

Optimal Sizing of Hybrid Renewable Energy Systems for Rural Electrification

Prepared for

A/Prof S.P. Chowdhury

Dr S. Chowdhury

The University of Cape Town

Prepared by

Gabrielle Coppez

CPPGAB001

Submitted to the Department of Electrical Engineering, University of Cape Town, in fulfilment of the requirements for the degree: Masters of Science in Electrical Engineering.

29 August 2011



Key Words: Rural Electrification, Hybrid Renewable Energy System, Off-Grid Electrification, Optimisation

Declaration

I declare that the work contained in this thesis is my own and no part was created by another party. All references and sources have been appropriately acknowledged.

This work is submitted to the Department of Electrical Engineering, University of Cape Town, in fulfilment of the requirements for the degree: Masters of Science in Electrical Engineering, and has not been submitted for any other academic purposes before this.

Gabrielle Coppez
University of Cape Town
Rondebosch
Cape Town

29 August 2011

In Memory of Doug Banks (2 April 1965- 4 July 2008)

A man of passion for Africa, its people, rural electrification and renewable energy



Gaby Coppez is the first young professional to benefit from the Doug Banks Renewable Energy Vision scholarship which funded a significant part of her research and thesis.

The Doug Banks Renewable Energy Vision is a South African initiative aimed at building intellectual capital in the field of Renewable Energy.

Dr Doug Banks was a man who was passionate about meeting Africa's energy challenges through the development of Renewable Energy. Through a deep understanding of people and technology, Doug was able to speak to and shape national renewable energy policies. A number of young professionals owe their career choice to Doug's enthusiastic mentorship.

The initiative is set on finding undergraduate students, preferably from an engineering, scientific or technical background who are willing and able to carry forward Doug's passion and vision.

After his untimely death in July 2008, friends and colleagues of Dr Doug Banks decided to create something that would become a legacy of a truly remarkable man. The Doug Banks Renewable Energy Vision Trust resulted.

Acknowledgements

There are many people to thank for me getting to the point of finishing this work and writing it up:

To the Doug Banks Renewable Energy Vision for carrying me financially, for allowing me opportunities to attend conferences in Wales and China, for introducing me to many people who expanded my vision on rural electrification and talked to me about the real implications of this, and to the mentors who have walked this journey alongside me, asking good questions and being available when I was in need. I would like to especially thank Wendy Anneke and Dave Gale for their mentoring and support during this time. It has been a real privilege to be the first Doug Banks Renewable Energy Vision scholar.

To Prof Gaunt of UCT for making rural area load data available to me from the National Load Research Project. To Schalk Heunis of Enerweb for making load data and climatic data available for the areas which I was researching.

To Prof and Dr Chowdhury for always having an open door for me to come and discuss my project, for encouraging me to write papers and attend conferences and financially supporting me in that when necessary, for direction in my work and for making me feel like part of your family, thank you.

To my family, Mum, Dad, Pascale and Klos, thank you for your encouragement and support, for listening to me when I was feeling disillusioned, for being proud of me and celebrating my achievements with me.

To my housemates, past and present, Kate and Sarah, thank you for listening to me talk for ages about things that you probably didn't even want to know, for your encouragement and for the many cups of coffee, chats, dancing and love.

To my friends, thank you for walking alongside me, being with me through thick and thin, for the chats, for the creativity, for the prayers and for the love, it has meant so much to me. To my specifically renewable friends, Brian and Christine, I look forward to long lovely chats about the things we've learned and the places we've been. Thanks for being inspirational to me.

To my fiancé, Barry Pitman, thank you for being an encourager, a shoulder to cry on, a loving presence in my life, for working with me, for helping me to focus, for distracting me, for putting things in perspective, for being a light and for being the love of my life.

Lastly, to the One who encourages me, loves me unconditionally and everlastingly, who guides me and who is hope in every situation, I could not have done this without You.

Abstract

Rural areas in South Africa face large challenges when it comes to electricity supply. Grid extension projects are time intensive and require a large capital investment. Non-grid electrification is an option in these areas, but must be sustainable and easily maintainable to give maximum energy supply efficiency for the area. As South Africa has a large amount of the resources needed for current renewable energy technology application, it has great potential for implementation of this kind. In addition to renewable energy techniques of energy generation being environmentally friendly, there is no necessity for fuels and therefore after initial capital investment, there are only minor operating costs associated with this. For rural environments, this is important. For non-grid electrification, different renewable energy technologies must be investigated to ascertain the most efficient and productive means of energy generation and distribution in each area to enable the area to be able to generate, store and distribute electricity and become independent and self-sustainable. The implication of implementation of this scheme must then be considered.

This project has the objective of creating a tool for feasibility assessment and recommendations of sizing of hybrid renewable energy systems in rural areas in South Africa. This involves the development of a tool which would analyse information input about the climate of the area and the load demand. As the load demand is variable, other electrified rural areas with similar loads or population structures can be used to estimate the load profile of the proposed area for electrification. This is done to ensure the correct sizing of the system. Climatic data of temperature, wind speed and solar irradiance will be needed for the accurate execution of the tool.

With the information specified above, this tool is then used to calculate the size and type of the Hybrid Renewable Energy System (HRES) that is best suited, in view of the energy demands calculated for that area. For the purposes of rural electrification, wind and solar renewable techniques are considered the most appropriate at this point in time as they are the most technologically mature options and have been proven in many applications and therefore the reliability of these methods are assured.

Another aspect of this model would be energy storage. Because of the inherent intermittency of renewable energy techniques which are reliant on wind speed and irradiance levels, it is important to store energy when there is an excess of energy and to be able to supply energy when there is insufficient being generated.

The objective of this tool is therefore to optimise the size of the HRES needed for an area for which the climatic and load data is supplied. The optimisation will occur to minimise the cost of the system whilst keeping the probability of the load being supplied to a specified constraint.

Following initial model development, rural areas which are currently electrified are used as case studies using their load and climatic data and designing and sizing HRES for these areas. The result from this optimisation must be checked through various methods to ensure that the specified reliability of the system is kept consistent.

Table of Contents

Declaration.....	i
Acknowledgements.....	iii
Abstract.....	iv
Table of Contents.....	v
List of Tables	ix
List of Figures	x
Nomenclature	xii
1. Introduction	1
1.1. Rural Electrification in South African context.....	1
1.2. Renewable Energy.....	1
1.3. Hybrid renewable energy systems.....	1
1.4. Problem definition	2
1.5. Thesis objective.....	2
1.6. Scope and Limitations.....	3
1.7. Thesis outline	3
2. Literature Review.....	5
2.1. Introduction	5
2.2. PV systems	5
2.2.1. Modelling PV	6
2.2.2. Maximum Power Point Tracking.....	10
2.3. Wind Turbine Systems	11
2.3.1. Modelling Wind.....	12
2.4. Energy Storage	13
2.4.1. Storage Method Selection	14
2.4.2. Types of Energy Storage.....	14
2.5. Batteries.....	15
2.5.1. Types of Batteries	16
2.5.2. Lead acid batteries.....	17
2.5.3. Modelling lead acid batteries.....	18
2.6. System and Battery Controller.....	20
2.6.1. High level supervisory control.....	21
2.6.2. Directional Convertor control	21

2.6.3.	Battery Management Control System	22
2.7.	System Sizing Optimisation.....	23
2.7.1.	Graphical Construction	23
2.7.2.	Probabilistic and Deterministic Techniques.....	24
2.7.3.	Artificial Neural Network	24
2.7.4.	Genetic Algorithm	25
2.8.	Genetic Algorithms	26
2.8.1.	Generate Initial Population.....	27
2.8.2.	Natural Selection.....	28
2.8.3.	Select Mates.....	28
2.8.4.	Mating.....	30
2.8.5.	Mutation	31
3.	Methodology.....	32
3.1.	Introduction	32
3.2.	Climatic Data Set.....	32
3.3.	Load Data Set	32
3.4.	Optimisation objectives and overview	32
3.1.1.	PV Panels.....	33
3.1.2.	Wind turbine	35
3.1.3.	Batteries.....	37
3.1.4.	Calculating LPSP	39
3.5.	Objective function of cost of system	39
3.1.5.	Annualised Cost of the System	39
3.1.6.	Total Cost of the System	41
3.1.7.	Implemented Cost of the System.....	41
3.6.	Setting up the genetic algorithm	43
3.1.8.	Generating Initial Population.....	43
3.1.9.	Natural Selection.....	44
3.1.10.	Select Mates.....	44
3.1.11.	Mating.....	44
3.1.12.	Mutation	44
3.7.	Calculating LPSP for checking results.....	44
3.8.	Controller and simulation for checking GA results	45
3.1.13.	Mode 1.....	46

3.1.14.	Mode 2	47
3.1.15.	Mode 3	47
3.1.16.	Mode 4	48
4.	Case Study 1: Garagapola	49
4.1.	Introduction	49
4.2.	Climatic Data Set	50
4.3.	Load Data Set	51
4.4.	Results of Optimisation.....	51
4.1.1.	PV Panels.....	53
4.1.2.	Wind turbine	53
4.1.3.	Batteries.....	54
4.1.4.	Calculating LPSP	54
4.5.	Resultant Controller and Simulation Results	54
4.6.	Conclusions	58
5.	Case Study 2: Antioch	59
5.1.	Introduction	59
5.2.	Climatic Data Set	60
5.3.	Load Data Set	61
5.4.	Results of Optimisation.....	61
5.4.1.	PV Panels.....	63
5.4.2.	Wind turbine	63
5.4.3.	Batteries.....	64
5.4.4.	Calculating LPSP	64
5.5.	Resultant Controller and Simulation Results	64
5.6.	Conclusions	68
6.	Case Study 3: Gasese	69
6.1.	Introduction	69
6.2.	Climatic Data Set	70
6.3.	Load Data Set	71
6.4.	Results of Optimisation.....	71
6.1.1.	PV Panels.....	73
6.1.2.	Wind turbine	73
6.1.3.	Batteries.....	74
6.1.4.	Calculating LPSP	74

6.5.	Resultant Controller and Simulation Results	74
6.6.	Conclusions	78
7.	Discussion of Results.....	79
7.1.	Introduction	79
7.2.	Climatic Data Set	79
7.3.	Load Data Set	81
7.4.	Results of Optimisation.....	82
7.1.1.	PV Panels.....	82
7.1.2.	Wind turbine	82
7.1.3.	Batteries.....	83
7.5.	Conclusions	84
8.	Conclusions and Recommendations.....	85
8.1.	Conclusions	85
8.2.	Recommendations	86
9.	References	88
10.	Papers Published.....	92
	Appendix: Datasheets	93
	PV Panel Datasheet: Tenesol TE200	94
	Wind Turbine Datasheet: Kestrel e400i.....	96

List of Tables

Table 2.1: Comparison of Energy Storage Methods	14
Table 2.2: Key Battery Attributes Comparison	17
Table 4.1: Average Monthly Climatic Data	50
Table 4.2: Monthly Average Load for Garagapola	51
Table 4.3: Genetic Optimisation Results per Generation	51
Table 5.1: Average Monthly Climatic Data	60
Table 5.2: Monthly Average Load for Antioch	61
Table 5.3: Genetic Optimisation Results per Generation	61
Table 6.1: Average Monthly Climatic Data	70
Table 6.2: Monthly Average Load for Gasese	71
Table 6.3: Genetic Optimisation Results per Generation	71
Table 7.1: Comparison of Results	82

List of Figures

Figure 2.1: Voltage-Current Curve of PV Panel [2]	7
Figure 2.2: PV Single Diode Equivalent Circuit Model	7
Figure 2.3: Component Values for PV Array	9
Figure 2.4: PV Double Diode Equivalent Circuit.....	10
Figure 2.5: P&O MPPT Flow Diagram [9]	11
Figure 2.6: Relationship between Wind Speed and Power Output of Wind Turbine.....	12
Figure 2.7: Simple Circuit Model.....	18
Figure 2.8: Thevenin Battery Model Circuit.....	19
Figure 2.9: Non-linear Battery Model	20
Figure 2.10: Improved Non-linear Battery Model.....	20
Figure 2.11: Bi-directional Convertor Control Algorithm [22]	22
Figure 2.12: GA Optimisation Flowchart [27]	26
Figure 2.13: Genetic Algorithm Flowchart.....	27
Figure 2.14: Representation of Chromosome for Hybrid Power System	28
Figure 2.15: Example of Ranking Selection of Chromosomes to be Paired.....	29
Figure 2.16: Single and 2-Point Crossover Mating.....	30
Figure 3.1: Wind Speed - Power Profile of Kestrel e400i with Datasheet Details [35].....	36
Figure 3.2: Generated Wind Speed-Power Profile of Kestrel e400i from Matlab	37
Figure 3.3: Simple Flowchart of Genetic Algorithm.....	43
Figure 3.4: Flowchart of modes of control for HRES.....	45
Figure 3.5: Mode 1 Flow Chart of Operation	46
Figure 3.6: Mode 2 Flow Chart of Operation	47
Figure 3.7: Mode 3 Flow Chart of Operation	48
Figure 4.1: Map showing Location of Garagapola [40].....	49
Figure 4.2: Satellite Image of Garagapola [40]	49
Figure 4.3: Garagapola Daily Average Temperature over Year	50
Figure 4.4: Histogram showing Average Monthly Load for Garagapola.....	51
Figure 4.5: Power able to be supplied by PV Panels.....	53
Figure 4.6: Power able to be supplied by Wind Turbines	53
Figure 4.7: Load over the Year	54
Figure 4.8: Power Supplied by the Wind Turbines	55
Figure 4.9: Power Supplied by the PV Panels	55

Figure 4.10: Capacity of Batteries.....	56
Figure 4.11: Histogram of Modes of System.....	56
Figure 4.12: Load and Total Supply over Year	57
Figure 4.13: Enlargement of figure 4.12 showing Load not being met	58
Figure 5.1: Map Showing Location of Antioch [42].....	59
Figure 5.2: Satellite Image of Antioch [42]	59
Figure 5.3: Antioch Daily Average Temperature over Year	60
Figure 5.4: Histogram showing Average Monthly Load for Antioch.....	61
Figure 5.5: Power able to be Supplied by PV Panels.....	63
Figure 5.6: Power able to be Supplied by Wind Turbines.....	63
Figure 5.7: Load over the Year	64
Figure 5.8: Power supplied by the Wind Turbines.....	65
Figure 5.9: Power Supplied by the PV Panels	65
Figure 5.10: Capacity of Battery.....	66
Figure 5.11: Histogram of Modes of System.....	66
Figure 5.12: Load and Total Supply over Year	67
Figure 5.13: Enlargement of figure 5.12 showing Load not being met	68
Figure 6.1: Map Showing Location of Gasese in South Africa [43]	69
Figure 6.2: Satellite Image of Gasese [43]	69
Figure 6.3: Gasese Daily Average Temperature over Year	70
Figure 6.4: Histogram Showing Average Monthly Load for Gasese	71
Figure 6.5: Power Able to be Supplied by PV Panels	73
Figure 6.6: Power Able to be Supplied by Wind Turbines	73
Figure 6.7: Load over the Year	74
Figure 6.8: Power Supplied by the Wind Turbines	75
Figure 6.9: Power Supplied by the PV Panels	75
Figure 6.10: Capacity of Batteries.....	76
Figure 6.11: Histogram of modes of System.....	76
Figure 6.12: Load and Total Supply over Year	77
Figure 7.1: Average Monthly Temperature Bar Chart	79
Figure 7.2: Average Monthly Solar Irradiance Bar Chart	80
Figure 7.3: Average Monthly Wind Speed Bar Chart	80
Figure 7.4: Average Monthly Load Bar Chart.....	81

Nomenclature

DC	Direct Current – A non-alternating current.
DOD	Depth of Discharge – The lowest State of Charge allowed for a battery.
EMF	Electromotive Force – The potential across the terminals of a battery.
GA	Genetic Algorithm – Optimisation method using biological principles.
HRES	Hybrid Renewable Energy Systems – Renewable energy systems using more than one source of energy generation.
LPSP	Loss of Power Supply Probability – Probability that the load will not be met by the supply over a period of time.
MPPT	Maximum Power Point Tracking – A method of control used to track the maximum power obtainable from a energy source where the maximum power changes dependant on factors such as temperature or solar irradiance.
PV	Photo-voltaic – A method of converting solar energy to electricity.
SoC	State of Charge – Amount of capacity in battery at a specific point in lifecycle, at 100% State of Charge, the battery is at maximum capacity, at 0% at minimum
SoH	State of Health – The state of a battery taking capacity, number of cycles and lifetime into account.
STC	Standard Temperature Conditions – Set temperature conditions used as the benchmark in tests for standardisation of datasheets. It is defined as 1000W/m ² solar irradiance, temperature of 25°C and airmass of 1.5.

1. Introduction

1.1. Rural Electrification in South African context

South Africa is a large country and has many rural areas. There is not always grid connection to outlying rural areas and many of these rural areas remain without electricity. Grid extension projects are time intensive and require a large capital investment. Because of the large distance needed to be covered by the grid to reach these outlying rural areas, it is often too expensive to be feasible. In addition, as these areas are sparsely populated and have a low power demand, the expense of extending the grid may not be worth the benefit that it would bring. In addition, the grid in South Africa is currently operating very close to its maximum capacity and therefore cannot afford to increase the load it is supplying over the next period of time until more power stations are built.

However, to encourage economic growth in these rural areas, some form of electricity is needed. Non-grid electrification is an option in these areas, but must be sustainable and easily maintainable to give maximum energy supply efficiency for the area.

1.2. Renewable Energy

The use and applications of renewable energy is on the incline. As the amount of fossil fuels lessens and the environmental concerns of continuing to use fossil fuels increases, there is a heightened need to search for alternative solutions. As South Africa has a large amount of the resources needed for current renewable energy technology application, it has great potential for implementation of this kind. In addition to renewable energy techniques of energy generation being environmentally friendly, there is no necessity for fuels and therefore after initial capital investment, there are only minor operating costs associated with this. For rural environments, this is important. For non-grid electrification, different renewable energy technologies must be investigated to ascertain the most efficient and productive means of energy generation and distribution in each area to enable the area to be able to generate, store and distribute electricity and become independent and self-sustainable.

1.3. Hybrid renewable energy systems

When considering the electrification of a rural area it is important to design systems that are reliable and require little maintenance as in these areas frequent repairs and replacements might not be easy. Using a singular form of renewable energy, such as solar PV, to supply a rural area is possible, however no electricity will be generated when sunlight is not available and therefore no electricity will be supplied during that time. If more than one independent source is employed for energy generation, for example a combination PV panels and wind turbines, the energy demand generation can be split between these two sources and therefore the system depends less on one intermittent energy source. This improves energy supply security. To make the system further reliable, energy storage must be added to the

system to store energy in times of excess generation and supply energy in times of a lack of generation. Hybrid Renewable Energy Systems, using a combination of energy sources and storage are preferred in the area of rural electrification.

1.4. Problem definition

Hybrid Renewable Energy Systems have been accepted as a possible means of electrifying rural outlying areas where it is too expensive to extend the grid to supply them. One of the main problems identified with these systems which are not connected to the grid is that the sources themselves are reliant on climatic conditions and therefore inherently intermittent. In addition to this the load to be supplied is also fluctuating and therefore it is even more difficult to predict the load and supply together. As these stand-alone systems run without any grid connection, they must be designed to be reliable systems with only a small loss of power supply probability. In addition to this, as there is generally limited funding for rural areas, the design of such systems must be cost-effective as well.

The problem, therefore, that this thesis deals with is that of sizing an HRES to ensure a specified reliability, through the use of a specified Loss of Power Supply Probability and to design a system that minimises the necessary cost as much as possible to ensure its affordability for necessary rural electrification.

1.5. Thesis objective

This project has the objective of creating an optimisation tool for feasibility assessment and optimal sizing of HRESs in rural areas in South Africa. This involves the development of a tool which would analyse information input about the climate of the area and the load demand. As the load demand is variable, other electrified rural areas with similar loads can be used to estimate the load profile of the proposed area for electrification. This is done to ensure the correct sizing of the system. Climatic data for temperature, wind speed and solar irradiance will be needed for the accurate execution of the tool.

With the information specified above, this tool would then be used to calculate the size and type of the Hybrid Renewable Energy System (HRES) that is best suited, in view of the energy demands calculated for that area. Another aspect of this model would be energy storage: the method of modelling energy storage, sizing the optimal amount of energy storage and its operation and control in HRE Systems. Because of the inherent intermittency of renewable energy techniques which are reliant on wind speed and irradiance levels, it is important to store energy when there is an excess of energy and to be able to supply energy when there is insufficient being generated.

The objective of this tool is therefore to optimise the size of the HRES needed for a rural area for which the climatic and load are supplied. The optimisation will be done to minimise the cost of the system whilst keeping the probability of the load being supplied to a specified constraint.

The result from this optimisation must be checked through various methods to ensure that the specified reliability of the system is kept consistent.

1.6. Scope and Limitations

For the purposes of rural electrification, wind turbines and solar PV are considered the most appropriate renewable technologies at this point as they are the most technologically mature options. They have also been proven in many applications and therefore the reliability of these methods is assured. The scope of this thesis is, therefore, to optimise the size of a HRES system to be used in a rural area using PV panels, wind turbines and for energy storage, batteries.

No other methods of renewable energy generation are considered, however other methods could be used in a system such as the one designed in this thesis.

It is understood that the issue of rural electrification is not purely technical. There are other factors which must be taken into account when implementing an electricity solution in a rural area. These include social factors, such as the adoption and acceptance of the system by the community for which it is designed; economic factors, such as the repayment of the system or subscription fees to be paid by members of the community. It also includes other economic factors such as the growth of the community once electricity is available, the growth in size of the community as well as growth in industry and functions of the community which would increase the load to be supplied to the community.

These are all important factors to rural electrification, however they are large areas of research in themselves and therefore purely the technical aspect of designing a HRES system for an off-grid area is discussed. A surplus of 5% is added onto all load data received for designing the system to ensure that there is room for growth of the community, but no further areas of growth have been included or accounted for.

1.7. Thesis outline

Chapter 2 begins by reviewing the energy generation technologies specified for this thesis, such as solar PV systems and wind turbine systems. These are reviewed in terms of their applications and the possible methods of modelling these technologies. Methods of energy storage and varieties of batteries are then explored along with the methods of modelling lead-acid batteries. Methods of controlling HRES systems to supply the load of the system are discussed with special emphasis on the manner of charging and discharging the battery to ensure the maximum lifetime of the battery. Finally methods of optimisation are reviewed, focussing on Genetic Algorithms, as the chosen method of optimisation of the system.

Chapter 3 presents the methodology used in the optimisation tool as well as the result checking algorithms. The chapter explains the climatic and data sets needed for this optimisation problem as well as where these data sets were obtained. The selected methods of modelling the power generated by each of the energy generation methods and the method of modelling the input of the batteries into the system are discussed. The genetic

algorithm is discussed in detail along with the assumptions and methods used for setting up the genetic algorithm with respect to the objective function of the cost of the system. Finally the controller algorithm used for validating the results obtained by the genetic algorithm is explained.

Chapters 4, 5 and 6 describe three case studies undertaken in the areas of Garagapola, Antioch and Gasese respectively. These chapters look at the climatic and load data sets used in the study as well as the results of the optimisation of each. The controller used to validate the results is run and the results of this are also discussed.

Chapter 7 discusses the results from the case studies. It compares the various data and load sets used as well as the results of the optimisations, drawing parallels between the three case studies and noting any irregularities that have arisen.

Chapter 8 draws conclusions from the various results discussed in chapter 7 and the rest of this thesis. Recommendations for further work are made with respect to limitations in the scope of this project as well as from information learned as a result of this work.

2. Literature Review

2.1. Introduction

Renewable energy systems (RESs) using renewable and low carbon power sources are being increasingly preferred for power generation. As the world moves towards the end of its finite supply of fossil fuel resources, being able to use them sparingly, as well as refining ways of generating electricity without them, becomes increasingly important. At the same time the adverse effects of burning fossil fuels on the environment have been acknowledged and the move towards cleaner methods of energy generation is imperative. There are many advantages to renewable power generation especially within remote areas where access to established grids is limited and large distances between the existing grid and the area cause the cost of extending the grid to be impractical.

Hybrid renewable energy systems are becoming increasingly used within the context of rural electrification. For the scope of this thesis, hybrid renewable energy systems consisting of wind turbines, PV panel and lead acid batteries are considered. Each of these elements adds complexity to the system introducing new parameters, new changing values based on the weather, but ultimately new energy sources to areas where previously there was none and where connection to the grid would be a very expensive exercise. The following section discusses each of the mentioned sources as well as looking at methods of optimisation and control of hybrid renewable energy systems. The optimisation is used in the design phase to size the best system to supply the load whilst minimising the cost of the system and the control is used within the running system to get the most out of each component.

2.2. PV systems

The use of photovoltaic systems around the world is increasing and the ways that it is being used is constantly changing and evolving. Most applications of photovoltaic systems are currently grid connected, distributed systems supplying only a few kilowatts of power. However, with the increasing sophistication of technology and new methods of Maximum Power Point Tracking (MPPT) and of implementing systems, the use and different applications of PV systems is expected to grow. The introduction of feed-in tariffs in South Africa, as well as many other countries, imitates that the use of small system PV will continue to rise as well [1].

Photovoltaic systems are used within power generation to convert energy from the sunlight into electrical energy. Photovoltaic systems are comprised of cells at a basic element level. These cells can be connected together in series to form panels. Connecting the photovoltaic cells together in series increases the output voltage of the system. For example the KC200GT solar panel consists of 54 PV cells connected together in series to generate an open circuit voltage of 32.9V [2].

In typical power generation applications panels are joined together in series and in parallel to enable the correct power to supply the load to be generated. A collection of panels such

as this is called an array. Panels connected together in series increase the voltage of the system, while panels connected in parallel to the system increase the current that the PV array can supply.

The PV array can then be connected straight to a DC load, but is most commonly connected to a convertor or controller to control the voltage and power to the load and to track the Maximum Power Point (MPP) of the PV array. MPPT is generally used to ensure that the maximum power that the array can provide at the given temperature and irradiance is achieved [2].

As the use of PV sources in on the incline, the importance of modelling these components is high to ensure that we can predict the behaviour of these systems before they are installed. Using data from real experimental systems when modelling helps us to see the impact of aging, and consistency of the systems to allow for us to include this in the models we design. It is also very important to know how PV systems interact with other renewable and non-renewable sources to supply a common load. Modelling is also necessary for the sizing of a system, in knowing that the load will always be met by the energy sources used for different size systems. The power generated from a PV cell is a function of the properties of the material that the PV cell is made from, as well as the temperature of the PV surface and the irradiance on the surface of the cell [3].

For the purposes of this project, the PV source is modelled to ensure that the load is met by the PV panels, wind turbine and battery energy sources and storages. The PV source is modelled with a varying irradiance and temperature based on the varying hourly data over a day.

2.2.1. Modelling PV

There are many different approaches to how one can model photovoltaic systems. A PV panel has a very distinct voltage-current curve which has the general appearance shown in figure 2.1. This needs to be accounted for when modelling the PV system. This V-I curve has three distinct points of interest which can be used in modelling to calculate parameters of the model. The first is the short circuit current point, where voltage is zero and current is equal to the short circuit current, I_{SC} . The second is the Maximum Power Point (MPP). This is the point where the maximum power is generated by the PV panel. The current has a value of I_{MP} at this point and the voltage, V_{MP} . The third is open circuit voltage point where the current is zero and the voltage is at open current voltage. Each of these voltages and currents are distinct to the particular PV array and are detailed on the manufacturer's data sheet.

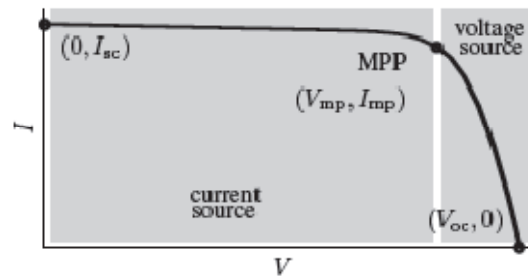


Figure 2.1: Voltage-Current Curve of PV Panel [2]

Equation Model

The first method of modelling a PV array involves simply using mathematical equations to calculate the power generated at the specified temperature and irradiance from the power generated at Standard Temperature Conditions (STC) by analysing the factors concerned and determining how they would affect the power generated. STC is defined as $1000\text{W}/\text{m}^2$ irradiance, temperature of 25°C and airmass of 1.5. The power generated at the specified temperature conditions is therefore:

$$P_m = P_p \cdot n_t \cdot \frac{G}{G_{STC}} \quad (2.1)$$

Where P_m is the power generated at the specified temperature conditions, P_p is the nominal power produced by the PV panel as STC, n_t is a coefficient which contains the effect of factors such as the deviation of temperature from 25°C , the aging of the panel, deviation from MPP and ohmic resistances in conductors as well as other factors which affect the power generated, G is the irradiance at the specified site and G_{STC} is the irradiance at STC [1].

Equivalent Circuit Model

A second method of modelling PV arrays is using electrical equivalent circuits. There are two electrical equivalent circuits that are in general use.

The first is a single diode model where the PV cell is modelled as a circuit containing a single diode and two resistors as shown in figure 2.2 below.

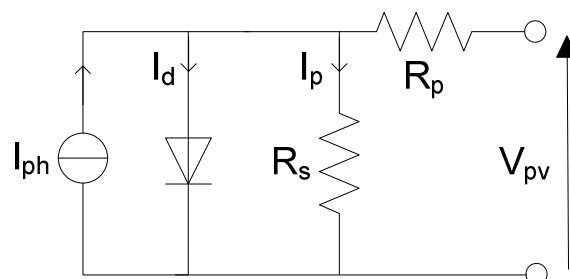


Figure 2.2: PV Single Diode Equivalent Circuit Model

The PV cell is modelled as a current source with a diode in parallel to the current source as well as one resistor in parallel and one in series with the current source, as shown in figure 2.2. The DC source, I_{ph} , represents the current generated by the

photon-electron interaction in the PV cells, the diode illustrates the p-n junction effect, the parallel resistance, R_p , represents the current losses and the series resistance, R_s , represents the metallic contact voltage losses [4].

The characteristic equation for this equivalent circuit is shown in equation 2.2:

$$I_{pv} = I_{ph} - I_d - I_p \quad (2.2)$$

There are many ways of solving this equation for a solar panel and specified temperature conditions. Some of these methods taken from journal articles will be discussed in varying depths.

Belfkira et al [5] state that the output current I_{pv} at an hour denoted by t , can be expressed as a function of the output voltage of the panel, V_{pv} . Equation 2.3 is used to calculate this relationship:

$$I_{pv}(t) = K_1 \cdot G(t) \cdot [1 + K_2 \cdot (G(t) - G_{ref})] + K_3 \cdot (T(t) - T_{ref}) - \frac{V_{pv}(t)}{R_p} - K_4 \cdot T^3(t) \cdot \exp\left(-\frac{E_g}{k \cdot T(t)}\right) \cdot [\exp(q \cdot (V_{pv}(t) + R_s \cdot I_{pv}(t)) / (k \cdot A \cdot n_s \cdot T(t))) - 1] \quad (2.3)$$

where K_1 , K_2 , K_3 and K_4 are the constant parameters, G_{ref} is the reference solar irradiation of 1000 W/m², which is the irradiance at STC, T_{ref} corresponds to the reference temperature of cell (25°C), which is the temperature of the cell at STC, k is the Boltzmann constant (1.38 10⁻²³ J/K), q is the elementary charge (1.6 10⁻¹⁹ C), A is the ideality factor of junction, E_g is the gap energy and G and T corresponds to the solar irradiance and solar cell temperature, respectively. The cell temperature can be expressed as in equation 4.

$$T(t) = T_a(t) + \left(\frac{NOCT-20}{800}\right) \cdot E_s(t) \quad (2.4)$$

Where T_a is the ambient temperature and Normal operating cell temperature, NOCT, is the cell temperature when the PV panel operates under 800 W/m² of solar irradiation and 20°C of ambient temperature, NOCT is usually between 42°C and 46°C.

The power of the panel can then be calculated by multiplying the voltage and current of the output of the PV array [5].

Ashraf A. Ahmed et al [6] and Villalva [2] translate equation 2.2 into the following equation:

$$I_{pv} = I_{ph} - I_o \left(e^{\frac{V+I \cdot R_s}{A}} - 1 \right) - \frac{V+I \cdot R_s}{R_p} \quad (2.5)$$

$$\text{Where } A = \frac{mKT}{q}$$

The last term which represents I_p can be ignored if one assumes that the value of R_p is very large.

In this model, one can assume that the temperature is the same over the whole solar cell. This equation is considered by many to be the standard PV panel calculation [2,6].

Cells are generally connected together in series and parallel to form panels and arrays. When the same types of cells are connected in this arrangement, the equivalent circuit can be shown as in the figure below.

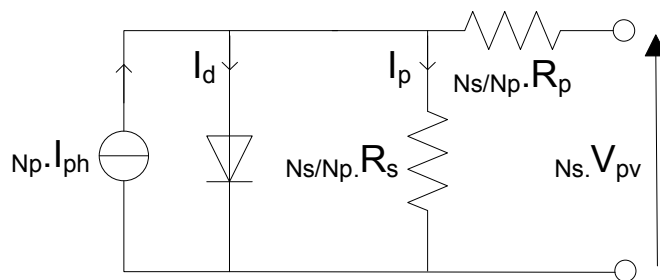


Figure 2.3: Component Values for PV Array

This translates to the following amendments when one is calculating array values as opposed to cell values:

$$R_{sa} = \left(\frac{n_s}{n_p}\right) \cdot R_s \quad (2.6)$$

$$R_{pa} = \left(\frac{n_s}{n_p}\right) \cdot R_p \quad (2.7)$$

$$I_{pha} = n_p \cdot I_{ph} \quad (2.8)$$

$$V_{pva} = n_s \cdot V_{pv} \quad (2.9)$$

The second method of equivalent circuits is the double diode equivalent circuit model. This model is similar to the single diode equivalent circuit model, however a second diode is connected in parallel in addition to the first diode, shunt and series resistances. This second diode is added to represent the effect of recombination of electrons in the PV cell [2].

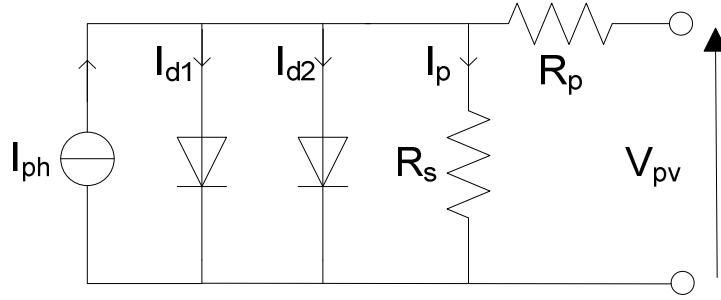


Figure 2.4: PV Double Diode Equivalent Circuit

The characteristic equation for the equivalent circuit shown in figure 4 is then as follows:

$$I = I_{ph} - I_{O1} \left[e^{\frac{V+I.R_s}{V_{Tcell}}} - 1 \right] - I_{O2} \left[e^{\frac{V+I.R_s}{A.V.T}} \right] - \frac{V+I.R_s}{R_p} \quad (2.10)$$

$$\text{Where } V_{Tcell} = \frac{k.T}{q} \quad (2.11)$$

Where k is the Boltzmann's constant, T is the absolute temperature and q the charge of an electron.

In equation 2.10, V represents the terminal voltage of the PV panel or array and I the terminal current, I_{ph} the photocurrent, I_{O1} and I_{O2} the saturation currents of each of the diodes, R_s represents the series resistance and R_p the parallel or shunt resistance. A refers to the diode constant used to represent the Shockley-Read-Hall recombination in the space-charge layer in the photodiode. This value is usually set to 2 [7].

The parameters of this model can then be calculated in a number of manners, mostly similar to those presented for the single diode equivalent model.

2.2.2. Maximum Power Point Tracking

There are many methods of tracking the MPP, some include: constant voltage, open and short circuit method, perturb and observe method, incremental conductance algorithm, fuzzy logic and artificial neural networks.

The constant voltage is the simplest method of MPPT. It is however, still quite effective. This method uses the voltage at MPP and sets this as the voltage reference for the output of the PV system. A voltage regulator is then used to keep the output voltage as close to MPP voltage as possible. This keeps the system operating close to the MPP [8].

The open and short circuit method uses PV curves supplied by the manufacturers to calculate MPP current and voltage and then determine curves for the PV module. The voltage and current can then be monitored in the simulation and the voltage can be adjusted to ensure MPP voltage at that point.

Perturb and observe (P&O) MPPT method is the most commonly used method in commercial PV products. The P&O MPPT method uses trial and error in that the controller adjusts the reference output power of the inverter up fractionally and monitors the output power of the system. If the power increases, the controller will once again adjust the reference output power fractionally upwards and again monitor the output. It will continue to do this until the output power begins to decrease, at which point the controller will decrease the output power reference by a little bit to maintain the MPP found.

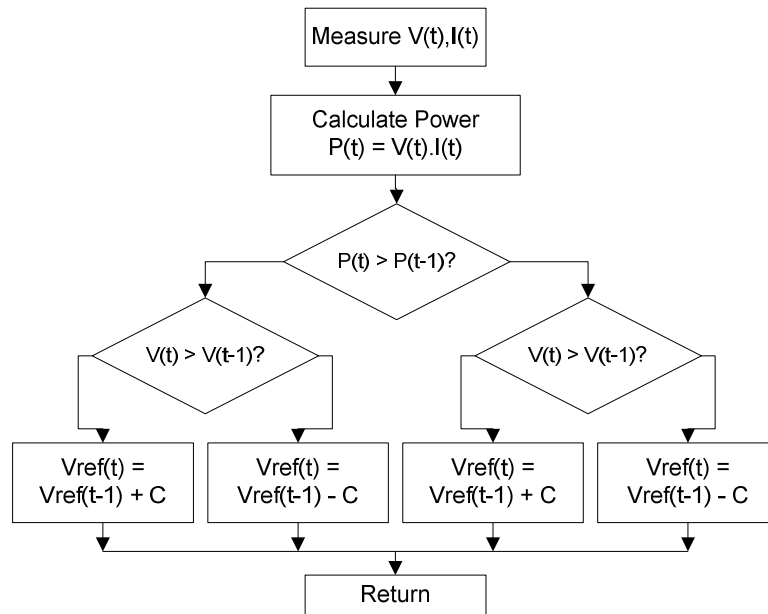


Figure 2.5: P&O MPPT Flow Diagram [9]

Incremental conductance works on the principle that when the derivative of the PV output power divided by the derivative of the output voltage approaches zero, the maximum output power is achieved. The controller therefore calculates $\frac{dP}{dV}$ from the output power and voltage and adjusts the voltage slowly until the derivatives approach zero [8].

2.3. Wind Turbine Systems

The use of wind turbine systems is growing considerably around the world. The use of onshore as well as the implementation of off shore wind turbines has let wind energy increase to the fifth most popular form of energy generation based on amount of energy generated worldwide in 2007 [10] producing 4% of Europe's total electricity demand in 2007 [11]. Wind is proving to be a very successful source of renewable energy as it still is able to provide a high amount of energy, whilst the cost not being too much higher than other traditional sources of energy generation [10]. The number of wind turbine systems in use is expected to continue to rise as countries prepare for the targets set by the European

Commission for 2020 that carbon emissions need to be reduced by 20% and the share of renewable energy sources in the energy generation mix must be 20%.

Within the context of rural electrification, wind turbines are used for their diversity of size and as they are the most proved form of renewable energy. Wind turbines of different types can range from generating power of 1kW to 7MW and therefore can be suited to whatever load size is needed to be supplied. As with PV panels, MPPTs are used to ensure that the maximum power that can be produced by the wind turbine at the particular wind conditions is produced. MPPTs for wind turbine systems are very similar to those discussed for PV panels and therefore will not be discussed again with regards to wind turbines.

The wind turbine needs to be modelled to ascertain the power added to the hybrid renewable energy system by the wind turbine(s) at the given wind speeds and tower heights. This will ensure that the system is accurately designed.

2.3.1. Modelling Wind

A wind turbine has a very distinct wind-power curve, which is shown in figure 2.6. As can be seen from figure 2.6 there is a very detailed relationship between the speed of the wind and the power that the wind turbine generates. This relationship is usually said to be a cubic one, in that for a specific change in wind speed there is a cube response to the power generated as is shown in equation 2.12.

$$p_1 = p_0 \left(\frac{ws_1}{ws_0} \right)^3 \quad (2.12)$$

Where p_0 is the power generated at the initial wind speed, ws_0 , and p_1 is the power generated at ws_1 .

It is therefore very important to generate a very precise wind speed data model or have detailed wind speed data. Weibull distribution is generally accepted as the best way of modelling wind speed probability distribution [10].

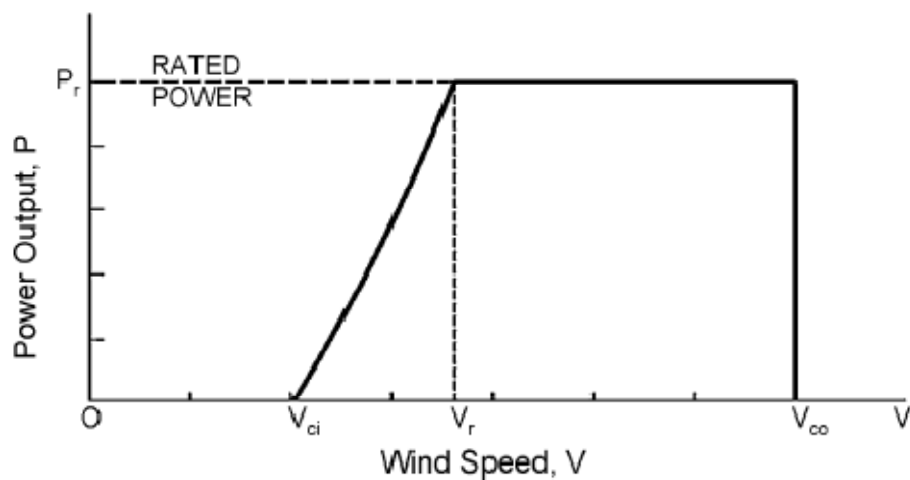


Figure 2.6: Relationship between Wind Speed and Power Output of Wind Turbine

Once wind speed has been properly modelled or enough accurate data is obtained, the power generated by the wind turbine can be estimated. Energy is generated between the cut-in wind speed, shown as V_{ci} in figure 2.6, and the cut-out wind speed, shown as V_{co} in figure 2.6. Between the rated wind speed, shown as V_r in figure 2.6, and the cut-out wind speed the power generated remains constant.

The power output of a wind turbine is therefore generally represented as a spline curve, as is shown in equation 2.13 [12].

$$P_W = \begin{cases} 0 & (v < v_{ci}) \\ a_1 v^2 + b_1 v + c_1 & (v_{ci} < v < v_1) \\ a_2 v^2 + b_2 v + c_2 & (v_1 < v < v_r) \\ c_3 & (v_r < v < v_{co}) \\ 0 & (v > v_{co}) \end{cases} \quad (2.13)$$

In equation 2.13, v_1 represents a point in change of gradient in the line between the cut-in wind speed and the rated wind speed, as some wind turbines don't have a straight line gradient but a more curved gradient between these two points.

The values for the constants in equation 2.13 can be found using the wind turbine characteristic curve supplied by the manufacturer.

2.4. Energy Storage

There are inherently some difficulties associated with Renewable Energy Hybrid Systems of this kind. Firstly, renewable energy is by nature intermittent and unpredictable. Secondly, the supply of energy, as well as the load needed, fluctuates. This creates imbalances within the system and therefore the potential for load to be unmet with supply.

There are a few ways of introducing stability into the system to ensure that there is always sufficient supply for the load demand. Hybrid RESs have a better chance of being able to supply the load more consistently as they combine more than one type of renewable technology which have different times of low and high generation. This distributes the consistency of supply more evenly, but in some cases will not be sufficient.

Energy storage is introduced in order to maintain the energy balance within the RES with consistency. It enables energy to be stored when there is an excess of supply, such as during daylight hours when PV generation is high and load is low; and supplies excess energy to the loads to compensate for the deficit of supply, such as during night time hours when PV generation is low and load is high. Energy storage can fulfil other functions such as load leveling and enhancing the power factor and overall efficiency and quality of the power system [13].

Batteries form a large part of the capital investment of RESs and therefore it is important to manage the system to ensure that the maximum lifespan of the battery is achieved by controlling its charging and discharging cycles. In addition the system must be sized correctly to ensure that the load is always met by the supply and to minimise the total cost of the system.

2.4.1. Storage Method Selection

The selection of an energy storage type for the optimal system is based on many different criteria. It is dependent on the project and the people involved as to which criteria are considered most critical and which are of lesser importance. Some criteria which can be used for optimisation are:

- *Reliability – the ability of the system to meet the load at all times.*
- *Efficiency – the ability to use the components in a way as to minimise losses.*
- *Cost – the lifecycle cost of the system including the initial investment plus running costs over the lifespan of the system.*
- *Technical maturity – commercial availability and proven reliability of the technologies used*
- *Life span – the length of time that the system will be able to operate*
- *Environmental impact – the impact that each component and therefore the overall system will have on the area surrounding it [14,15].*

Within hybrid wind and solar power generation applications, the parameters used for optimisation of the system are decided dependant on the project and the project stake holders. Multi Criteria Decision Making Management (MCDM) can be used to aid in system selection.

2.4.2. Types of Energy Storage

There are many types of energy storage that can be used in hybrid renewable energy systems. Some are: Compressed Air Energy Storage (CAES), Pumped Hydro Storage (PHS), Hydrogen Fuelcells, Flywheels, Super-capacitors, Super-conducting Magnetic Energy Storage (SMES) and chemical energy storage, also known as batteries. Key characteristics of each of the mentioned energy storage types are shown below in table 2.1. The application of storage selection methods are shown with regards to energy storage selection for HRES.

Table 2.1: Comparison of Energy Storage Methods

Attributes	Efficiency	Maturity of Technology	Cost	Energy Density	Power Density
CAES	70%	Mature	High	High	High
PHS	75-85%	Mature	High initial costs	Depends on size of reservoir	Dependant on height distance between reservoirs
Hydrogen	50-60%	Early stages of maturity	High	Depends on hydrogen reservoir	Dependant on speed of reaction
Flywheel	80-90%	Mature	Low	Low	High
Super-capacitor	80-95%	Immature	High	Low	High

SMES	90-95%	Immature	High	Low	High
Chemical	75-85%	Mature	Low	High	High

Table 2.1 compares the salient features of each storage method discussed above. In terms of hybrid RESs such as the discussed PV-wind generation system, important aspects are efficiency, maturity and therefore reliability of the storage method as well as cost. Looking at the energy storage methods it can be seen that SMES has the highest efficiency. However, SMES is a relatively new technology and is very expensive due to the use of superconductive wiring in the coil. Hydrogen storage and super-capacitors, as relatively new methods of storage, are not preferred for applications where adequate technical support is not readily available. The efficiency of hydrogen storage also does not qualify the cost of the system. For a small power application, the use of CAES as well as PHS is not justified as there are large initial costs involved with the systems, particularly in the case of PHS. While CAES is a relatively cheap form of energy storage, system location is limited by the need for underground compressed-air storage caverns. Flywheels are efficient and low cost systems, their self discharge rate is high and the energy density that they can supply is low. This makes them unsuitable for these types of applications. Chemical storage in the form of cell batteries is the ideal solution for hybrid RESs as there are no auxiliary systems which need to be run in conjunction with batteries. In addition, batteries are a very mature form of storage and can yield high energy density and high power density at low cost.

It is seen for this context that chemical storage offers the best trade for reliability, efficiency, maturity of technology and cost, as it is a reliable and technically mature type of energy storage as well as having an efficiency of between 75% and 85%. While costs fluctuate between types of batteries, they are on the whole a cheaper method of energy storage.

2.5. Batteries

Batteries form a large part of the capital investment of RESs and therefore it is important to manage the system to ensure that the maximum lifespan of the battery is achieved by controlling its charging and discharging cycles. In addition the system must be sized correctly to ensure that the load is always met by the supply and to minimise the total cost of the system.

Modelling and simulation of batteries within a RES design has a twofold purpose: firstly, to study their performance in a stand-alone system as an energy storage device, and secondly to enable the optimization of the size of batteries in order to minimise the overall operating costs. Modelling batteries can be a challenging task as there are many parameters to take into account, such as the State of Charge (SoC) of the battery, various voltages, internal resistances, battery capacitance, charge resistance, discharge resistance and other values which do not remain constant. These parameters are difficult to measure and predict within

a system where the charging and discharging cycles are often unpredictable and the temperature of the system is not constant, as is the case with most RESs.

2.5.1. Types of Batteries

Cell batteries are currently the most used form of energy storage in RESs. Cell batteries come in various forms and various types. When comparing types of batteries, important comparison criteria are: possible depth of discharge of the battery, cost, number of charge/discharge cycles the battery can tolerate, efficiency, self-discharge, maturity of the technology and energy density.

Lead Acid Batteries

Within the cell battery group, lead acid batteries are the cheapest and most popular. They can tolerate a depth of discharge of 75% and have a life span of 1000-2000 cycles on this depth of discharge. Lead acid batteries are 72-78% efficient and are currently the most mature battery technology type [16].

Lithium Ion (Li Ion) Batteries

Lithium ion batteries are mostly used within portable electrical equipments, such as laptops. This is because they have a very high efficiency of almost 100%. In addition, they have a lifespan of 3000 cycles at a depth of discharge of 80% [16]. However, lithium ion batteries are very expensive and therefore are not currently considered for larger applications where a larger energy density is needed.

Sodium Sulphur (NaS) Batteries

Sodium sulphur batteries are efficient batteries which work well with the pattern of daily charge and discharge. These batteries have a lifespan of 2500 cycles for a depth of discharge of 100%, 4500 cycles for a depth of discharge of 90%, and 6500 cycles for a depth of discharge of 65% [17]. Sodium Sulphur batteries have an efficiency of 89% but must be kept at a temperature of 300°C. While these batteries themselves are not expensive, maintaining them at 300°C requires energy which decreases the overall efficiency of the storage system and increases the cost [16].

Nickel Cadmium (NiCd) Batteries

Nickel cadmium batteries have efficiency between 72 and 78%. They can store up to 27MW of power which makes them very useful. Nickel Cadmium batteries have a lifespan of 3000 cycles with a depth of discharge of 100% and are thus well suited to the daily discharge and charge of a RES. They have high self-discharge rate losing between 5 and 20% of charge held per month [16]. However, they are also expensive and toxic [13].

Zinc Bromine (Zn-Br) Batteries

Zinc bromine batteries have an efficiency of 75% and negligible self-discharge. They have high power and energy density [16]. The technology related to Zn-Br batteries is

still relatively new and therefore not as technologically mature as others. In addition, these batteries are toxic [13].

Table 2.2: Key Battery Attributes Comparison

Attributes	Lead Acid	Li Ion	NaS	Ni-Cd	Zn-Br
Depth of Discharge	75%	80%	100%	100%	100%
Cost	Low	Very High	High and auxillary heating systems needed	High	High
Lifespan (Cycles)	1000	3000	2500	3000	2000
Efficiency	72-78%	100%	89%	72-78%	75%
Self-discharge	Average	Negligible	Negligible	High	Negligible
Maturity of Technology	Mature	Immature	Mature	Mature	Immature

Table 2.2 compares the key features of the batteries discussed. Within these types, lead acid and nickel cadmium are the most technologically advanced [16]. The ease of use of the lead acid batteries and their low cost make them the most preferred type of energy storage. Lithium ion batteries, whilst having great efficiency and lifespan at high depths of discharge, are currently too expensive to be used in large applications. Sodium sulphur batteries are also expensive and there is an additional need to maintain it at 300°C for optimal use. While Nickel cadmium batteries have a good lifespan with 100% depth of discharge, they have a very high self-discharge rate, making them less ideal for long term energy storage. Zinc bromine batteries are relatively immature in their technology and use, so still have to be proved in application. For the reasons stated above, lead acid batteries have been chosen as the focus for energy storage in this thesis. In addition lead acid batteries have been proven in their use in isolated power systems and remain the cheapest option in terms of cell batteries. The need for maintenance and their short lifespan is still an area where improvements need to be made; however when compared with other battery types, specifically for an isolated hybrid renewable energy system, minimization of costs is very important, lead acid batteries are still considered the best option.

2.5.2. Lead acid batteries

Lead acid batteries are currently the most used types of batteries in power applications. They are used for varying energy density requirements, but are most effective for lower power densities. While they have a good energy density, their power density is limited and therefore the amount of energy that can be supplied to the system and the time taken to charge the battery is significant [18]. Lead acid

batteries have a relatively short lifespan and therefore need to be replaced periodically. This is therefore the limiting factor in isolated power generation.

Due to the inherent unpredictable nature of renewable energy sources and the significant dependence of the power generated on climatic conditions, it is very important to simulate all components of the system together before implementation to ensure that the power supply needed for the load is met at all times. Therefore the extent to which the battery can store and supply energy is very important within a standalone system and must be simulated to ensure that the system will be able to meet the load.

2.5.3. Modelling lead acid batteries

Modelling of lead acid batteries can be done in a number of ways depending on how accurate the model needs to be as well as which parameters are needed to be taken into account. Some methods of battery modelling use experimentation to ascertain the characteristics and plot response curves for the battery, by measuring voltages and currents during the charge and discharge processes [17]. Another way of modelling the battery is by using an electrical equivalent circuit to represent the various parameters and characteristics of the battery and ascertain their values or equations to represent their values at different points in the process. Some of these models are discussed below.

Simple Battery Model

The simple battery model, as shown in Figure 2.7, represents the battery by an open circuit ideal voltage source and a fixed resistance. This model does not take the battery internal resistance or SoC into account, both of which are both very crucial to accurate dynamic modelling of the system. This model can be upgraded by introducing a variable resistance instead of the fixed resistance. This variable resistance is then dependent on the SoC of the system [19]. This model can then be used for applications where the SoC is irrelevant to calculations, such as for sizing a system where the system has a fairly constant charge.

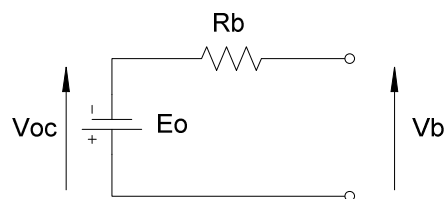


Figure 2.7: Simple Circuit Model

Thevenin Battery Model

The Thevenin Battery Model, as shown in Figure 2.8, uses an ideal voltage source, the internal battery resistance in series with the ideal voltage source and two parallel branches connected in series to the rest of the circuit to determine the battery voltage. The first parallel branch contains a resistor which represents the battery over-voltage resistance and the second parallel branch contains a capacitor which represents the

capacitance between the electrolyte and the electrodes. None of these parameters are dynamic parameters and therefore this model is also limited in its dynamic accuracy as it does not take the SoC of the battery into account [20, 21]. This model can be used effectively for applications which do not need to consider the dynamic SoC.

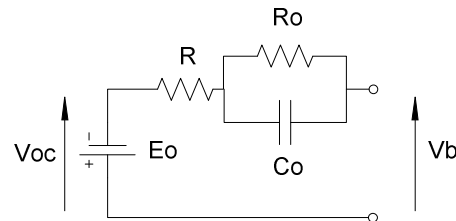


Figure 2.8: Thevenin Battery Model Circuit

Non - Linear Dynamic Battery Model

To improve accuracy on the Thevenin Battery Model established above, the non-linear dynamic battery model is introduced as shown in Figure 2.9. This model uses a capacitor, C_b , to represent the charge of the battery and a shunt resistor, R_p , to represent its self-discharge. Two parallel branches are connected to the circuit, each containing a resistor, R_{id} and R_{ic} respectively, and a diode, each diode facing the opposite direction. This is to enable different resistances to be used to model the charging and discharging behaviour of the internal resistance of the battery. Following this, 3 parallel branches are connected to the circuit. Similar to the Thevenin battery model, the first branch contains a capacitor, C_o , which represents the static charge between the electrolyte and the electrodes. The second and third parallel branches contain resistors, R_{do} and R_{co} respectively, and a diode, each facing opposite directions. These resistors, R_{co} and R_{do} represent the over-potential resistance and the under-voltage resistance respectively during charging and discharging. This model represents the SoC of the battery as well as the internal resistance and therefore provides high modelling accuracy. As all these components change with the SoC of the battery, it is complicated to derive equations for each parameter and tests must be carried out on the battery to validate the model [19,20]. This model can be used for modelling systems dynamically, to assess at each point what the battery voltage is and what current can be fed into the system. This allows the system to be optimised in terms of its sizing to ensure that the load will always be met by the energy supply with the battery as the energy supply backup for the generation system.

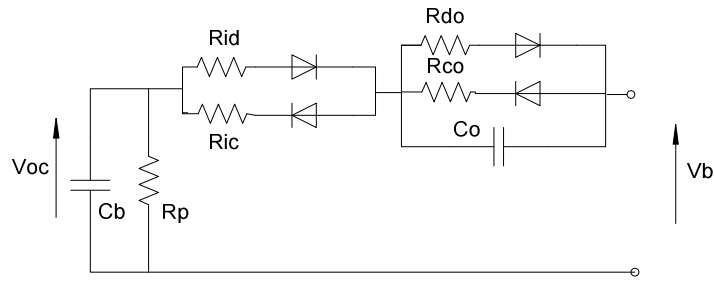


Figure 2.9: Non-linear Battery Model

An improvement on this model is suggested by Jantharamin et.al. [14] where the battery EMF is modelled as a voltage source, E_o , dependant on the SoC of the battery. The self-discharge is still represented by the shunt resistor, R_p , shown across the voltage source in Figure 4. Three parallel branches are connected to the circuit, with the first branch containing the capacitor, C_o , representing the static charge between the electrolyte and the electrodes. The second and third branches contain resistors and diodes, R_d , representing the entire resistance of the battery as it is discharging, and R_c representing the entire resistance of the battery as it is charging. The diodes control the direction of the flow of current. All of these parameters can be determined by fitting the curves with the curves supplied by the battery manufacturers. A charging test will only need to be done to determine the charging resistance. This does suggest an easier but accurate way to model the battery circuit.

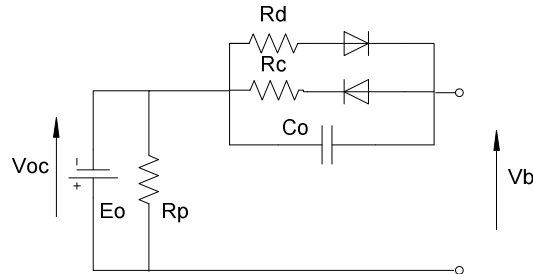


Figure 2.10: Improved Non-linear Battery Model

For the context of the HRES, it is therefore crucial that the model used incorporates the State of Charge (SoC) of the battery. The SoC of the battery shows the state of the battery at any point of its lifetime and allows more accurate control of the system, thereby increasing the reliability of the system. The simple battery model and the Thevenin battery model would therefore be improper choices of types of models to be used in simulating the system as neither of them are dynamic models. The non-linear battery model and improved non-linear battery models would therefore both be better choices for dynamic modelling of the system.

2.6. System and Battery Controller

Batteries form a large part of the capital investment of hybrid RESs, and therefore it is important to preserve and extend the battery life where possible [20]. This means ensuring

that the battery always remains within the maximum and minimum boundaries of State of Charge (SoC) set out by the manufacturers; that the battery is not allowed to stay at a low SoC for long periods of time and that high frequency of partial charging and discharging is avoided. There are different techniques of controlling this and some of these will be discussed in this section.

2.6.1. High level supervisory control

Torres-Hernández et al [21] use high level control using a supervisory controller in a wind and PV hybrid generation system. The supervisory control consists of 5 modes. In Modes 1 and 2, the PV and wind systems generate enough energy to supply the load as well as charge the battery. In Mode 3, PV and wind supply at their maximum capability and the battery supplies stored energy to meet the load. In Modes 4 and 5, the load is greater than what the PV, wind and battery can supply and the supervisory control connects to the grid to enable the necessary load to be met. In Modes 1, 2, and 3 sliding mode control is used to ensure that the supply meets the load. This is done by monitoring the power needed by the load and the power of the power generating mechanism and controlling the DC output using a DC-DC convertor to match them. This control is very effective as constraints can be added into the system as needed and each mode can be controlled separately; for example, in Mode 3, the battery is only used until it reaches the minimum allowed SoC. At this point, the system transitions to another mode.

Another use of sliding mode control and high level supervisory control is presented by Valenciaga et al [20] in a PV-wind hybrid system with battery storage. This system operates using 3 modes. Wind is chosen as the primary energy generation mechanism and therefore mode 1 is used when solely the wind power generated is sufficient to power the system. This power is regulated using sliding mode control as described above. In mode 2, increased energy is required by the load, so the wind power is generated at its maximum and solar energy generation then tracks the load power using sliding mode control. In both mode 1 and 2, the battery is recharged and therefore adds to the load on the system. In mode 3, further energy is required and the battery is utilised along with the wind and PV power generated to supply the load.

2.6.2. Directional Convertor control

Hasan et al [22] use a high efficiency bidirectional convertor system with high gain buck-boost operations and a battery charger controller. The battery charger controller monitors the DC bus power and the SoC of the battery and depending on the monitored values puts the battery in charge, discharge or halt mode as shown in figure 2.11.

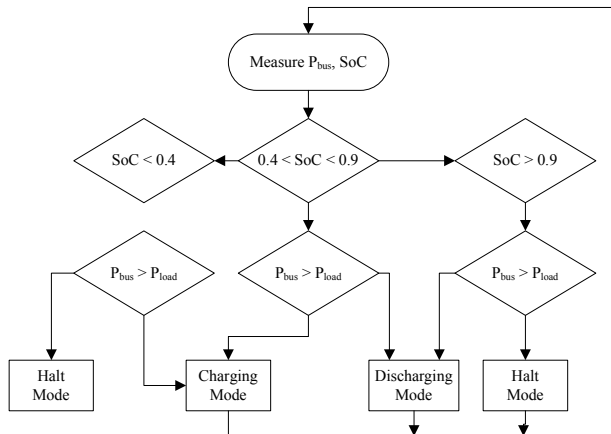


Figure 2.11: Bi-directional Converter Control Algorithm [22]

Qiang et al [23] use a four directional converter system within a hybrid wind-PV system with battery storage. The four directional DC-DC converter is a four winding transformer which has two input stages, connected respectively to the wind generation system and the PV generation system and two output stages, connected to the load and battery storage respectively. This system also functions using modes in which the 4-directional converter becomes a 2, 3 or 4 port converter dependant on which inputs and outputs are in use.

2.6.3. Battery Management Control System

Kaiser et al [24] have developed a system using parallel strings of batteries which are each switchable in or out of the circuit. Each string is monitored in terms of its SoC and State of Health (SoH). A DC-DC converter is connected to the DC bus and each string via a switch to be used for intensive full charging. Each string is then monitored separately and only used within approved range of SoC. If the SoC reaches the minimum value, the battery string is detached from the load using a switch. In addition, the controller takes account of the age and stability of each battery string and does an intensive full charge of each battery string every 14 days using the DC-DC converter for higher and more constant charging currents. The SoH and ageing characteristic of each battery string is determined by a capacity test which is done every 6 months.

Each of these methods has advantages and disadvantages and the nature of the system in which it is to be implemented is a very crucial part of the decision process. A Battery Management Control system or high level supervisory control system would be very useful within a complex system, but would possibly become overcomplicated and uneconomical for a simpler system. Directional Converter control could be implemented very well in a smaller system. The amount of control and flexibility of the system to adjustment may also be a criterion when choosing which battery controller to use.

For use in the off-grid stand-alone RES being designed to be used in rural areas, an accurate battery controller which takes into account the health of the battery and

ensures the maximum possible battery life cycle is necessary. This is because when the system is placed in the rural area, there will be little support for the system. It is therefore important that the battery controller be intelligent so as to maximise the uptime of the system before maintenance is required.

2.7. System Sizing Optimisation

While designing a hybrid RES, the reliability of supply of the system must be kept in mind to ensure that the load will be met by the supply at all times. There are many different variations of hybrid power systems which will ensure that the system is reliable. However, economically the system must be optimised to ensure the lowest cost possible whilst maintaining the system integrity. A common parameter used to measure the system integrity and reliability is Loss of Power Supply Probability (LPSP). This is the probability that load will encounter an insufficient load supply [3]. LPSP must be monitored as the key constraint to ensure that in optimising the system, the likelihood of the system supply not being able to meet the load at all times is kept very low [25]. Cost of the system can be measured in different ways, but most commonly is measured by the total annualised cost of the system or the total cost of the system.

Annualised cost is made up of annual capital cost, annual maintenance and operation cost and annual replacement cost [26]. The total cost of the system is generally calculated over 20 years and therefore includes the capital cost of the system, the maintenance cost of the system over 20 years as well as the installation costs [5, 28].

Some techniques used for optimising renewable energy system in terms of LPSP and cost are as follows: Graphical Construction, Probabilistic Methods, Adaptive Neural Network and Genetic Algorithm Approaches [3]. These are outlined below.

2.7.1. Graphical Construction

Graphical construction is used to optimise in terms of two criteria. This is an accurate way of optimising the system; however, it restricts which parameters can be used [3]

Graphical construction techniques require time series chronological data for the systems involved. This enables the graph to be plotted using this information. For example in a Hybrid renewable power generation system, where wind power generation, solar generation and battery storage are used, one could only choose two parameters, such as the size of the battery storage and the size of the solar panels to be optimised in terms of one parameter, for this instance, probability of Loss of Load. This method would therefore not take into account other factors, such as how many wind turbines are included, the angles of the wind turbine blades, the height of the blades above ground, etc.

This is therefore useful for simple systems with few parameters, however if a more complex system is to be optimised, other techniques will prove more useful.

2.7.2. Probabilistic and Deterministic Techniques

Probabilistic techniques can be used in situations where actual hour by hour long-term data is not available and more general data needs to be used. This method then takes the data that is available and predicts future values, taking into account (in the case of a hybrid renewable energy system) the fluctuation of supply and load. The second method is less computationally intense and requires minimal time series data [3]. Roy et al. [28] uses an initially probabilistic approach to optimize a wind-battery hybrid system by creating a Probability Density Function (PDF) of the wind speed at the site. This is done by gathering information from the site and creating an empirical model of the wind turbine. Belfkira et al. [5] use statistical models of wind speed and irradiation values as inputs to optimize a wind, PV and battery system.

Both of these approaches then use a deterministic algorithm to optimize the system. This is done by initially creating a 'design space' of feasible solutions which adhere to the maximum LPSP. This design space is then optimized by minimizing an objective function in the space. The objective function in each case is a variation of the cost of the system. Belfkira et al. [5] use a DIRECT (DIviding RECTangles) algorithm approach to minimising where a vector of the input parameters such as number of wind turbines, size of PV panels, size of battery storage are input to minimise within the feasible area restricted by the power input and requirements. Further constraints can be added to this optimization process, such as to only use the battery within the recommended State of Charge (SoC) and to use the battery as little as possible. This appears to be an effective method of optimizing the system and is non-restrictive in terms of the constraints that can be used to optimize the system.

2.7.3. Artificial Neural Network

Artificial Neural Networks (ANNs) are methods of optimisation based on the biological principle of the nervous system. The network is made up of neurons which have an input and output and a black box between them. A weighting function related to the suitability of the neuron to the solution of the problem is attached to each neuron and at each level the neuron outputs are summed with respect to their outputs and weighting functions to produce an output for the level. This is a parallel processing approach. Different layers of the neurons can be placed in series if needed for higher accuracy.

ANNs are adaptive by nature and therefore need to be trained. Different topologies are used for different instances. As the main calculation occurs by the learning of the neural network, neural networks are appropriate for instances where there is limited data available. The available data can be used to train the neural network and then the neural network will use what it has learnt to calculate further values. Training occurs by initially giving the neuron different inputs and corresponding output data so that it can calculate the process in between [3].

2.7.4. Genetic Algorithm

Genetic Algorithm (GA) technique uses the biological principles of genetics, namely, crossover, recombination and mutation in the optimisation procedure. This occurs as the system solves values of entered parameters for certain conditions. Different solutions of the values of the set of parameters are grouped together to form a 'chromosome' and then these chromosomes are crossed over and recombined until the optimal solution is found. These different sets of optimal solutions are then recombined to create more optimal solutions. The selection of the chromosomes for cross-over and advancing to the next generation is generally controlled by a fitness factor. These fitness factors are assigned to the chromosomes based on the accuracy of the solution for the scenario.

GA is very useful for solving non-linear problems, in this case for situations where renewable energy system's supply fluctuates and the load fluctuates randomly [2].

A sample set of parameters that can be considered for optimizing a wind-PV-battery hybrid system is as follows: Number of wind turbines, height above ground of the blades, number of solar panels with a specified size, size of battery storage. The conditions that must be met are that the system LSLP must be minimised, that the battery SoC must never go below 40% and the cost must be minimised. Only those 'chromosomes' which then meet these conditions will be considered for the next generation of solutions [29].

Sharhirinia et al. [26] use a GA technique to optimize a PV, battery and wind hybrid renewable energy system. A roulette wheel selection method is used, where the size of the roulette wheel slot is proportional to the chromosome fitness factor. This enables the chromosomes most suited to the scenario to have a higher chance of advancing to the next generation and cross-over. Different irradiation values and average wind speeds were used to simulate different scenarios.

Ould Bilal et al. [30] shows a case study of an optimisation of a wind, PV and battery renewable energy system in Senegal. An optimisation using Genetic Algorithms to minimise the total cost of the system whilst maintaining a low LPSP is used with parameters of number of PV modules, power output of wind turbines, battery capacity and number of inverters and regulators.

Another example of optimizing a PV-wind-battery system is reported by Koutroulis et al. [27]. A flow chart of the optimization process is shown in figure 2.12 [27]. A roulette method of selection based on the chromosome fitness factor is used in this optimisation. The flow chart shown in figure 2.12 is repeated until a predefined number of generations have been completed and the system is then considered optimised. The constraints evaluation and chromosome repair after each step consists of testing each resulting chromosome to ensure that they still comply to the restrictions in terms of LPSP. If they do not, chromosome repair occurs by replacing the chromosome with its parent.

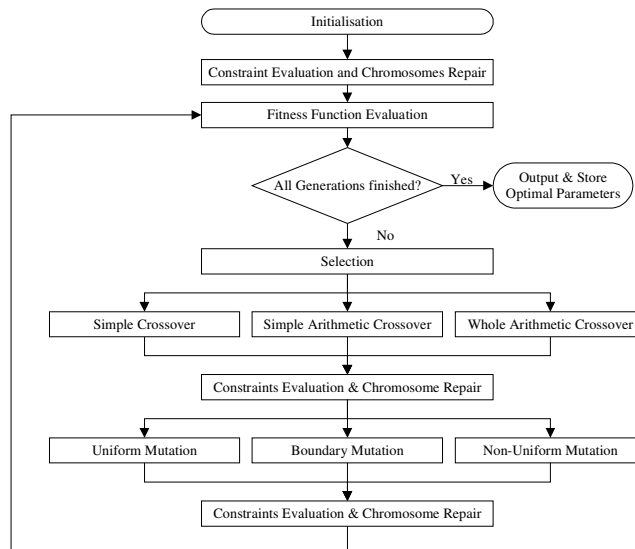


Figure 2.12: GA Optimisation Flowchart [27]

In the case where the chromosome resulted from cross over, the chromosome is replaced by the parent with the highest fitness factor. Genetic algorithms are seen to have a lot of success in these optimisation problems and their use is increasing in related areas.

Comparing the different methods, we see that graphical construction is a good way to achieve accurate results, but requires a lot of data which is not always readily available. Probabilistic techniques are more feasible for reasons that they need less input data, but however are then less accurate. In terms of this thesis, genetic algorithms and neural networks are the favoured method of optimising the system. This is because of their high accuracy and ability to be used with varying amounts of data. Genetic algorithms have finally been selected as the method of optimisation for this project and will therefore be discussed in more detail in the following sections.

2.8. Genetic Algorithms

As discussed there are various methods of optimisation of problems, searching for the best solution to a problem, whilst looking at a single variable to optimise or looking at many variables to optimise. Genetic algorithm is a type of minimum seeking optimisation which mimics the behaviour of chromosome genetics and survival of the fittest in biology.

This is done by creating a number, or population, of ‘chromosomes’, which represent possible solutions to the problem to be optimised. These ‘chromosomes’ are then measured against some criteria, and the specified percentage of those that match the criteria the best are kept, while those that match the criteria least are discarded. This is in keeping with the biological principles of natural selection. The kept chromosomes are then sorted and some chosen to ‘crossover’ with other chromosomes. This can be done in a number of ways, but the outcome is that the two chromosomes are combined to form new chromosomes. The population are then crossed over in this way to make up the population size to replace those that were discarded. Another important biological aspect of genetics which is used in genetic

algorithms is mutation. In genetic algorithms, a percentage of the population will undergo mutation which can also happen in a variety of ways which will be discussed, but essentially where a random section of a chromosome is changed or mutated to give a different chromosome. This introduces some change especially when the parent chromosomes are all very similar. The process of crossover and mutation is then reiterated until either the specified number of population generations has been reached or until some other stopping criterion is reached.

Genetic algorithms have the advantage of being able to solve discrete or continuous problems, because of the fact that there is a population of solutions, of being able to look at a wide variation of solutions at the same time and therefore is more able to find a global optimum solution rather than get stuck in a local optimum, of not being restricted in the number of variables it uses and of being able to handle very tricky objective functions with ease, amongst other advantages. Whilst in some simpler cases, it may not be the best or quickest method of finding a solution, when it comes to complex problems with many constraints as many variables, such as the problem that is presented in this project, it is a very effective way of tackling a problem.

Matlab has an optimisation toolbox which can be used for genetic algorithms, however it does not account for all situations and can therefore be adapted to the needs of the user. The remainder of this section will deal with the different elements of genetic algorithms, as seen in figure 2.13, how they are used in this thesis and how they are approached in Matlab.

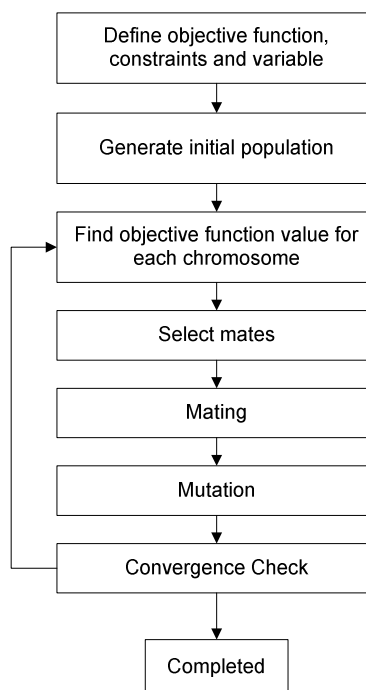


Figure 2.13: Genetic Algorithm Flowchart

2.8.1. Generate Initial Population

As mentioned previously, genetic algorithms use a population of chromosomes to find the solution to the problem. A chromosome in this type of problem is made up of the variables that need to be optimised. For this project, the variables that need to be used

to optimise the objective function are the number of PV panels, N_{pv} , the number of wind turbines, N_{wt} , the height of the wind turbine tower, h , and the number of batteries, N_b . The chromosome can therefore be represented as in figure 2.14 below.

N_{pv}	N_{wt}	h	N_b
----------	----------	-----	-------

Figure 2.14: Representation of Chromosome for Hybrid Power System

The user determines the size of the population and the initial population is generated randomly. This can be represented in a matrix sized by the number of variables x the size of the population. Generally all the chromosomes are created and normalised to be real numbers between 0 and 1 unless stipulated by lower and upper bounds. This is represented by the equation 1 as follows.

$$v = (v_h - v_l).v_{norm} + v_l \quad (2.14)$$

Where v_h is the upper bound of the variable, v_l is the lower bound of the variable and v_{norm} is the normalised variable between 0 and 1.

As the current problem requires the variables to be integers, the output value of v for each variable must be rounded to the nearest integer.

2.8.2. Natural Selection

Once the initial population has been generated and the objective function calculated with each chromosome's values, the chromosomes which give the minimum values of the objective function need to be kept as part of the population and those that give the highest value for the objective function need to be discarded from the population. This is done by one of two ways.

The first is by sorting the chromosomes and ranking them from lowest objective function value to highest objective function value. The user must then specify what percentage of chromosomes is kept from each population. If for example 50% is selected, once the chromosomes are sorted according to their objective function values, those chromosomes that fall into the half which have the higher objective function values will be discarded and the rest will go on to the next generation as well as be parents of the chromosomes created to replenish the amount of chromosomes in the population.

The second is by setting a threshold for the objective function and any chromosomes whose objective function value falls above the set threshold is discarded and any that fall below the threshold are kept and move forward to the next generation. In this way the population does not need to be ranked, however, there is no control as to how many chromosomes go forward from one generation to the next generation.

2.8.3. Select Mates

The chromosomes which are not discarded become part of the next generation of chromosomes and may become parents of the chromosomes which will make up the

remainder of the population size. The pairing of chromosomes for mating can be done in many different ways, some of which are discussed here.

The first is the simplest method and takes the chromosomes from the top of the ranking and works down to those at the bottom, pairing them two by two. In this pairing method, the chromosome at the top of the ranking would be paired with that which is second in the ranking, the third with the fourth and so on until the number of chromosomes needed to make up the population size have been created.

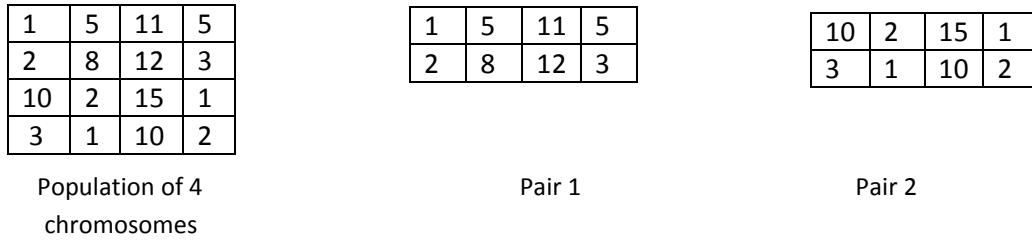


Figure 2.15: Example of Ranking Selection of Chromosomes to be Paired

The second method is random pairing where an array of random numbers representing chromosome A is generated and an array of random numbers representing chromosome B is generated and multiplied by the number of chromosomes that are being kept for the following generation and that is then rounded to the nearest integer to give the index of the chromosome As to be mated with chromosome Bs.

The third method is Rank Weighted Random pairing. This method looks at the chromosomes according to the ranking of objective function values and assigns each a probability of being chosen as a parent according to its ranking. Those chromosomes with the best objective function values have the smallest probability of being chosen as parents whilst those with the worst objective function values in the population which are being kept for the next generation have the highest probability of becoming parents. This method is also referred to as the roulette wheel method of selection. The probability assigned to each chromosome is calculated as in equation 2.15.

$$P_n = \frac{N_{keep} - n + 1}{\sum_1^{N_{keep}} n} \quad (2.15)$$

Where n is the rank of the chromosome and N_{keep} is the number of chromosomes which are kept for the next generation.

The fourth and last method to be discussed is tournament selection pairing. This method takes a subset of the chromosomes to be kept and automatically selects the best ranking chromosome in the subset as a parent and then repeats this, choosing new subsets and new parents until the number of parents needed is reached.

2.8.4. Mating

Once the parents have been selected and paired, mating occurs. This is done by combining parts of chromosome A with chromosome B, creating a chromosome with a different chromosome make up to both the mother and father chromosome. This can be done in many different ways; two of the main ways which will be discussed as follows are crossover and blending.

Crossover can occur at one or more points of the chromosome to create the offspring chromosomes. Crossover implies that a point(s) in the chromosome is selected and everything before that point would be from chromosome A and everything after would be from chromosome B. Figure 2.16 illustrates this with a single crossover point after variable 1 and a 2 point crossover after variable 1 and 3.

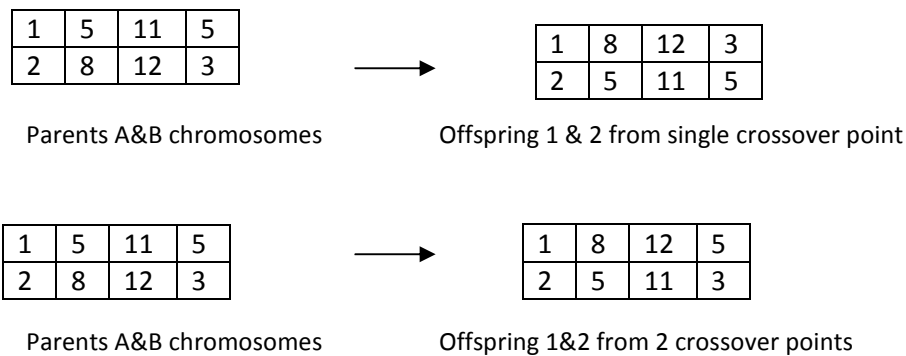


Figure 2.16: Single and 2-Point Crossover Mating

While crossover does create a new chromosome from chromosome A and chromosome B, it does not introduce new solutions into the algorithm. When using crossover mating, one is relying completely on mutation to ensure new solutions are added to the algorithm.

The second manner of mating the chromosomes combines chromosome A and B whilst also introducing new values into the algorithm. The blending method uses the value of chromosome A and the value of chromosome B to create a new chromosome as shown in equation 2.16. A second chromosome can be formed from the complement of equation 2.16 as shown in equation 2.17.

$$v_{new1} = \beta v_{an} + (1 - \beta)v_{bn} \tag{2.16}$$

$$v_{new2} = (1 - \beta)v_{an} + \beta v_{bn} \tag{2.17}$$

Where β is a random number between 0 and 1, v_{an} is the nth variable in chromosome A and v_{bn} is the nth variable in chromosome B.

Blending can be used on each variable when mating the chromosomes, or can be used on one variable or any number in between. Blending can also be used in conjunction with crossover, where blending occurs to the variable which fall to the right of the

crossover point or some combination as such. If using blending in the current problem, it must be ensured that the resulting variable value is an integer and therefore the value should be rounded before the next step commences. Blending effectively introduces new solutions to the algorithm through mating.

2.8.5. Mutation

In some cases, using the above methods of selection and mating lead to a quick convergence to a minimum value. If this convergence happens too quickly, it is possible that the system may converge to a local minimum rather than a global minimum. To avoid this and to introduce new solutions to the algorithm, mutation occurs. This occurs by selecting a percentage of chromosomes in the population and purposefully changing one or more variables to introduce new solutions into the algorithm. If, for example 20% of the population is selected as the percentage to undergo mutation, the system will make $0.2 \times N_{pop}$ mutations. The variables to be mutated are selected using randomly generated numbers to point to the index of the variable. This variable is then replaced by a random number within the bounds of the system constraints. New solutions are thereby introduced to the algorithm.

Once mutation has occurred, the new generation of chromosomes is complete and can again begin the cycle of computing the objective function value, selection, sorting, mating and mutation. This will continue until the genetic algorithm reaches the number of generations listed as the number of generations wished to be achieved or another stopping condition such as convergence of the objective function to a specific value. Other stopping criteria can be stipulated based on various tolerances and lack of change in the chromosome over a number of generations. [31]

The methods of modelling and the methods of optimisation included in this chapter are included for the sake of fullness of background to the task set out for this thesis. From these methods discussed, the actual method of optimisation and modelling are outlined in the following chapter. There is a vast amount of material written on this subject and therefore only the relevant and most popular methods have been discussed here.

3. Methodology

3.1. Introduction

The aim of this thesis is to accurately size a hybrid renewable energy system for stand-alone use in rural areas, by sizing the system for the smallest cost, whilst maintaining a specified level of system integrity, by keeping the LPSP lower than 0.1. This chapter outlines the methods used to size these systems as well as the methods used to check the results of the aforementioned optimisation problem.

After the optimisation and checking methods were developed, 3 areas were selected as case studies and the climatic data and load data of each village was collected and is used in these calculations. The areas chosen are Antioch, Garagapola and Gasese. More on each of these areas will be discussed in the case study chapters 4,5 and 6 that follow.

3.2. Climatic Data Set

As the load profile for a residential area has peaks and valleys and therefore the load is not constant for a daily period, it is better to not work with a daily average value for the load and rather better to work with a matching climatic data set. In addition to the fluctuating load values, the solar and wind profiles are also fluctuating, therefore to ensure the power match between the load and the supply, it was decided to use hourly climatic values.

For power calculations for the PV panels, the hourly solar irradiance as well as the hourly temperature is required. For the wind turbines, the hourly wind speed is required for power calculations.

Wind speed and temperature data for the areas was provided by Enerweb using SAWB raw data. Solar irradiance data was gathered from Helioclim using the data available from SoDa Services. [32]

3.3. Load Data Set

As discussed, hourly load data is required to ensure that the outcome of the optimisation is accurate and the system sizing suggested accounts for the fluctuations of both supply and load. Hourly data for each of the three sites was obtained from the National Load Research Program through UCT.

For the purposes of growth in the communities and the power being used, an additional 5% of the load was added onto the amount used for the optimisation process.

3.4. Optimisation objectives and overview

For a hybrid system where PV arrays, wind turbines and batteries are supplying a load in an isolated area where no grid connection is possible it is important to optimise the system to ensure that the load is met by the supply as much as possible. This criterion is referred to as the Loss of Power Supply Probability (LPSP). In an ideal system where the load is always met

by the supply, LPSP = 0 and in a system where the load is never met, LPSP = 1. In this optimisation, we optimise the number of PV panels, wind turbines and batteries as well as the height of the wind turbines to ensure that LSLP is less than a specified limitation.

As renewable energy systems are fairly costly, it is also of importance to optimise the system for the least total cost possible. This total cost includes the initial capital cost, the annual operating cost and the maintenance costs of the system over a period of time. This is then the second criterion for optimisation.

The factors affecting the cost and LPSP which can be changed are the number of PV panels used, the number of wind turbines used, the height of the wind turbine and the number of batteries used. These make up the variables to be optimised in this simulation.

The PV panels, wind turbines and batteries need to be examined as to how to be represented in this optimisation in terms of the power that they generate and the cost that they add to the systems. This follows this section.

3.1.1. PV Panels

Some methods of calculating the power produced by a PV panel are presented in the previous chapter. A few more are presented here for completeness and the method used in the simulation is shown.

Method 1

Xu et al [3] use an analytical model to define the current voltage relationship using the PV panel electrical characteristics. Values for panel temperature and the irradiance on the panel are needed as inputs to this model as well as the PV panel electrical characteristics.

Equation 3.1, 3.2 and 3.3 below outline the method presented. It is assumed that the system has a MPPT controller for the PV panel. Equation 3.1 calculates the maximum power generated by the PV panel.

$$P_{mp} = V_{mp} \cdot I_{mp} \quad (3.1)$$

Where V_{mp} and I_{mp} are the PV panel voltage and current at the maximum power point taking into account the temperature and irradiance effects on the panel.

V_{mp} is calculated as per equation 3.2 below and I_{mp} as in equation 3.3.

$$V_{mp} = V_{mpn} + K_V(T - T_n) \quad (3.2)$$

Where V_{mpn} is the maximum power point voltage at STC, K_V is the temperature coefficient for open circuit voltage, T is the panel operating temperature and T_n is the STC temperature.

$$I_{mp} = I_{mpn} + I_{sc} \left(\frac{G}{G_n} \right) + K_I(T - T_n) \quad (3.3)$$

Where I_{mpn} is the maximum power point current at STC, I_{sc} is the panel short circuit current, G is the irradiance, G_n is the irradiance at STC, K_I is the temperature coefficient for short circuit current, T is the panel operating temperature and T_n is the STC temperature [33].

Method 2

Koutroulis [27] present the following method of calculating the power of the PV panels at the specified temperature and irradiance:

$$P_{mp} = N_s \cdot N_p \cdot V_{oci} \cdot I_{sci} \cdot FF \quad (3.4)$$

Where N_s is the number of series PV panels connected in the system, N_p is the number of parallel panels connected to the system, V_{oci} is the open circuit voltage at the specified temperature and irradiance, and is calculated in equation 3.6, I_{sci} is the short circuit current at the specified temperature and irradiance, and is calculated in equation 3.5, and FF is the fill factor of the panel.

$$I_{sci} = [I_{sc} + K_I(T_c - T_n)] \cdot \frac{G}{G_n} \quad (3.5)$$

Where I_{sc} is the short circuit current at STC, K_I is the temperature coefficient for short circuit current, T_c is the calculated temperature, T_n is the STC temperature, G is the irradiance and G_n is the irradiance at STC.

$$V_{oci} = V_{oc} - K_V \cdot T_c \quad (3.6)$$

Where V_{oc} is the open circuit voltage at STC, K_V is the temperature coefficient for open circuit voltage and T_c is the calculated temperature, as calculated in equation 3.7.

$$T_c = T + \frac{NCOT-20}{800} \cdot G \quad (3.7)$$

Where T is the PV panel operating temperature, $NCOT$ is the Nominal Cell Operating Temperature as specified by the manufacturer and G is the irradiance [27].

Method 3

The last method of calculating the PV panel power presented here is from Yang et al [36]. Two sets of temperature and irradiance data as well as the corresponding open circuit voltage and short circuit current are needed for this form of power calculation.

$$P_{module} = \frac{\frac{V_{oc} \cdot q}{n_{MPP} \cdot K \cdot T} \cdot \ln\left(\frac{V_{oc} \cdot q}{n_{MPP} \cdot K \cdot T} + 0.72\right)}{1 + \frac{V_{oc} \cdot q}{n_{MPP} \cdot K \cdot T}} \cdot \left(1 - \frac{R_s \cdot I_{sc}}{V_{oc}}\right) \cdot I_{sc0} \left(\frac{G}{G_0}\right)^\alpha \cdot \frac{V_{oc0}}{1 + \beta \ln \frac{G_0}{G}} \cdot \left(\frac{T_0}{T}\right)^\gamma \quad (3.8)$$

Where T, G, V_{oc} and I_{sc} are the temperature, irradiance, open circuit voltage and short circuit current for one set of temperature and irradiance values and

T_0, G_0, V_{oc0} and I_{sc0} are the data for the second set of temperature and irradiance values. q is the electric charge constant, n_{MPP} is the ideality factor between 1 and 2 of the maximum power point, K is the Boltzmann constant, R_s is the series resistor value in the single diode equivalent circuit model, α is the photodiode non-linear effect factor, β is a module technology coefficient and γ is the nonlinear temperature-voltage effect factor.

The power of the PV array is then calculated as:

$$P_{PV} = N_s \cdot N_p \cdot P_{module} \cdot n_{MPPT} \cdot n_{oth} \quad (3.9)$$

Where N_s and N_p are the number of PV modules in series and parallel, n_{MPPT} is used to represent the efficiency of the maximum power point tracking and n_{oth} is used to represent any other losses in the system.

Each of these methods was implemented in Matlab using data from the Tenesol TE200 PV panel [34]. Method 3 was found to be most difficult to implement due to the number of factor and coefficient parameters which needed to be calculated and derived. It was found that method 2 gave the most consistent answers with those of the datasheet.

3.1.2. Wind turbine

It is agreed upon by Daming Xu et al [33], S.C.Gupta et al [12], Eftichios Koutroulis [27] and Hongxing Yang et al [36] that when approaching modelling the power output of wind turbines, it is best to use the power curve supplied by the manufacturers to calculate the power of the system. This is assuming that the wind turbine has a MPPT controller attached to it, ensuring that the system is as often as possible following the maximum power point of the wind turbine in the specified wind conditions.

As discussed in chapter 2, a piecewise spline function is used to represent the wind power as in equation 3.10.

$$P_W = \begin{cases} 0 & (v < v_{ci}) \\ a_1 v^2 + b_1 v + c_1 & (v_{ci} < v < v_1) \\ a_2 v^2 + b_2 v + c_2 & (v_1 < v < v_2) \\ a_3 v^2 + b_3 v + c_3 & (v_2 < v < v_{co}) \\ 0 & (v > v_{co}) \end{cases} \quad (3.10)$$

Where P_W is the wind power at the given wind speed, v is the wind speed, v_{ci} is the wind cut in speed, v_1, v_2, v_3 are various point of wind speed on the wind speed/power profile where the gradient of the profile changes and v_{co} is the wind cut out speed for the wind turbine. a, b, c are various coefficients denoting the profile gradient and features to describe the various splines of the profile.

Using the piecewise spline function method on the Kestrel e400i, a 3kW DC-DC wind turbine [35] would give us values of 2 for v_{ci} as this is the cut in speed for the wind turbine, and values of roughly 6.5, 9.5 and 11.5 for v_1, v_2, v_3 where the gradient of

the profile changes significantly. We can then use these values to calculate the values of the power generated by the wind turbine.

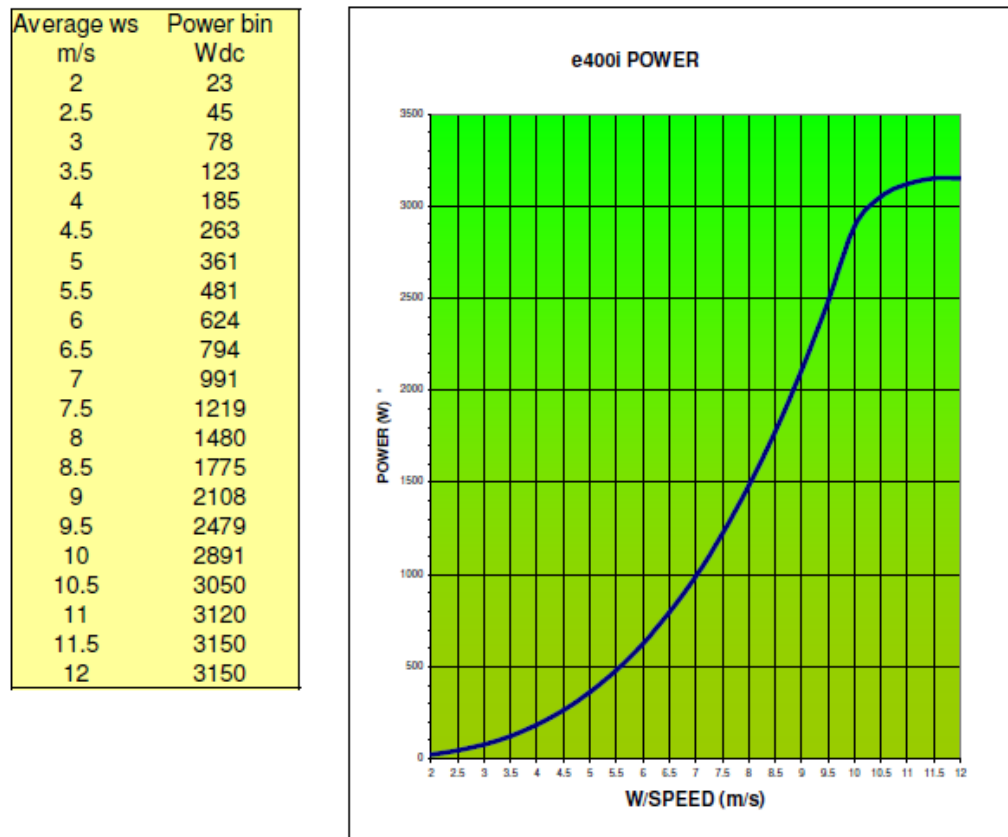


Figure 3.1: Wind Speed - Power Profile of Kestrel e400i with Datasheet Details [35]

However, Koutroulis [27] and Hongxing Yang [36] suggest the approach of creating a look up table using the wind speed/power profile and details supplied by the manufacturer as the data generally supplied by the manufacturer is usually substantial enough to do this and interpolate values without losing much accuracy in the system.

This is the approach that I've taken considering Matlab's vast ability to interpolate and store data efficiently. The following code was used to implement the initialisation of the look up table.

```

WSda = transpose([2:0.5:12]);
WPda =
[23;45;78;123;185;263;361;481;624;794;991;1219;1480;1775;2108;2
479;2891;3050;3120;3150;3150];
WSdai = 2:0.01:12;
WPdai = interp1(WSda,WPda,WSdai);

```

Where *WSda* and *WPda* represent the wind speed and wind power data supplied by the datasheet and *WSdai* and *WPdai* represent the interpolated data with values at every 0.01 interval.

The wind power can then be looked up by finding the value closest to the input of windspeed from the user and allocating the matching wind power value.

```
[diff,Row]= min(abs(WSdai-Wsi)); %returns the difference
between the actual wind value and closest reference on table
and the index position
Wp = nturbine*WPdai(Row); %matches power with index of
speed
```

The resulting interpolated generated wind speed/power profile generated by Matlab is as below in figure 3.2:

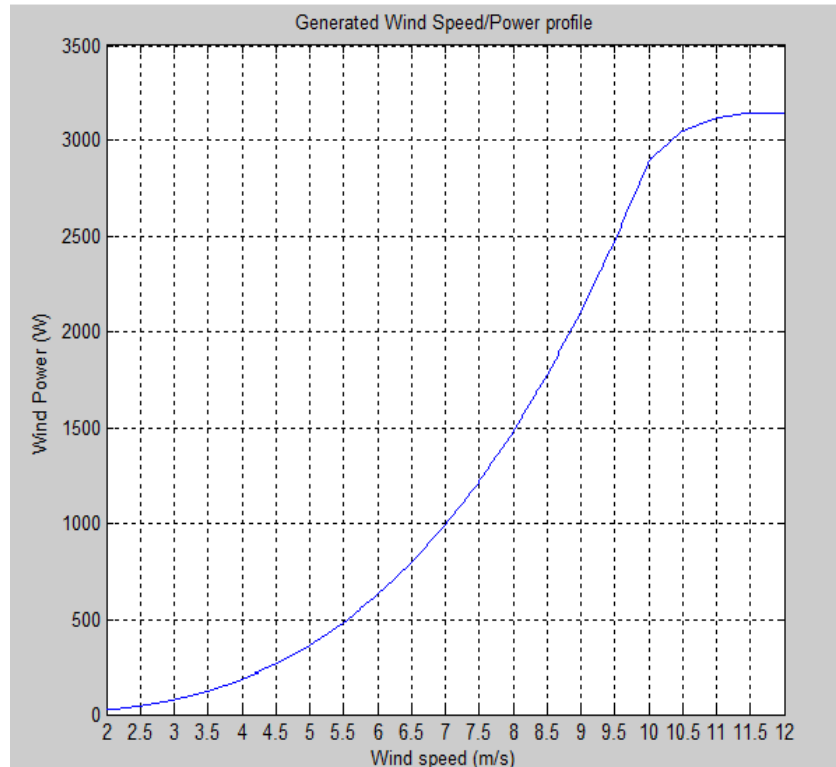


Figure 3.2: Generated Wind Speed-Power Profile of Kestrel e400i from Matlab

As wind speed measurements are not always taken at the same height as the proposed height of the wind turbine, the wind speed must be altered to ensure that the wind speed at the proposed height of the wind turbine is used rather than the wind speed at the height measured.

Equation 3.11 is used to calculate the wind speed at the appropriate height:

$$v = v_0 \cdot \left(\frac{h}{h_0}\right)^\alpha \quad (3.11)$$

Where v is the wind speed at the height of the wind turbine, h , and v_0 is the reference wind speed at the height of measurement, h_0 . α is the wind speed power law coefficient, which varies from $\frac{1}{4}$ to $\frac{1}{7}$, depending on the type of terrain at the site. For open land, $\frac{1}{7}$ is used as the standard factor [12].

3.1.3. Batteries

In the optimisation procedure batteries can either add to the load or supply the load depending on amount of energy generated by the other energy sources (PV panels and wind turbine). Whether the batteries act as supply or load is also dependant on the state of charge of the batteries. Battery manufacturers stipulate that discharging

the batteries below a specific State of Charge (SOC) is harmful for the number of cycles that the battery can complete and therefore the lifetime of the battery. This minimum SOC is called the Depth of Discharge (DOD). The battery can therefore supply power between full SOC and DOD.

The minimum battery capacity is therefore as shown in equation 3.12:

$$E_{Bmin} = (1 - DOD)E_{Bmax} \quad (3.12)$$

Where E_{Bmax} is the maximum battery capacity and DOD is the recommended depth of discharge of the battery [33].

There are various methods of incorporating the energy supplied and used by the battery into the model. Xu [33] uses the following equation to calculate the energy used when the battery is being charged:

$$E_{B(t)} = E_{B(t-1)} \cdot (1 - \sigma) + \left[E_{g(t)} - \frac{E_{l(t)}}{n_{inv}} \right] n_{bat} \quad (3.13)$$

Where $E_{B(t-1)}$ is the energy stored in the battery the previous hour, σ is the rate of self-discharge per hour of the batteries, $E_{g(t)}$ is the energy generated in that hour by the wind turbine and PV panels, $E_{l(t)}$ is the load that needs to be supplied, n_{inv} is the efficiency of the inverter (assuming that the load is AC) and n_{bat} is the round trip efficiency of the battery.

When the energy required by the load is greater than the energy generated by the PV panel and wind turbine, the energy supplied by the battery is calculated as follows in equation 3.14:

$$E_{B(t)} = E_{B(t-1)} \cdot (1 - \sigma) - \left[\frac{E_{l(t)}}{n_{inv}} - E_{g(t)} \right] \quad (3.14)$$

Koutroulis [27] calculates the capacity of the battery at a point in time, t , as follows in equation 3.15:

$$C(t) = C(t - 1) + n_{bat} \cdot \left(\frac{P_B(t)}{V_{BUS}} \right) \Delta t \quad (3.15)$$

Where $C(t - 1)$ is the battery capacity at the previous increment of time, n_{bat} is the battery round trip efficiency, $P_B(t)$ is the power supplied or used by the battery V_{BUS} is the voltage of the bus that the system is connectd to and Δt is the increment of time used, in this case, 1 hour.

$$P_B(t) = E_g(t) - E_l(t) \quad (3.16)$$

$P_B(t)$ is therefore negative when the energy generated by the other energy sources is not sufficient to supply the system and the battery supplies additional power to the system and the value is positive when the battery is charging [27].

The method used in equation 3.15 was decided to be the best method of calculation as this method takes into account the value of the DC bus and therefore the current that is being drawn from the battery. Using this method, a maximum amount of

current can be set to be drawn from the battery, to further ensure that that battery is never overdrawn and maintains a long expected life of the battery.

3.1.4. Calculating LPSP

Once the power generated or used by each of these sources is modelled, it possible to calculate the LPSP of the system. As previously stipulated, the LPSP is a measurable probability of the load being supplied. The load will be supplied when the energy generated plus the energy supplied by the battery is greater than the energy required by the load.

Xu [33] and Gupta [12] calculate the LPSP as shown in equation 3.17:

$$LPSP = \sum_{t=1}^T LPS_t / \sum_{t=1}^T E_{Lt} \quad (3.17)$$

Where E_{Lt} is the energy required by the load at time t,

$$LPS_t = E_{Lt} - (E_{gt} + E_{Bt-1} - E_{Bmin}) \cdot n_{inv} \quad (3.18)$$

Where E_{gt} is the energy generated by the PV panels and wind turbines at time t, E_{Bt-1} is the energy stored in the battery at time t-1, E_{Bmin} is the minimum capacity of the battery and n_{inv} is the efficiency of the inverter [12,33].

3.5. Objective function of cost of system

When working with genetic algorithms, there is the option of creating a multi-objective genetic algorithm or creating a single objective genetic algorithm. Creating a multi-objective genetic algorithm increases the complexity of the problem as well as the time taken to solve the problem. To avoid this, it is possible to choose a solitary objective function for the system and set other objectives as constraints of the system. In the problem presented in this project, it is quite simple to take this approach. The two possible objective functions would firstly be that of minimising the cost of the system and secondly minimising the LPSP. While cost is something that we want to minimise as much as possible, it is possible to make the LPSP a constraint of the system by stipulating that the LPSP must be lower than a specific value, for example $LPSP < 0.1$. In this manner we have simplified the problem to which we apply the genetic algorithm.

There are a variety of ways in which the cost of the system can be calculated. The first way that we encounter is that of the annualised cost of the system and the second method is that of using the total cost of the system. Each take into account the capital cost, operating cost and maintenance cost of the elements of the system, but the annualised cost looks at the cost per year and the total cost looks at the cost over a specified length of time, generally 20 years.

3.1.5. Annualised Cost of the System

Shahirinia et al [26] calculate the annualised cost by looking at the capital cost, replacement cost, operation and maintenance cost and fuel cost, in the case that a

diesel generator is part of the system. Each of these factors will contribute to how profitable the proposed plant is to be.

The total annualised cost of the system is defined as the annualised cost of each of the components of the hybrid system where the annualised cost of each component is the annual capital cost plus the annual replacement cost plus the annual operation and maintenance cost.

The objective function to be minimised in this case would be as shown in equation 3.19.

$$Cost = \sum_t C_{arepi} + C_{acapi} + C_{aomi} \quad (3.19)$$

Where i is each component of the system, in this case – wind, solar and battery and C_{arepi} is the annualised replacement cost of each component, C_{acapi} is the annualised capital cost of each component and C_{aomi} is the operating and maintenance cost of each component of the system [26].

The annualised capital cost of each component of the system is calculated as follows in equation 3.20.

$$C_{acap} = C_{cap} \cdot CRF(i, Y_{proj}) \quad (3.20)$$

Where C_{cap} is the capital cost of the component, CRF is the Capital Recovery Factor as calculated in equation 3.21 to show the present value of the component, i is the annual interest rate as calculated in equation 3.22 and Y_{proj} is the lifetime of the component.

$$CRF(i, Y_{proj}) = \frac{(i \cdot (1+i)^{Y_{proj}})}{(1+i)^{Y_{proj}-1}} \quad (3.21)$$

$$i = \frac{i' - f}{1 + f} \quad (3.22)$$

Where i' is the nominal interest rate and f is the annual inflation rate.

The annualised replacement cost is the annualised value of each component that needs to be replaced during the project lifetime. For the hybrid configuration studied of wind turbine, PV panels and batteries. Generally the battery is the component which needs to be replaced most often and if the project is viewed over a life time of 20 years, only the battery will need to be replaced. The annualised replacement cost is calculated as in equation 3.23.

$$C_{arep} = C_{rep} \cdot SFF(i, Y_{rep}) \quad (3.23)$$

Where C_{rep} is the cost of replacement for the component which needs to be replaced and SFF is the Sinking Fund Factor used to calculate the future value of

payments as shown in equation 3.24, i is the interest as calculated in equation 22 and Y_{rep} is the lifetime of the component.

$$SFF(i, Y_{proj}) = \frac{i}{(1+i)^{Y_{rep}-1}} \quad (3.24)$$

The annualised maintenance cost then takes the inflation rate into account for all maintenance costs which will be incurred in each year. This is calculated as in equation 3.25.

$$C_{amain}(n) = C_{amain}(1) \cdot (1 + f)^n \quad (3.25)$$

Where $C_{amain}(n)$ is the maintenance cost of the system for the n th year [36].

3.1.6. Total Cost of the System

Koutroulis et al [27] calculate the cost of the system using the total cost over the lifetime of the project. In most cases when calculating the total cost over the lifetime of a project, an estimate of 20 years is used. The objective function in this case would then be:

$$Cost = \sum_t C_c + C_m + C_r \quad (3.26)$$

Which is the total cost over 20 years.

The total cost for the system equation can therefore be expanded to show the different components of the system as shown in equation 3.27 for the inputs of N_{pv} , the number of pv panels used, N_{wt} , the number of wind turbines used, h , the height of the wind turbine tower and N_b , the number of batteries used in the system.

$$Cost(N_{pv}, N_{wt}, h, N_b) = N_{pv}(C_{cpv} + 20 \cdot C_{mpv}) + N_{wt}(C_{cwt} + 20 \cdot C_{mwt} + h \cdot C_{cwt} + 20 \cdot h \cdot C_{mwt}) + N_b(C_{cb} + y_b \cdot C_{cb} + (20 - y_b - 1) \cdot C_{mb}) \quad (3.27)$$

Where C_{cpv} is the capital cost of the PV panels, C_{mpv} is the yearly maintenance cost of the PV panels, C_{cwt} is the capital cost of the wind turbines, C_{mwt} is the yearly maintenance cost of the wind tubines, C_{cwt} is the capital cost per metre of the wind turbine tower, C_{mwt} is the maintenance cost per metre of the wind turbine tower, C_{cb} is the capital cost of the battery, y_b is the number of replacements that need to be made to the battery over the 20 years and C_{mb} is the maintenance cost of the battery [27].

3.1.7. Implemented Cost of the System

The simulations created as part of this project use the total cost of the system, using the capital cost, maintenance cost over the 20 year period and replacement cost of each component of the system to calculate the total cost of the system. Using this method allows different panel types or turbine types with varying costs to be easily substituted into the cost equation by only replacing the term associated with the component.

For the purpose of this project, the wind turbine selected was the Kestrel e400i [35]. The datasheet of this 3000kW wind turbine can be found in the appendix of this thesis. The price used for this simulation was gathered from a company called MLT drives, a company in Cape Town who supplies goods of this manner. The price was found on their pricelist on their website [37]. The price used for the wind turbine is R 68 147 for the turbine and R42 169 for a 15m high lattice tower. The price for the wind tower was adjusted for heights between 10m and 15m.

This wind turbine was selected as it is a locally produced wind turbine and therefore there is no problem with acquiring parts or maintenance and no importing fees. It has also been used in rural projects in the past and was found suitable for the application.

The solar panel selected is the Tenesol TE2000 – 200W [34]. This is a PV panel that is designed for many different applications, but among those, designed for rural electrification. It is therefore a good choice for solar panel. The technical specifications are available in the appendix of this thesis.

These panels are supplied by Sustainable.co.za, an online eco-store and are available for R5000 per panel [38].

The battery was selected as a 12V 200Ah battery, and was sourced from Battery Experts, model number, LA122000 [39]. The price for these batteries is R1873.

The maintenance cost on each of these items is chosen to be 1% of the capital cost for each year of operation. It is assumed that half of the batteries supplied for the HRES will have to be replaced in the 20 year lifetime.

Using the cost of the system as the objective function, there are still a number of constraints to which the system must adhere. As discussed, the LPSP then becomes a constraint of the system which can be expressed as in equation 3.28.

$$LPSP - 0.01 < 0 \quad (3.28)$$

This is expressed in the format in which non-linear constraints of genetic algorithms must be expressed, in that the constraint is less than zero, in this case the LPSP is actually less than 0.01, however because of the format, it has been expressed to be less than zero.

Other constraints that the system must adhere to are as follows in equation 3.29:

$$\left\{ \begin{array}{l} N_{pv} \geq 0 \\ N_{wt} \geq 0 \\ N_b \geq 0 \\ h_{min} \leq h \leq h_{max} \\ N_{pv}, N_{wt}, N_b, h \in \mathbf{Z} \end{array} \right. \quad (3.29)$$

Using the constraints shown in equation 3.29 above as well as in equation 3.28, the system is constrained accurately. Using the objective function of equation 3.26, the genetic algorithm can be set up to give the most cost effective solution whilst still satisfying all the constraints shown.

3.6. Setting up the genetic algorithm

The genetic algorithm optimisation toolbox in Matlab is designed for real numbers and therefore calculates the optimum real values for each value comprised in the chromosome. As the present problem looks at the number and height of 3kW wind turbines, the number of 200W PV panels and the number of 200Ah batteries used within the hybrid system to satisfy the load constraints whilst taking the climatic data into account, the required solutions to the genetic algorithm are integer values. To account for this, the genetic algorithm functions needs to be altered to only develop integer values.

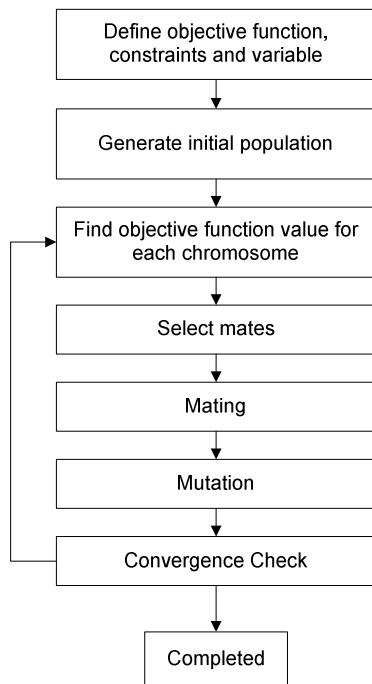


Figure 3.3: Simple Flowchart of Genetic Algorithm

Matlab allows one to use customised functions for generating the initial population, step 2 on the flowchart shown in figure 3.3, and mutation, step 6 on the flowchart, within the optimisation toolbox.

3.1.8. Generating Initial Population

A population of size 20 was selected for this optimisation. This is the standard size used for most optimisation problems. It was therefore deemed a satisfactory number of chromosomes to use.

The population was generated as in equation 3.30, which has been shown in the literature review as equation 2.16, using an upper limit, v_h , of 20000 for the number of

PV panels, wind turbines and batteries to avoid lengthening the procedure of optimisation by using values up to infinity in the chromosome variable generation. An upper bound of 15m was set for the height of the wind turbine, as this is the upper bound imposed by the manufacturer of the towers. The lower bound for the number of PV panels, wind turbines and batteries, v_l , was set to 1 to ensure a mix of energy sources was used. The lower bound for the wind turbine height was set to 10m, again as stipulated by the manufacturer.

$$v = (v_h - v_l).v_{norm} + v_l \quad (3.30)$$

To account for the use of integers instead of real numbers, the values were rounded.

3.1.9. Natural Selection

Ranking was selected as the method of sorting the chromosomes and therefore once the objective function of each chromosome has been calculated the chromosomes are ranked from lowest fitness function to highest fitness function in order to be selected for mating. This was chosen as it takes into account the best to worst objective functions rather than just sorting to a threshold as with threshold sorting. It is therefore more thorough and therefore preferred for this application.

3.1.10. Select Mates

Rank Weighted Random Pairing or the Roulette Selection method is chosen as the method of selection of mates as it makes use of the ranking which was used for natural selection. It is also the most popular method used for mate selection in genetic algorithms.

3.1.11. Mating

Scattered mating was chosen as the method for mating the chromosomes. This uses multiple point crossover at random points on the chromosome. As the chromosome only has four variables, using scattered crossover, helps to keep the children of the parents different as it adds a degree of randomness which is not available in single or two point crossover.

3.1.12. Mutation

Mutation is selected for $0.1 \times N_{pop}$. This means that in our population of 20, 2 chromosomes undergo mutation introducing new variables to the chromosomes. Again, it needs to be ensured that the variables introduced are integers and therefore the custom mutation function must include a round function to ensure that an integer variable is produced as an output.

Once the genetic algorithm has been set up as described here, it can be run with the various data from each of the areas chosen as case studies. The results of this are discussed in the following chapters.

3.7. Calculating LPSP for checking results

As an initial check for the result obtained from the genetic algorithm, the LPSP is again calculated. For this the climatic and load data of the area chosen and results from the

genetic algorithm are used. The results include the number of PV panels, wind turbines and batteries as well as the height of the wind turbine generated as the solution of the genetic algorithm.

As the set constraint of the genetic algorithm was a LPSP of 0.01, our preliminary check of calculating the LPSP should give an answer of less than 0.01 if the genetic algorithm is successful.

3.8. Controller and simulation for checking GA results

The second method of checking the genetic algorithm result is using a virtual controller and simulating the control of the system over the year period and monitoring the times of loss of supply, and the power supplied by the PV panels, wind turbines and battery in relation to the power required by the load.

A sliding control has been used for this, using wind energy generation as the primary source of energy, PV energy generation as the secondary source and battery as the supplement.

The system moves between different modes dependant on the power needed by the load and the power able to be supplied by each of the sources. Figure 3.4 outlines the flow between the different modes. This mode of control assumes that each energy source has a MPPT control system of its own.

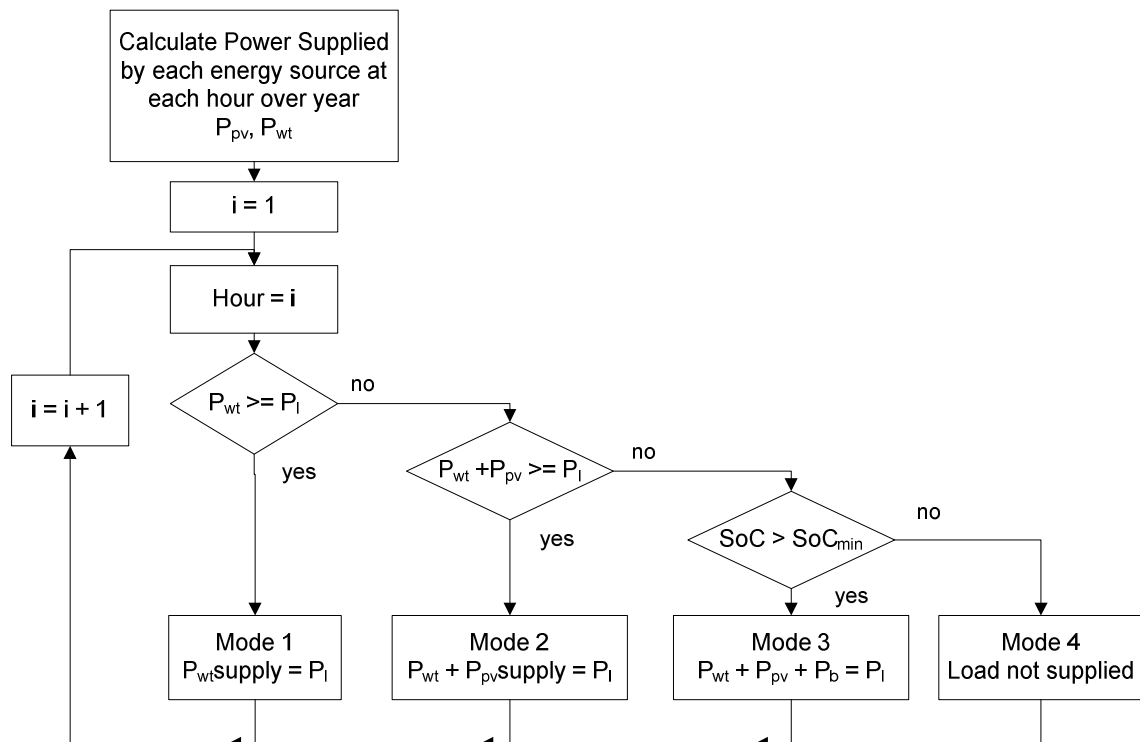


Figure 3.4: Flowchart of modes of control for HRES

Initially, the power supplied by the PV panels and the wind turbines is calculated for each hour over the year and stored in matrices, so that power availability in each hour can be accessed easily. The control process then begins at hour 1.

The first decision loop looks at the power that can be supplied by the wind turbine in this hour and the power required by the load. If the power generated by the wind turbine is sufficient to match the load, the system enters Mode 1.

If the wind turbine cannot provide sufficient energy for the load, the control looks at the total amount of energy that can be provided by the wind turbine and the PV panel together. If these together are sufficient to provide power for the load, the system enters Mode 2.

If the combined energy supplied by the wind turbines and the PV panels is not sufficient to supply the load, the state of charge of the battery is considered. If the battery SoC is not at its minimum value, the system enters Mode 3.

If the SoC of the battery is already at its minimum, the load is not able to be supplied and the system enters Mode 4.

3.1.13. Mode 1

Mode 1 uses solely the energy generated by the wind turbine to supply the load. When the system is in mode 1, sometimes the energy available from the wind turbine might be in excess of what is needed by the load and therefore the amount of energy supplied to the load must be matched to the load demand. This is called sliding control. As the PV panels are connected to the system, but not used to supply the load in this mode, the energy generated by the PV panels as well as any excess energy from the wind turbine can be used to charge the battery. Figure 3.5 outlines this process.

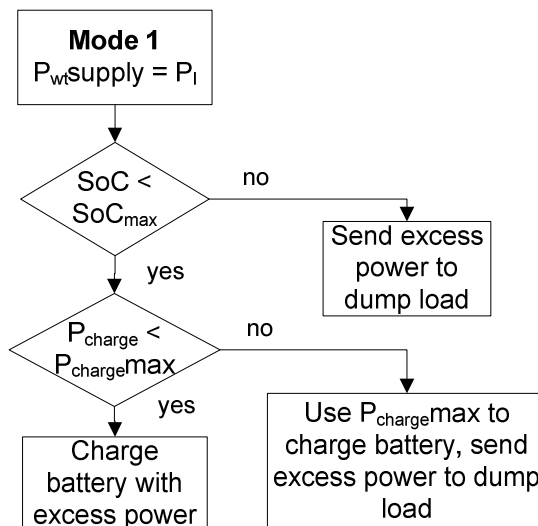


Figure 3.5: Mode 1 Flow Chart of Operation

If the SoC of the battery is at its maximum possible SoC value, the excess power is sent to a dump load, which can be defined according to the village's need, a water treatment facility, etc.

If the SoC of the battery is less than the maximum SoC, the amount of excess power is checked. The battery manufacturers advise not using a charging current of more than 60A. The power is then checked to make sure that the current used to charge the battery will be less than 60A. If the excess power is less than this maximum charging power, the battery is charged with the full excess power. If the power is above that of maximum charging for the battery, the maximum battery charge power is used to charge the battery and the excess is used for the dump load.

3.1.14. Mode 2

Mode 2 uses the power of the wind turbine plus the power of the PV panel to supply the load. In mode 2, if the energy available from the wind turbine and the PV panel combined is in excess of what is needed by the load, then the full power available from the wind turbine is used to supply the load and the power from the PV panel is supplied using sliding control to match the power required by the load. The excess energy from the wind turbine and the PV panels can be used to charge the battery, as in mode 1. Figure 3.6 shows this process.

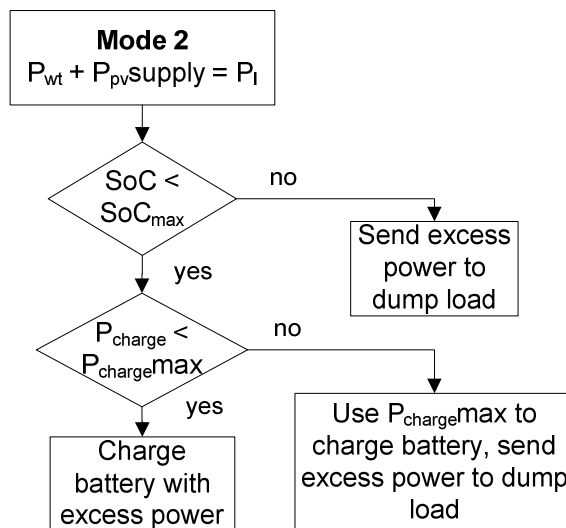


Figure 3.6: Mode 2 Flow Chart of Operation

The battery charging process is as described in mode 1.

3.1.15. Mode 3

The system enters mode 3 when the power generated by the wind turbine and PV panels is not sufficient to supply the load, but the SoC of the battery is greater than the minimum amount and therefore the battery is able to supply power to the load. The full power generated by the wind turbines and PV panels is supplied to the load. There is however a possibility that the amount of power required by the load is not able to be supplied by the battery. Figure 3.7 outlines this process.

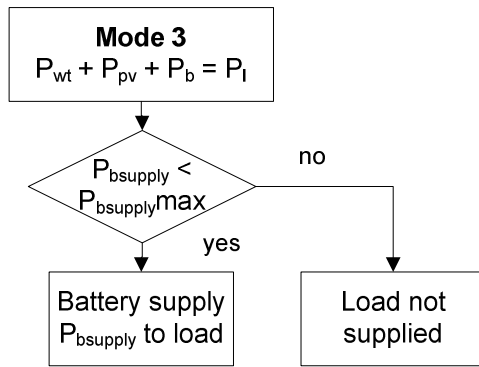


Figure 3.7: Mode 3 Flow Chart of Operation

Manufacturers specify that the batteries should not supply more than 80A current, and therefore the amount of power needed to be supplied by the batteries must be checked before it can supply that amount. If the load power needed to be supplied by the batteries is below this maximum, the battery then supplies the load power. Otherwise, load cannot be supplied.

3.1.16. Mode 4

When the system is in mode 4, the load cannot be supplied by the energy sources. The combined power of the wind turbine and the PV panels is not sufficient to supply the load and the battery is at its minimum SoC and therefore cannot be used to supply the deficit of power required.

From this control simulation we are able to see the performance of the system over the course of the year with the number of PV panels, wind turbines and batteries specified by the genetic algorithm. We will be able to see which modes the system spends most time in, the power supplied by each of the energy sources over the year, the power required by the load over the year and trend them against each other.

This is a very useful manner to check how the system is being supplied and which source of energy is the most proficient in supplying the load.

The climatic and load data for each of the selected areas is used to set up the genetic algorithm for optimisation. The genetic algorithm will then be run and the results will be used in testing the LPSP and the controller simulation to check whether the results match the criteria stipulated as well as to check the performance of the system in the different modes over the year of provided data.

4. Case Study 1: Garagapola

4.1. Introduction

Garagapola is an electrified village in Limpopo province, South Africa, situated at a latitude of -24.56° and a longitude of 30.16° . It is a good example of a rural village load and therefore a sample of 69 residential houses and loads has been used for the load data for this area.



Figure 4.1: Map showing Location of Garagapola [40]

Figure 4.1 above shows the location of the village on a map of Southern Africa and figure 4.2 below shows a closer satellite image of the area.

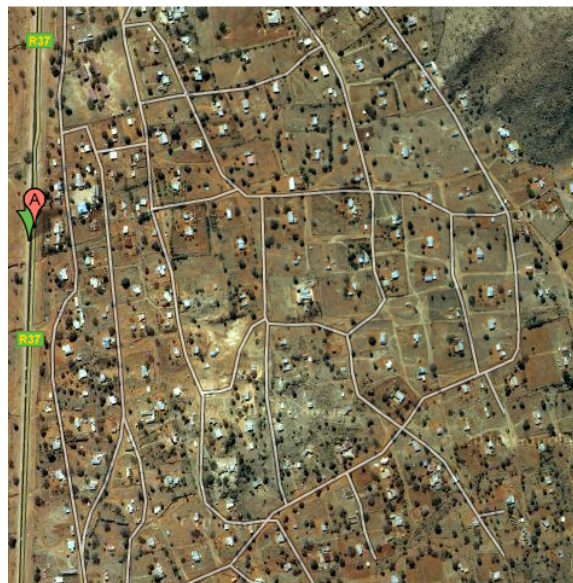


Figure 4.2: Satellite Image of Garagapola [40]

4.2. Climatic Data Set

As discussed in Chapter 3 of this thesis, the temperature and wind speed data is obtained from the South African Weather Bureau (SAWB), provided by Enerweb. The hourly temperature and wind speed data is obtained from the Pietersburg Weather Station situated at a latitude of -23.87° and a longitude of 29.45° in Polokwane.

The hourly solar irradiance data is provided by Helioclim through SoDa website [41]. The data is calculated from satellite pictures at the specified latitude and longitude required, in this case the co-ordinates of Garagapola.

Table 4.1: Average Monthly Climatic Data

	Temperature (°C)	Solar Irradiance (W/m ²)	Wind Speed (m/s)
January	22.16	307.56	3.27
February	21.45	315.88	3.17
March	21.23	259.69	3.09
April	19.25	207.49	2.89
May	15.42	196.35	3.03
June	12.09	171.78	2.63
July	12.35	180.32	2.27
August	15.59	218.62	3.35
September	16.88	266.05	3.43
October	20.163	292.57	3.90
November	20.50	295.01	4.03
December	22.18	299.23	3.75

While hourly data is used for the optimisation and checking algorithms, the average monthly values of the climatic data is presented in table 4.1 above. The trended temperature over the year is represented in the graph below in figure 4.3.

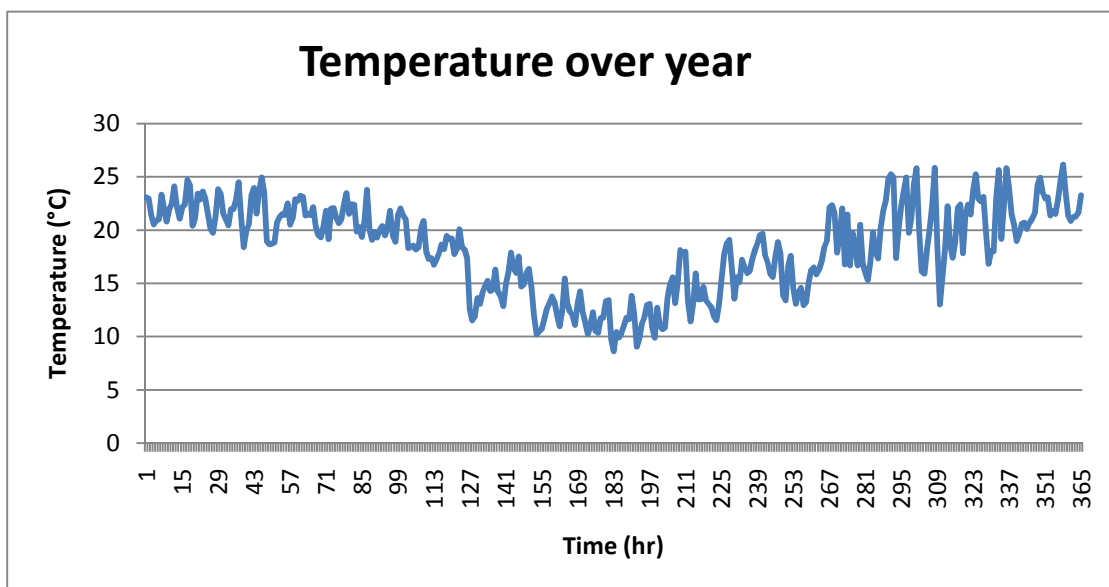


Figure 4.3: Garagapola Daily Average Temperature over Year

4.3. Load Data Set

The load data for 69 residential households in Garagapola is summed up to represent the hourly load profile for the entire village. The average monthly load values are shown in figure 4.4 and table 4.2 below. The load data is supplied by the National Load Research Program. This load data is used for the genetic algorithm after adding 5% onto them to allow for growth of load in the area.

Table 4.2: Monthly Average Load for Garagapola

	Load (W)
January	5021.97
February	8476.898
March	7934.379
April	8942.717
May	9784.03
June	10155.92
July	9732.388
August	9785.403
September	10381.79
October	10875.54
November	10815.64
December	10148.5

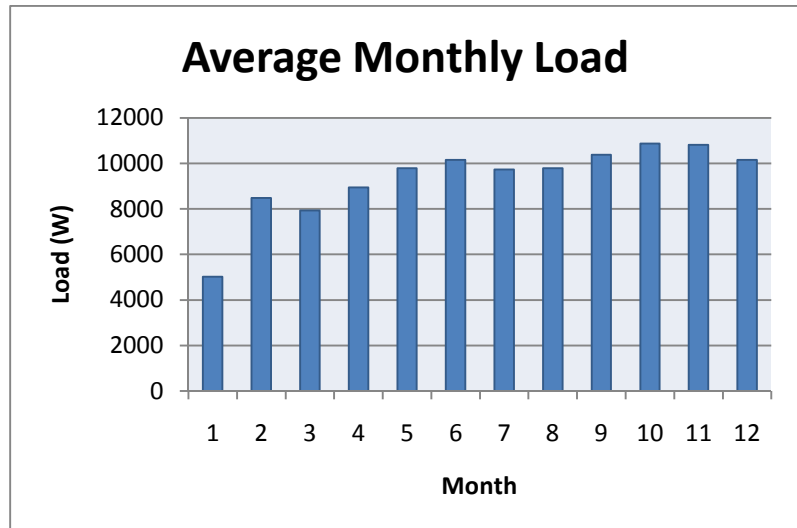


Figure 4.4: Histogram showing Average Monthly Load for Garagapola

4.4. Results of Optimisation

The genetic algorithm was run using the hourly values of climatic data and load data as specified above. The cost was minimised whilst keeping an LPSP of 1%. This means that the load will not be supplied a maximum of 1% of the year, this is 3.65 days of the year.

The resultant successive generations of populations of 20 in the genetic algorithm reduced the objective function cost as shown below in table 4.3:

Table 4.3: Genetic Optimisation Results per Generation

Generation	Max f(x)	Stall Generations	Generation	Max f(x)	Stall Generations
1	2.59987e+007	0	51	6.65578e+006	29
2	2.29087e+007	0	52	2.31243e+006	0
3	2.19766e+007	0	53	2.31243e+006	1
4	8.21218e+006	0	54	2.31243e+006	2
5	7.1799e+006	0	55	2.31243e+006	3
6	7.1799e+006	1	56	2.31243e+006	4
7	7.1799e+006	2	57	2.03043e+006	0
8	7.1799e+006	3	58	2.03043e+006	1
9	7.1799e+006	4	59	2.03043e+006	2
10	7.1799e+006	5	60	2.03043e+006	3
11	7.1799e+006	6	61	2.03043e+006	4

12	6.7959e+006	0	62	2.03043e+006	5
13	6.7959e+006	1	63	2.03043e+006	6
14	6.7959e+006	2	64	2.03043e+006	7
15	6.7959e+006	3	65	2.03043e+006	8
16	6.7959e+006	4	66	2.03043e+006	9
17	6.7959e+006	5	67	2.03043e+006	10
18	6.7959e+006	6	68	1.97324e+006	0
19	6.7959e+006	7	69	1.97324e+006	1
20	6.7959e+006	8	70	1.97324e+006	2
21	6.7959e+006	9	71	1.97324e+006	3
22	6.65578e+006	0	72	1.97324e+006	4
23	6.65578e+006	1	73	1.97324e+006	5
24	6.65578e+006	2	74	1.97324e+006	6
25	6.65578e+006	3	75	1.97324e+006	7
26	6.65578e+006	4	76	1.97324e+006	8
27	6.65578e+006	5	77	1.97324e+006	9
28	6.65578e+006	6	78	1.97324e+006	10
29	6.65578e+006	7	79	1.97324e+006	11
30	6.65578e+006	8	80	1.97324e+006	12
31	6.65578e+006	9	81	1.97324e+006	13
32	6.65578e+006	10	82	1.97324e+006	14
33	6.65578e+006	11	83	1.97324e+006	15
34	6.65578e+006	12	84	1.96124e+006	0
35	6.65578e+006	13	85	1.96124e+006	1
36	6.65578e+006	14	86	1.96124e+006	2
37	6.65578e+006	15	87	1.96124e+006	3
38	6.65578e+006	16	88	1.96124e+006	4
39	6.65578e+006	17	89	1.96124e+006	5
40	6.65578e+006	18	90	1.95267e+006	0
41	6.65578e+006	19	91	1.95267e+006	1
42	6.65578e+006	20	92	1.95267e+006	2
43	6.65578e+006	21	93	1.95267e+006	3
44	6.65578e+006	22	94	1.95267e+006	4
45	6.65578e+006	23	95	1.95267e+006	5
46	6.65578e+006	24	96	1.95267e+006	6
47	6.65578e+006	25	97	1.95267e+006	7
48	6.65578e+006	26	98	1.95267e+006	8
49	6.65578e+006	27	99	1.95267e+006	9
50	6.65578e+006	28	100	1.95267e+006	10

The genetic algorithm is set to stop if it reaches 100 generations or else when the objective function has remained the same for 50 generations. If the objective value does not change between generations, it is called a stall generation. Table 4.3 highlights the generation number, the objective function and the number of stall generations. This optimisation ended at the 100th generation as the maximum number of generations had been reached.

The output minimum cost of the system is R1 952 665.5, using 220 PV panels, 5 wind turbines at 10m heights and 19 batteries.

4.1.1. PV Panels

220x 200W PV panels were chosen as the optimal number of panels for the HRES for this area with the climatic data as shown above. At STC this gives 44kW of maximum solar PV power. Using the climatic data, the total PV power able to be supplied per hour to the system by all the PV panels is calculated and figure 4.5 shows the result over the period of the year, 0-8760 hours.

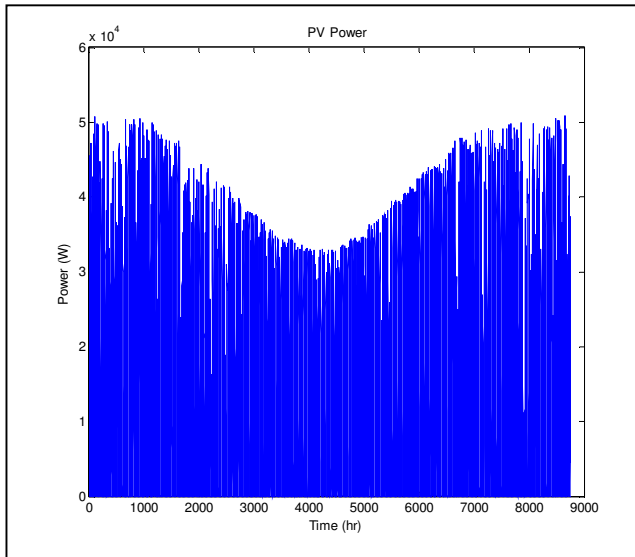


Figure 4.5: Power able to be supplied by PV Panels

4.1.2. Wind turbine

5x 3kW wind turbines were determined to be the optimal number of wind turbines for the HRES for this area with wind data as shown above. This gives a maximum of 15kW for the number of wind turbines. The turbines should be at a height of 10m to enable them to be most cost effective and provide as much power as possible. Figure 4.6 below shows the total power able to be provided to the system taking the wind speed into account.

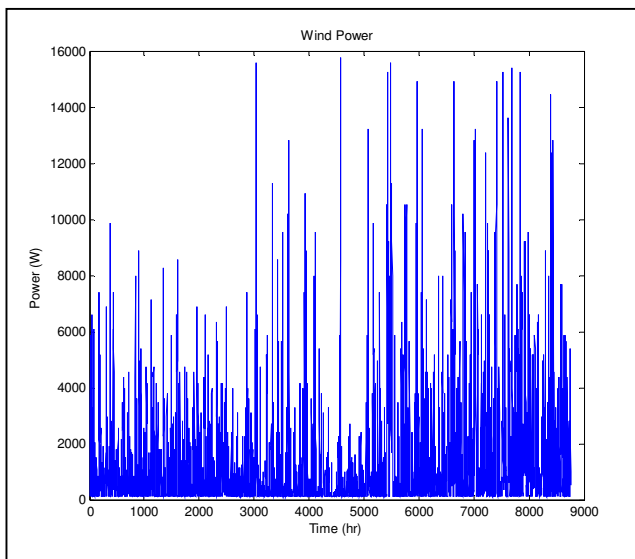


Figure 4.6: Power able to be supplied by Wind Turbines

4.1.3. Batteries

19x 200Ah batteries were selected for use for this system. There is therefore a capacity of 3800Ah. This will be used as energy storage to boost the power necessary to meet the load when weather conditions are not optimal.

4.1.4. Calculating LPSP

The LPSP calculated when checking the results from the genetic algorithm is 0.005, which is lower than 0.01 which is the set LPSP and therefore the load is supplied for 99.5% of the time. The load is therefore not supplied for only 43.8 hours, which is less than 2 days over the year.

4.5. Resultant Controller and Simulation Results

The controller consists of four modes for the system to run in depending on the load and generation values, as discussed in chapter 3. The system consists of 4 modes, the first where only the wind turbine supplies the load, the second where the PV panels and wind turbine supply the load, the third where the PV panels, wind turbine and batteries supply the load and the fourth where the load is not supplied as the load is greater than the energy that can be generated by the system. Running the controller with the results from the genetic algorithm gives us the following information about the system. Firstly, we can gauge the load over the year, hour by hour, as well as the amount of the load that is supplied by the PV panels and the amount of the load supplied by the wind turbines. The following graphs show these components.

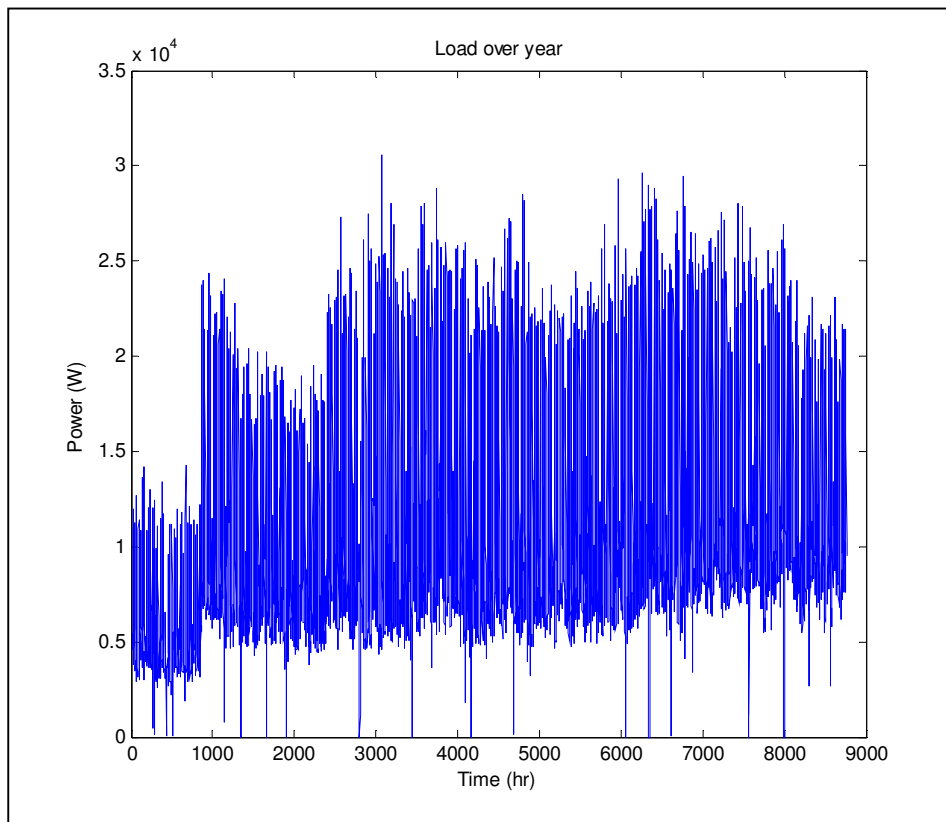


Figure 4.7: Load over the Year

The wind turbines supply the power to the system when the system is in mode 1, mode 2 and mode 3. In mode 1, the power generated by the wind turbine is sufficient to supply the system alone. Figure 4.8 shows the power supplied to the system by the wind turbines in mode 1, 2 and 3.

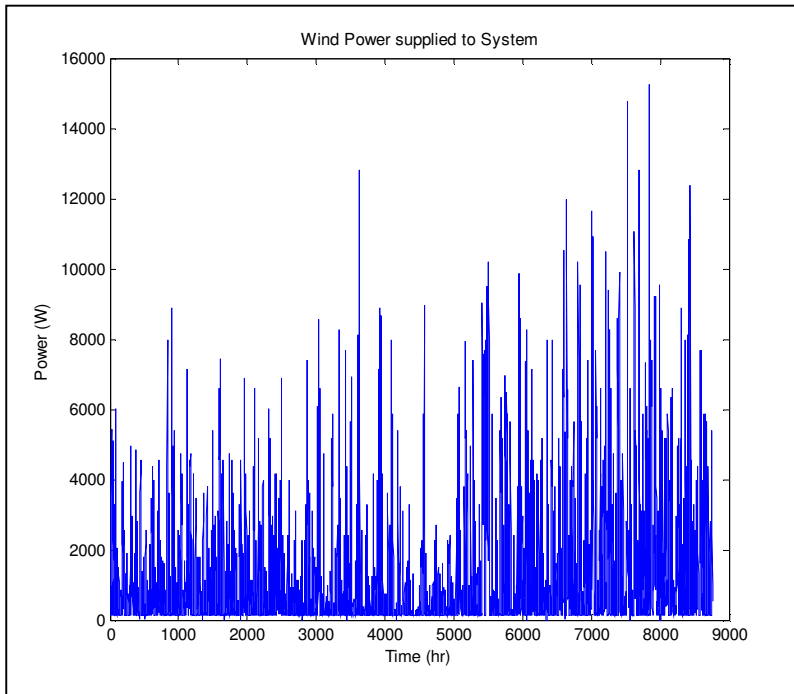


Figure 4.8: Power Supplied by the Wind Turbines

The PV panels supply power to the system in modes 2 and 3. Figure 4.9 shows the power that is supplied by the PV panels in those modes.

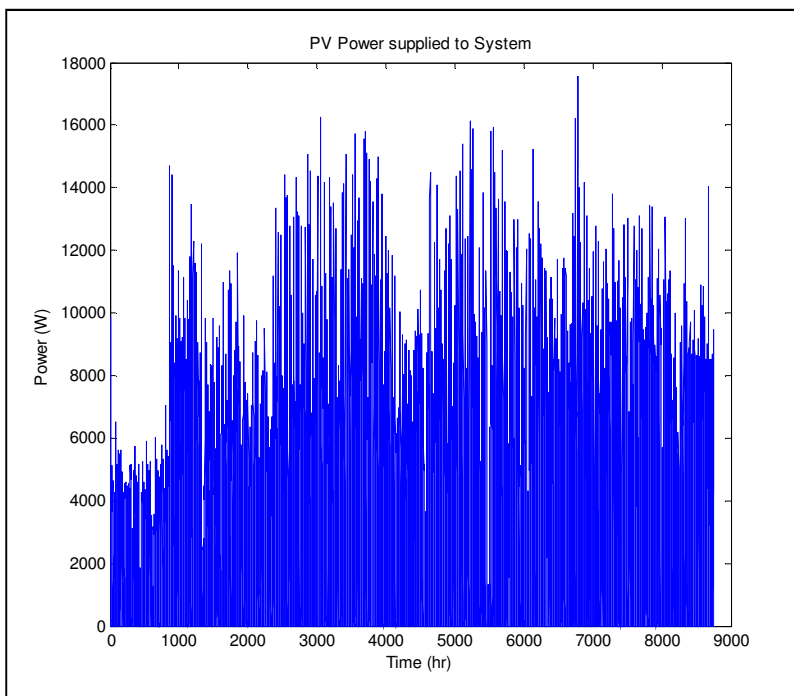


Figure 4.9: Power Supplied by the PV Panels

Another aspect of the system that can be monitored using the controller simulation is the State of Charge of the batteries and therefore the capacity of the battery system. The set depth of discharge for the batteries is 40%, which is 1520Ah for the battery system that we have for this system. Figure 4.10 outlines the battery capacity over the year. It can be seen that the battery capacity remains between around 1520 and 3800Ah and therefore the controller is working as required in keeping the battery between the minimum and maximum bounds.

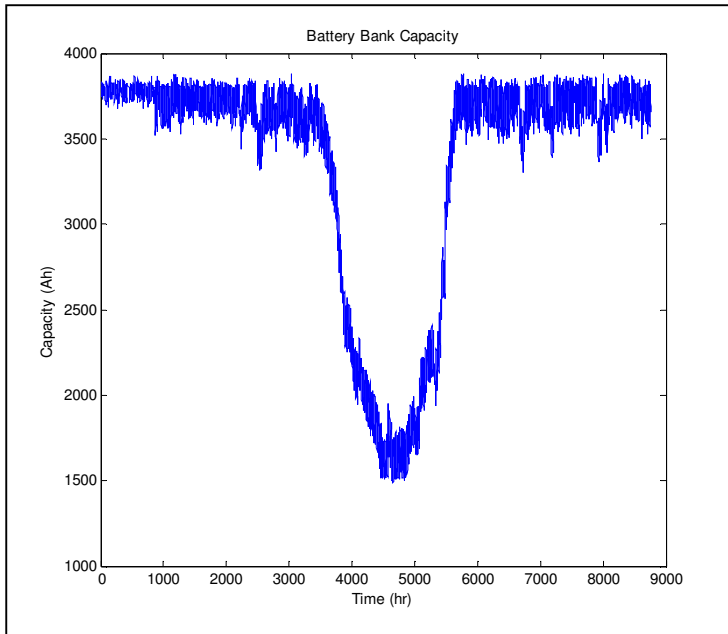


Figure 4.10: Capacity of Batteries

Figure 4.11 shows the histogram of the modes of the system. It can be seen that the system transitions between the different modes, as each mode accounted for on the histogram.

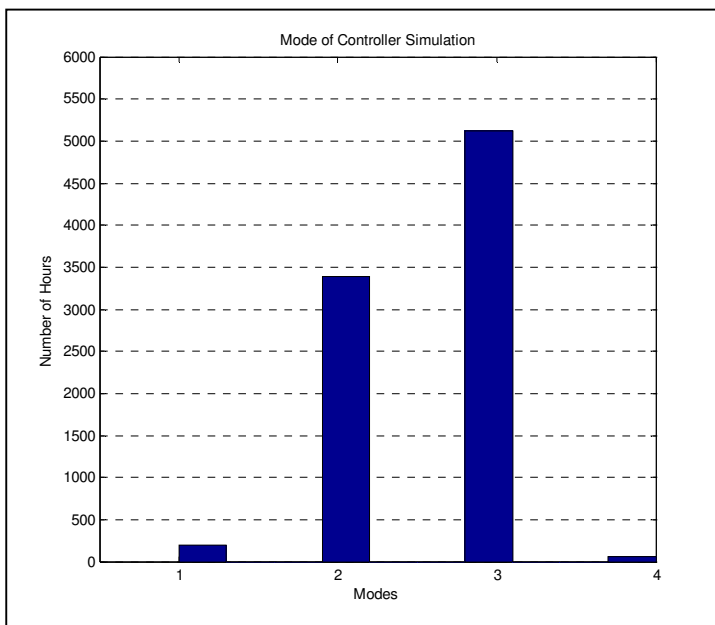


Figure 4.11: Histogram of Modes of System

Mode 4 is the mode where the system is not supplied by the PV panel, wind turbine and batteries. This is the mode where the load is not supplied. From figure 4.11 it can be seen that the system is mostly in mode 3 where the wind turbine, PV panels and batteries are supplying the load. As there are only 5 wind turbines in this system design, the amount of time in mode 1 where only the wind turbines supply the load is under 250 hours (3%), and the time spent in mode 2 where the PV panels and wind turbines supply the load is much higher due to the large number of solar panels (38%). From figure 4.11 we can also see that the time spent in mode 4 where the load is not supplied at all is very minimal, around 0.45% which is well within the limit of 1% set at the beginning of the optimisation.

Figure 4.12 shows the total load to be supplied, EI, and the total supply, TSupply. It can be seen from the graph that the load is met the majority of the time, however there is a section of time around 4500 hours where the load is not met. As the LPSP has not been set to zero and therefore some loss of load is expected over the year, the concern is not that the load is not always met. The main concern is the amount of time that the load is met and not met. From the histogram in figure 4.11 and the load and supply graph shown in figure 4.12, we see that the load is not met around 0.05% of the time. This is appropriate as we have selected a LPSP of 1%.

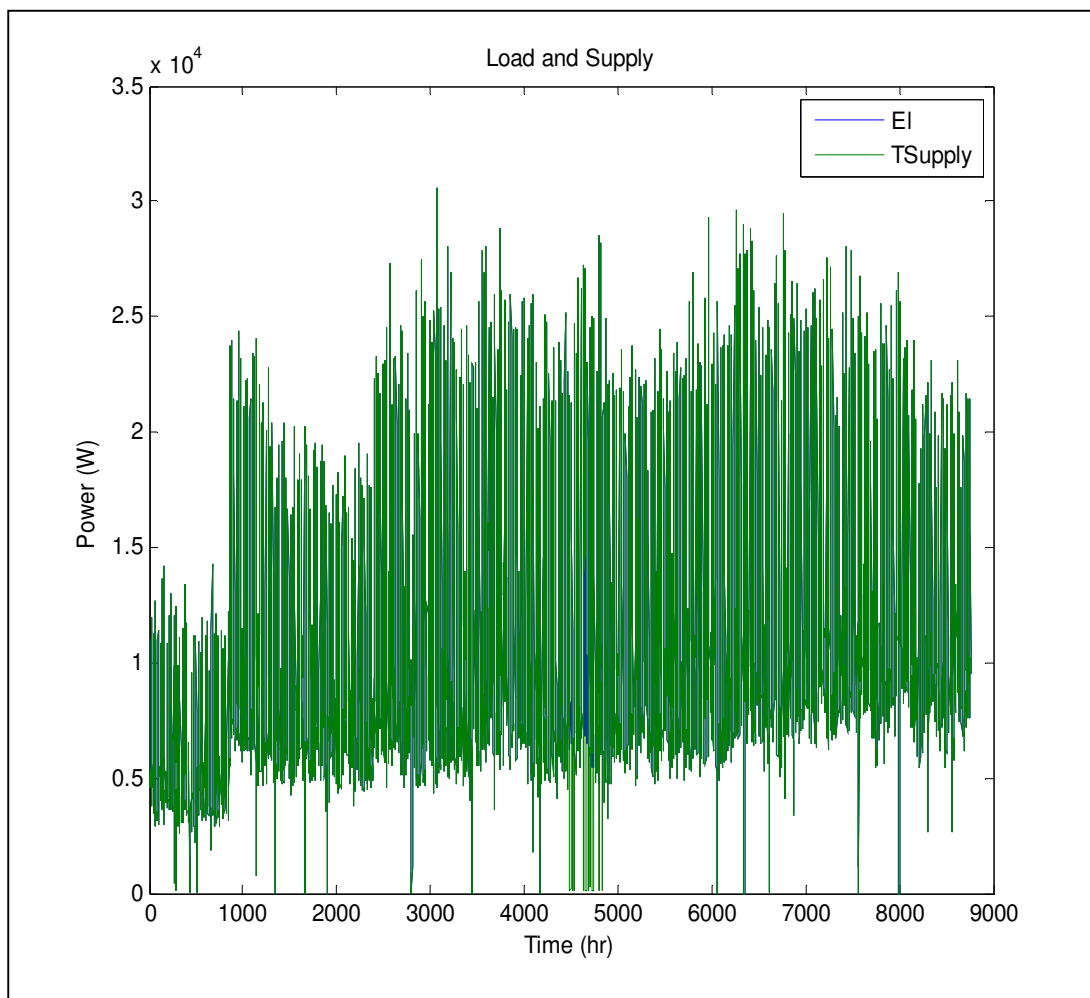


Figure 4.12: Load and Total Supply over Year

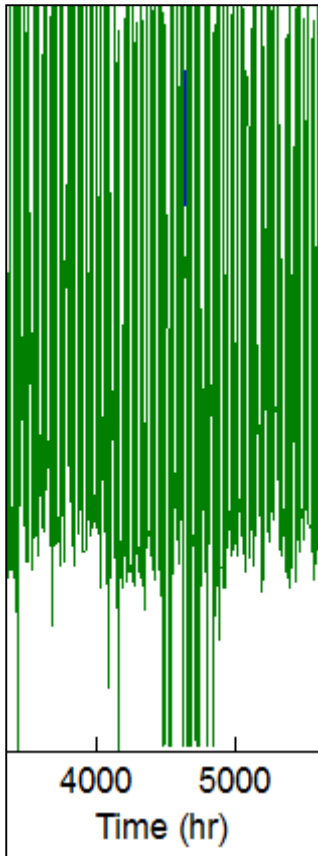


Figure 4.13: Enlargement of figure 4.12 showing Load not being met

4.6. Conclusions

Using the hourly climatic and load data for Garagapola over a year period, the genetic algorithm was run and a system of 220 PV panels, 5 wind turbines at 10m height and 19 batteries was deemed to be the most suitable for the conditions specified. This is an energy generation capacity of 59kW at optimal conditions and energy storage of 3800Ah. This has a cost of R1 952 665.5. Running the LPSP checking test, an LPSP of 0.0045 was calculated giving a 0.45% loss of load probability over the period of the year. The controller simulation is run as a checking mechanism. Running the controller simulation shows that the state of charge of the batteries stays between 40% capacity to 100% capacity, the minimum and maximum bounds of the batteries, which shows that the control is working well. The system enters all four modes at different points in the year and the load is not supplied around 0.5% of the year as can be seen from the histogram of modes in figure 4.11.

The outcome of this case study can be used to set up a HRES in an area similar in climate and population dynamics to Garagapola. Ideally the weather data for the area where the HRES is being designed for would be used in these calculations, but if it was not possible, this simulation could be used as a starting point for design. The outcome of this case study will be discussed in more detail in chapter 7, following the other case study results.

5. Case Study 2: Antioch

5.1. Introduction

Antioch is an electrified village in Kwazulu Natal Province, South Africa, situated at a latitude of -30.09° and a longitude of 29.81° . It is a good example of a rural village load and therefore a sample of 87 residential houses and loads has been used for the load data for this area.

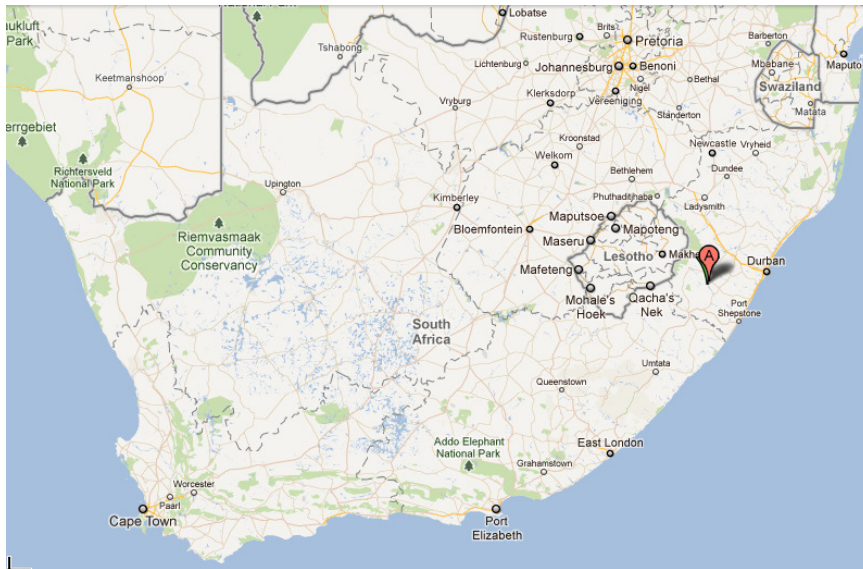


Figure 5.1: Map Showing Location of Antioch [42]

Figure 5.1 above shows the location of the village on a map of Southern Africa and figure 5.2 below shows a closer satellite image of the area.



Figure 5.2: Satellite Image of Antioch [42]

5.2. Climatic Data Set

As discussed in Chapter 3 of this thesis, the temperature and wind speed data is obtained from the South African Weather Bureau (SAWB), provided by Enerweb. The hourly temperature and wind speed data is obtained from the Durban Weather Station situated at a latitude of -29.97° and a longitude of 30.95° in Durban.

The hourly solar irradiance data is provided by Helioclim through SoDa website [41]. The data is calculated from satellite pictures at the specified latitude and longitude required, in this case the co-ordinates of Antioch.

Table 5.1: Average Monthly Climatic Data

	Temperature (°C)	Solar Irradiance (W/m ²)	Wind Speed (m/s)
January	24.4	286.4	5.06
February	23.5	276.2	3.93
March	24.4	244.3	4.00
April	22.5	199.6	3.85
May	19.7	167.8	3.43
June	17.3	145.7	3.68
July	16.6	163.2	3.42
August	18.6	190.4	3.78
September	19.4	226.7	4.15
October	20.5	247.1	5.13
November	20.8	267.4	5.75
December	23.6	299.5	4.66

While hourly data is used for the optimisation and checking algorithms, the average monthly values of the climatic data is presented in table 5.1 above. The trended temperature over the year is represented in the graph below in figure 5.3.

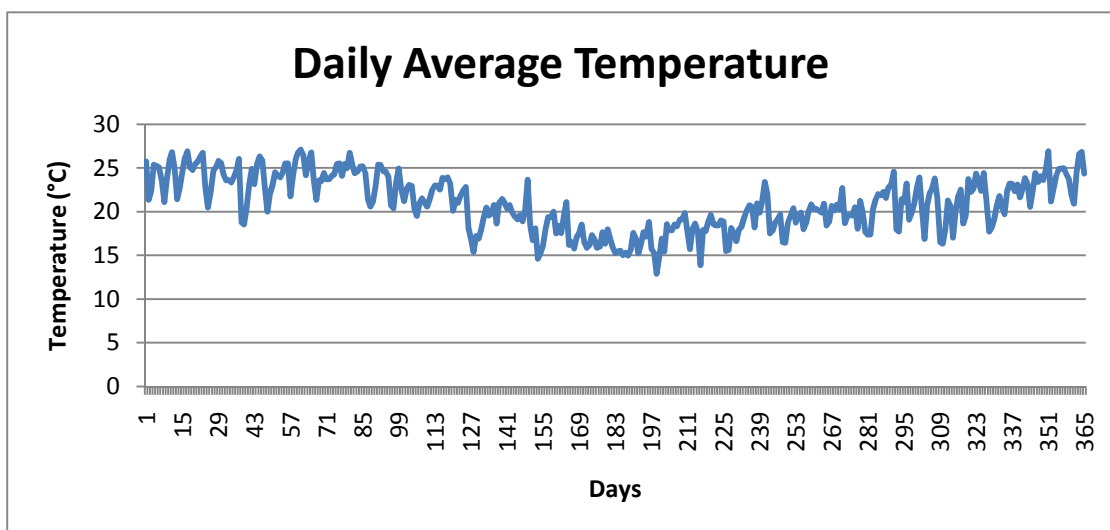


Figure 5.3: Antioch Daily Average Temperature over Year

5.3. Load Data Set

The load data for 87 residential households in Antioch is summed up to represent the hourly load profile for the entire village. The average monthly load values are shown in figure 5.4 and table 5.2 below. The load data is supplied by the National Load Research Program. This load data is used for the genetic algorithm after adding 5% onto them to allow for growth of load in the area.

Table 5.2: Monthly Average Load for Antioch

	Load (W)
January	5949.649
February	5465.443
March	5660.014
April	5921.789
May	8336.396
June	8279.907
July	8716.284
August	8619.324
September	7818.029
October	6687.78
November	6481.247
December	7176.931

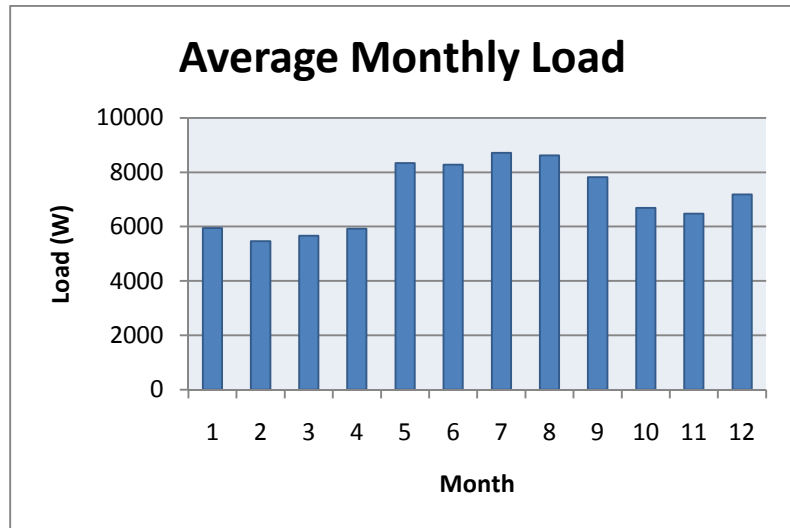


Figure 5.4: Histogram showing Average Monthly Load for Antioch

5.4. Results of Optimisation

The genetic algorithm was run using the hourly values of climatic data and load data as specified above. The cost was minimised whilst keeping an LPSP of 1%. This means that the load will not be supplied 1% of the time period that is included in this simulation.

The resultant successive generations of populations of 20 reduced the objective function cost as shown below in table 5.3:

Table 5.3: Genetic Optimisation Results per Generation

Generation	Max f(x)	Stall Generations	Generation	Max f(x)	Stall Generations
1	2.59987e+007	0	51	4.96782e+006	24
2	2.29087e+007	0	52	1.84181e+006	0
3	2.19766e+007	0	53	1.84181e+006	1
4	8.21218e+006	0	54	1.84181e+006	2
5	7.1799e+006	0	55	1.84181e+006	3
6	7.1799e+006	1	56	1.84181e+006	4
7	7.1799e+006	2	57	1.84181e+006	5
8	7.1799e+006	3	58	1.84181e+006	6
9	7.1799e+006	4	59	1.84181e+006	7
10	7.1799e+006	5	60	1.84181e+006	8
11	7.1799e+006	6	61	1.84181e+006	9

12	6.7959e+006	0	62	1.84181e+006	10
13	6.7959e+006	1	63	1.84181e+006	11
14	6.7959e+006	2	64	1.84181e+006	12
15	6.7959e+006	3	65	1.84181e+006	13
16	6.58716e+006	0	66	1.84181e+006	14
17	6.58716e+006	1	67	1.84181e+006	15
18	6.58716e+006	2	68	1.82751e+006	0
19	6.58716e+006	3	69	1.82751e+006	1
20	6.58716e+006	4	70	1.82751e+006	2
21	6.58716e+006	5	71	1.82751e+006	3
22	6.58716e+006	6	72	1.82751e+006	4
23	6.58716e+006	7	73	1.82751e+006	5
24	6.58716e+006	8	74	1.82751e+006	6
25	6.58716e+006	9	75	1.82751e+006	7
26	6.58716e+006	10	76	1.82751e+006	8
27	4.96782e+006	0	77	1.82751e+006	9
28	4.96782e+006	1	78	1.82751e+006	10
29	4.96782e+006	2	79	1.82751e+006	11
30	4.96782e+006	3	80	1.82751e+006	12
31	4.96782e+006	4	81	1.82751e+006	13
32	4.96782e+006	5	82	1.82751e+006	14
33	4.96782e+006	6	83	1.82751e+006	15
34	4.96782e+006	7	84	1.82751e+006	16
35	4.96782e+006	8	85	1.82751e+006	17
36	4.96782e+006	9	86	1.82751e+006	18
37	4.96782e+006	10	87	1.82751e+006	19
38	4.96782e+006	11	88	1.82751e+006	20
39	4.96782e+006	12	89	1.82751e+006	21
40	4.96782e+006	13	90	1.82751e+006	22
41	4.96782e+006	14	91	1.82751e+006	23
42	4.96782e+006	15	92	1.82751e+006	24
43	4.96782e+006	16	93	1.82751e+006	25
44	4.96782e+006	17	94	1.82751e+006	26
45	4.96782e+006	18	95	1.82751e+006	27
46	4.96782e+006	19	96	1.82751e+006	28
47	4.96782e+006	20	97	1.82751e+006	29
48	4.96782e+006	21	98	1.82751e+006	30
49	4.96782e+006	22	99	1.82751e+006	31
50	4.96782e+006	23	100	1.82751e+006	32

The genetic algorithm is set to stop if it reaches 100 generations or else when the objective function has remained the same for 50 generations. If the objective value does not change between generations, it is called a stall generation. Table 5.3 highlights the generation number, the objective function and the number of stall generations. This optimisation ended at the 100th generation as the maximum number of generations set had been reached.

The output minimum cost of the system is R1 827 510, using 202 PV panels, 5 wind turbines at 10m heights and 13 batteries.

5.4.1. PV Panels

202x 200W PV panels were chosen as the optimal number of panels for the HRES for this area with the climatic data as shown above. In STC this gives 40.4kW of maximum solar PV power. Using the climatic data, the total PV power able to be supplied per hour to the system by all the PV panels is calculated and figure 5.5 shows the result over the period of the year, 0-8760 hours.

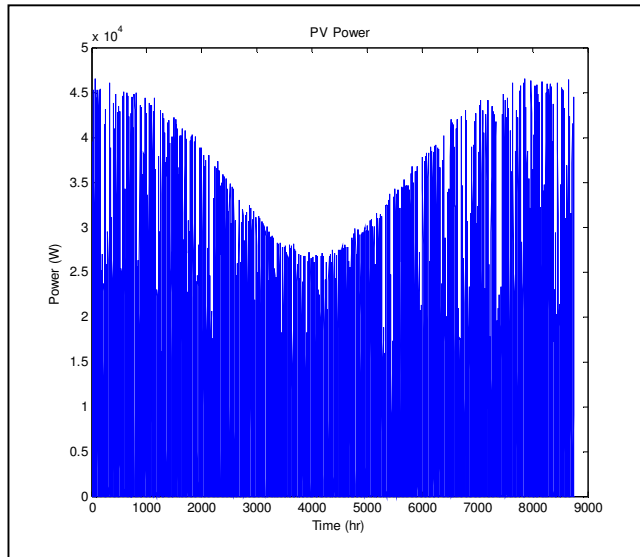


Figure 5.5: Power able to be Supplied by PV Panels

5.4.2. Wind turbine

5x 3kW wind turbines were determined to be the optimal number of wind turbines for the HRES for this area with wind data as shown above. This is a maximum of 15kW at optimal wind speed. The turbines should be at a height of 10m to enable them to be most cost effective and provide as much power as possible. Figure 5.6 below shows the total power able to be provided to the system taking the wind speed into account.

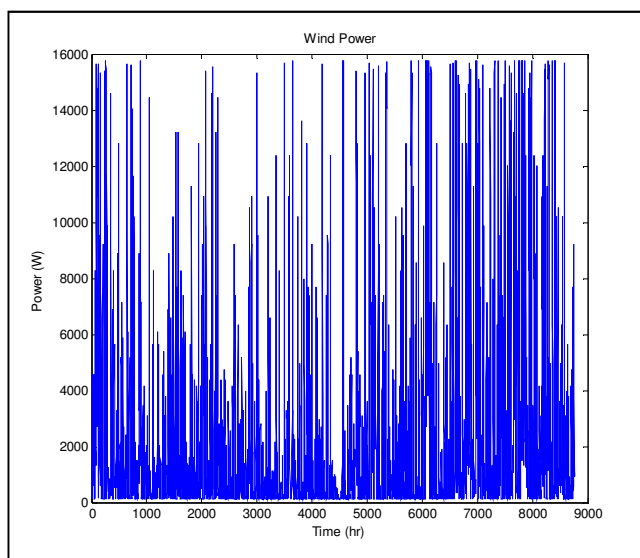


Figure 5.6: Power able to be Supplied by Wind Turbines

5.4.3. Batteries

13x 200Ah batteries were selected for use for this system. There is therefore a capacity of 2600Ah. This will be used as energy storage to boost the power necessary to meet the load when weather conditions are not optimal.

5.4.4. Calculating LPSP

The LPSP calculated when checking the results from the genetic algorithm is 0.0046, which is lower than 0.01 which is the set LPSP. This means that the load will not be supplied by the energy generation methods 0.46% of the time. This is 40.3 hours, 1.7 days.

5.5. Resultant Controller and Simulation Results

The controller consists of four modes for the system to run in depending on the load and generation values, as discussed in chapter 3. The system consists of 4 modes, the first where only the wind turbine supplies the load, the second where the PV panels and wind turbine supply the load, the third where the PV panels, wind turbine and batteries supply the load and the fourth where the load is not supplied as the load is greater than the energy that can be generated by the system. Running the controller with the results from the genetic algorithm gives us the following information about the system. Firstly, we can gauge the load over the year, hour by hour, as shown in figure 5.7, as well as the amount of the load that is supplied by the PV panels and the amount of the load supplied by the wind turbines. The following graphs show these components.

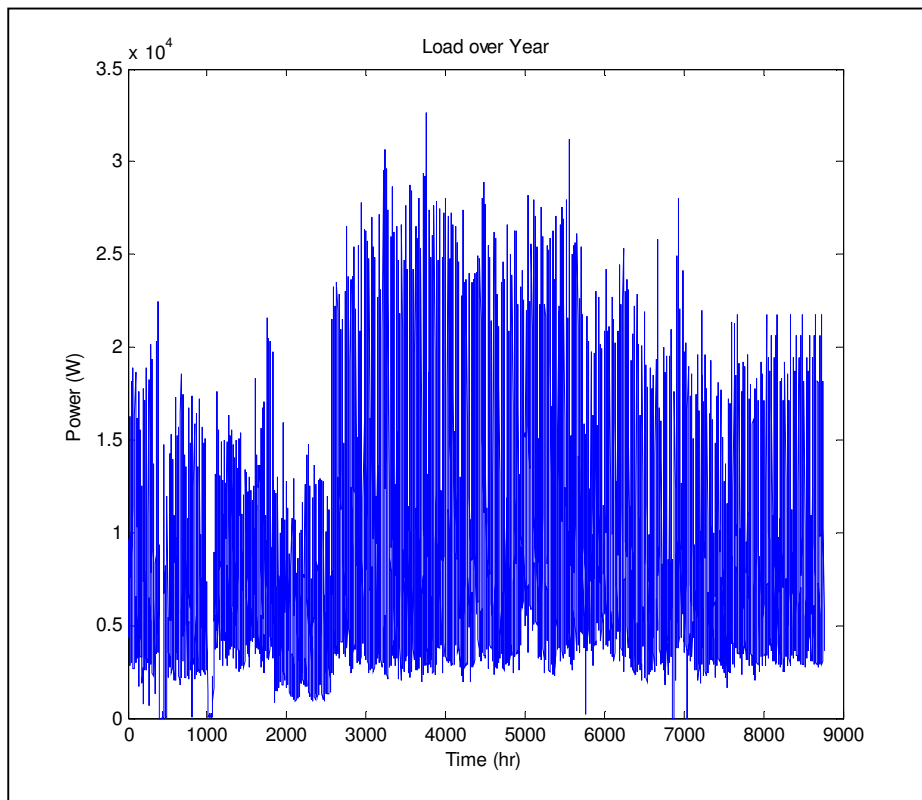


Figure 5.7: Load over the Year

The wind turbines supply the power to the system when the system is in mode 1, mode 2 and mode 3. In mode 1, the power generated by the wind turbine is sufficient to supply the system alone. Figure 5.8 shows the power supplied to the system by the wind turbines in mode 1, 2 and 3.

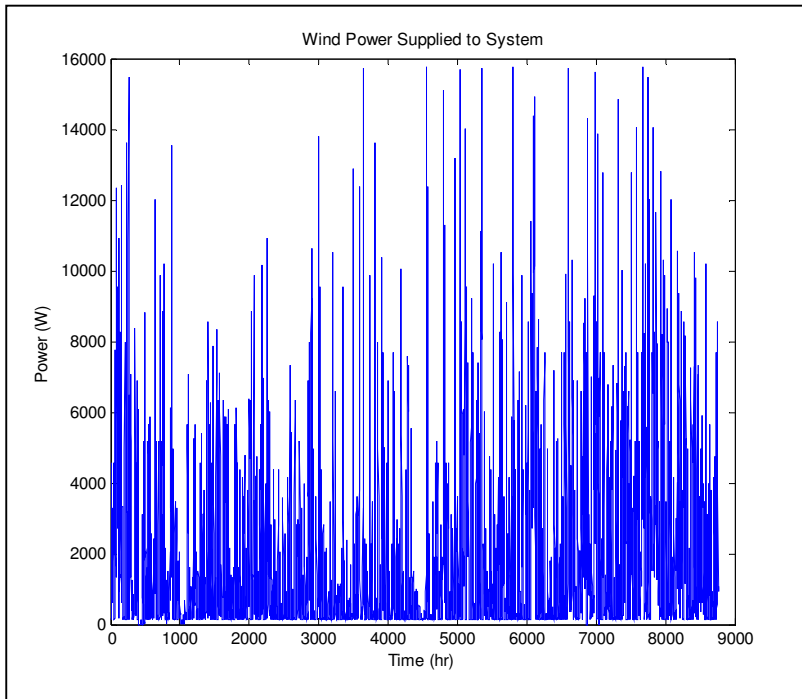


Figure 5.8: Power supplied by the Wind Turbines

The PV panels supply power to the system in modes 2 and 3. Figure 5.9 shows the power that is supplied by the PV panels in those modes.

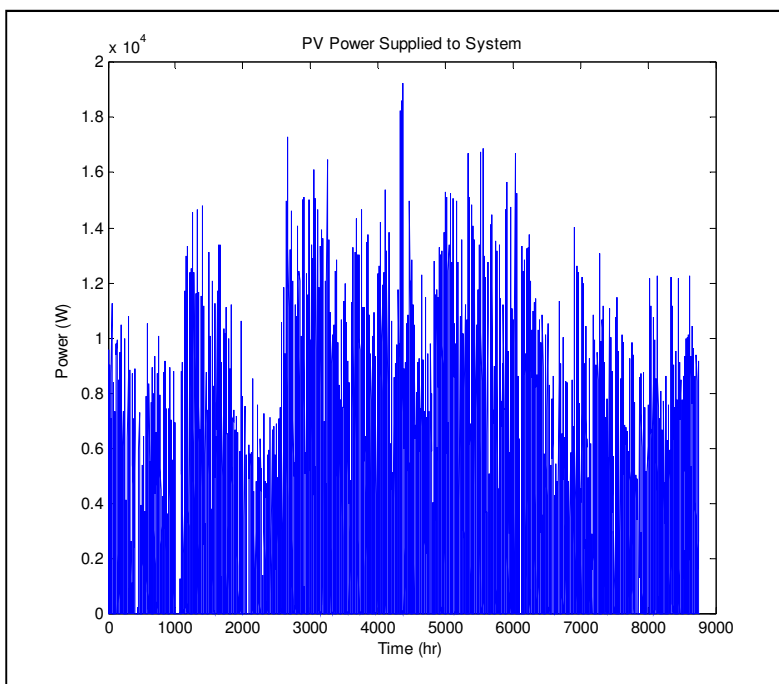


Figure 5.9: Power Supplied by the PV Panels

Another aspect of the system that can be monitored using the controller simulation is the State of Charge of the batteries and therefore the capacity of the system. The set depth of discharge for the batteries is 40%, which is 1040Ah for the battery system that we have for this system. Figure 5.10 outlines the battery capacity over the year. It can be seen that the battery capacity remains between 1040Ah and 2600Ah and therefore the controller is working as required in keeping the battery between the minimum and maximum bounds.

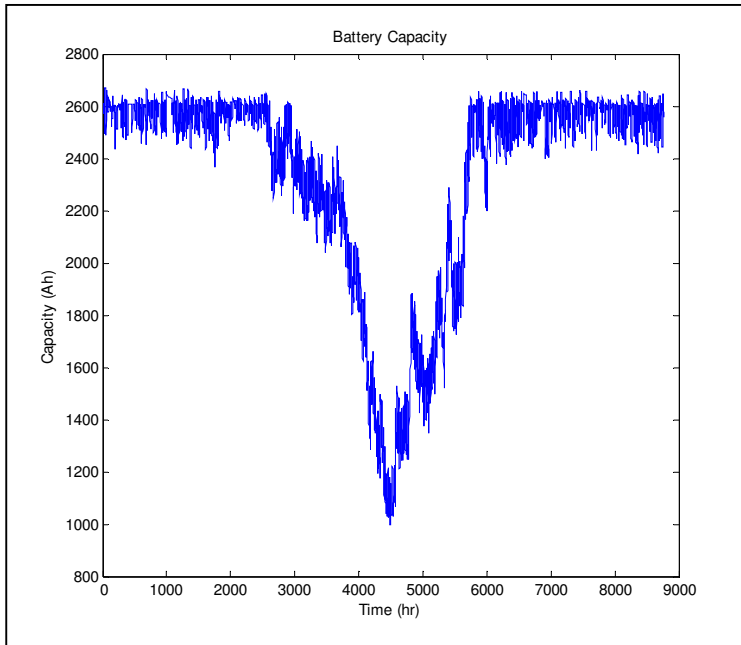


Figure 5.10: Capacity of Battery

Figure 5.11 shows the histogram of the modes of the system. It can be seen that the system transitions between the different modes, as each mode accounted for on the histogram.

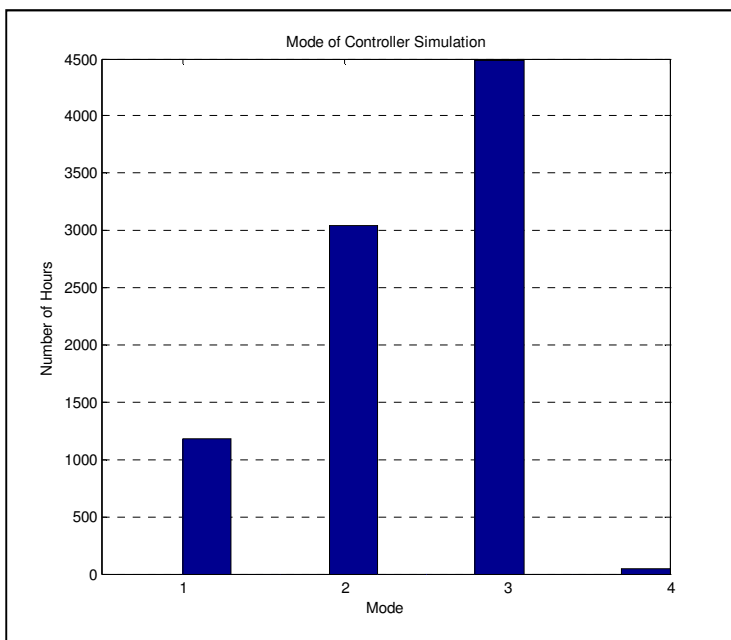


Figure 5.11: Histogram of Modes of System

Mode 4 is the mode where the system is not supplied by the PV panel, wind turbine and batteries. This is the mode where the load is not supplied. From figure 5.11 it can be seen that the system is mostly in mode 3 where the wind turbine, PV panels and batteries are supplying the load. As there are 5 wind turbines in this system design and the wind speed is generally high, the amount of energy able to be generated by the wind turbines is substantial and therefore the system is in mode 1 for a portion of time (15%). As there are many PV panels as part of this system, the system is in mode 2 - 35% of the time as the PV panels add a considerable amount of energy generation to the amount the wind turbines can generate. From figure 5.11 we can also see that the time spent in mode 4 where the load is not supplied at all is very minimal, around 0.5% which is within the limit of 1% set at the beginning of the optimisation.

Figure 5.12 shows the total load to be supplied, E_l , and the total supply, T_{Supply} . It can be seen from the graph that the load is met the majority of the time, however there is a section of time around 4500 hours where the load is not met. As the LPSP has not been set to zero and therefore some loss of load is expected over the year, the concern is not that the load is not always met. The main concern is the amount of time that the load is met and not met. From the histogram in figure 5.11 and the load and supply graph shown in figure 5.12, we see that the load is not met around 0.5% of the time. This is appropriate as we have selected a LPSP of 1%.

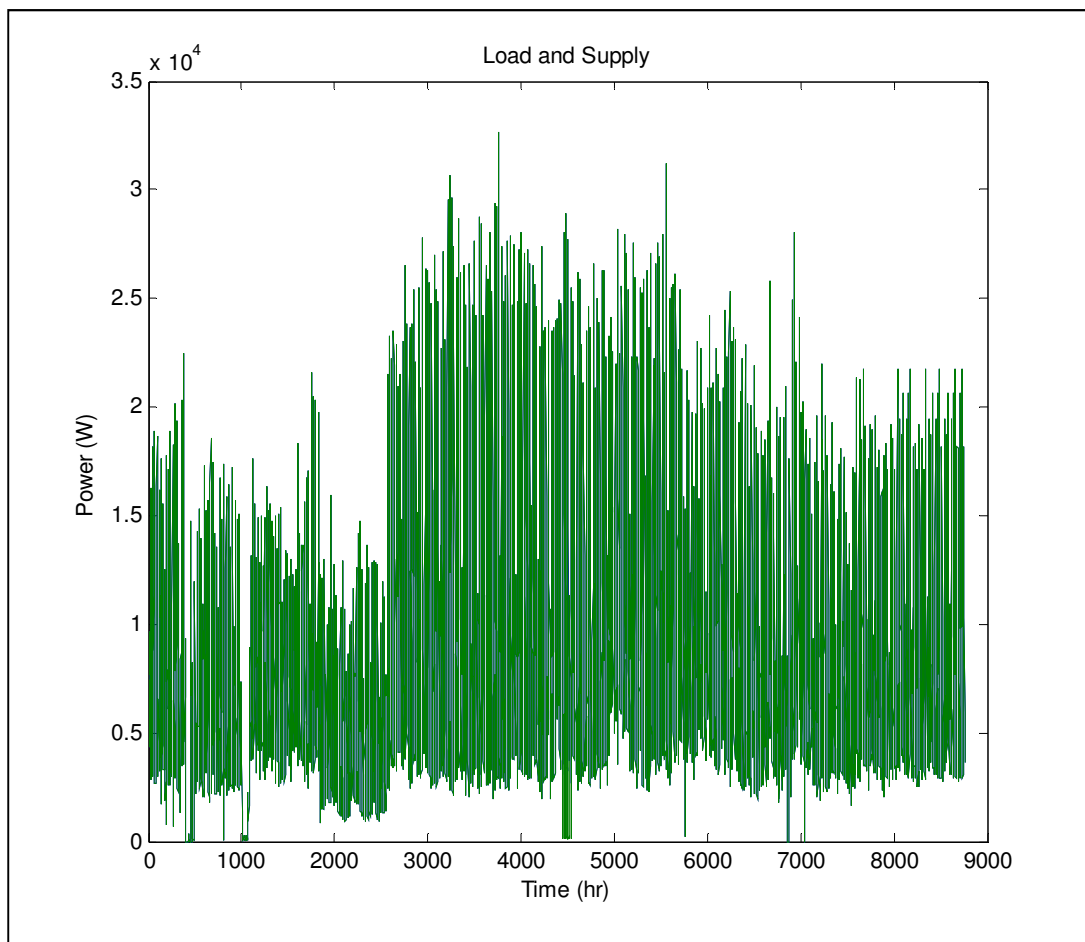


Figure 5.12: Load and Total Supply over Year

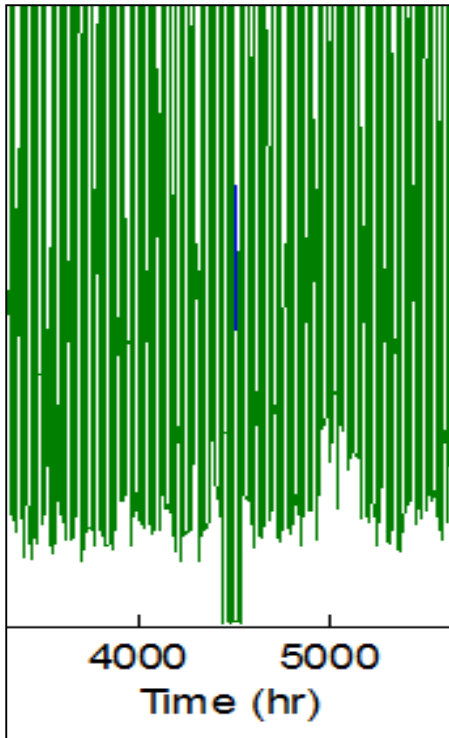


Figure 5.13: Enlargement of figure 5.12 showing Load not being met

5.6. Conclusions

Using the hourly climatic and load data for Antioch over a year period, the genetic algorithm was run and a system of 202 PV panels, 5 wind turbines at 10m height and 13 batteries was deemed to be the most suitable for the conditions specified. This is an energy generation capacity of 55.4kW and a storage capacity of 2600Ah. This has a cost of R1 827 510. Running the LPSP checking test, an LPSP of 0.0046 was calculated giving a 0.46% loss of load probability over the period of the year. The controller simulation is run as a checking mechanism. Running the controller simulation shows that the state of charge of the batteries stays between 40% capacity to 100% capacity, the minimum and maximum bounds of the batteries, which shows that the control is working well. The system enters all four modes at different points in the year and the load is not supplied around 0.05% of the year as can be seen from the histogram of modes in figure 5.11.

The outcome of this case study can be used to set up a HRES in an area similar in climate and population dynamics to Antioch. Ideally the weather data for the area where the HRES is being designed for would be used in these calculations, but if it was not possible, this simulation could be used as a starting point for design. The outcome of this case study will be discussed in more detail in chapter 7, following the other case study results.

6. Case Study 3: Gasese

6.1. Introduction

Gasese is an electrified village in the Northern Cape Province, South Africa, situated at a latitude of -27.11° and a longitude of 23.05° . It is a good example of a rural village load and therefore a sample of 84 residential houses and loads has been used for the load data for this area.

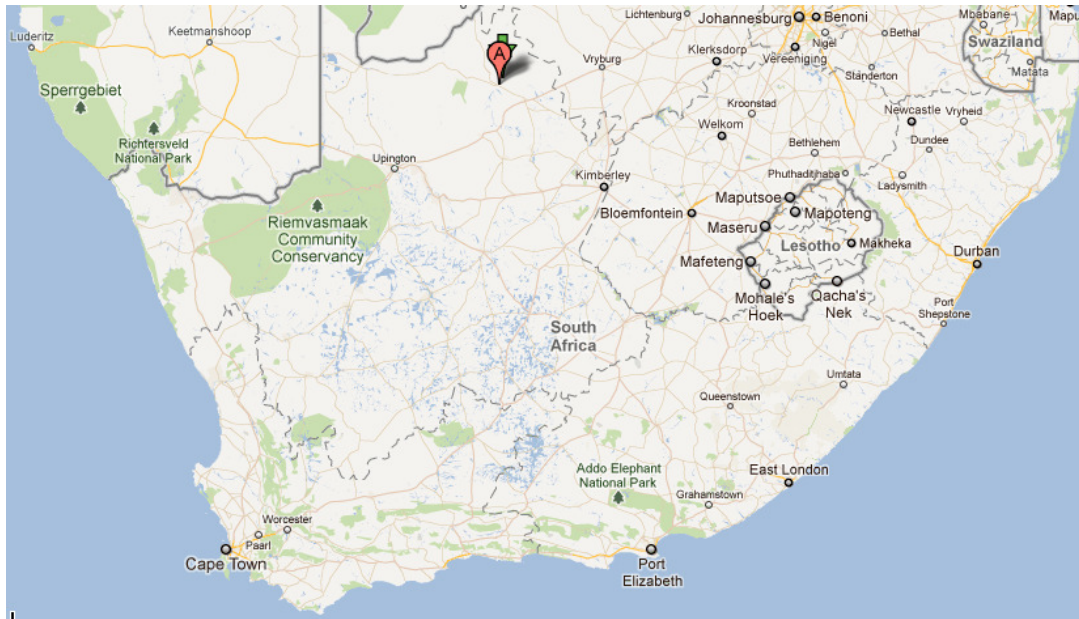


Figure 6.1: Map Showing Location of Gasese in South Africa [43]

Figure 6.1 above shows the location of the village on a map of Southern Africa and figure 6.2 below shows a closer satellite image of the area.



Figure 6.2: Satellite Image of Gasese [43]

6.2. Climatic Data Set

As discussed in Chapter 3 of this thesis, the temperature and wind speed data is obtained from the South African Weather Bureau (SAWB), provided by Enerweb. The hourly temperature and wind speed data is obtained from the Upington Weather Station situated at a latitude of -28.41° and a longitude of 21.26° in Upington.

The hourly solar irradiance data is provided by Helioclim through SoDa website [41]. The data is calculated from satellite pictures at the specified latitude and longitude required, in this case the co-ordinates of Gasese.

Table 6.1: Average Monthly Climatic Data

	Temperature ($^\circ\text{C}$)	Solar Irradiance (W/m^2)	Wind Speed (m/s)
January	26.84	3.95	317.34
February	27.93	3.52	310.78
March	25.69	2.93	264.40
April	21.96	3.17	216.92
May	15.29	2.98	181.60
June	11.20	3.13	161.02
July	10.70	3.10	176.68
August	14.34	3.09	207.75
September	19.62	3.42	261.89
October	23.75	4.05	291.33
November	24.31	4.27	314.65
December	28.014	3.92	348.74

While hourly data is used for the optimisation and checking algorithms, the average monthly values of the climatic data is presented in table 6.1 above. The trended temperature over the year is represented in the graph below in figure 6.3.

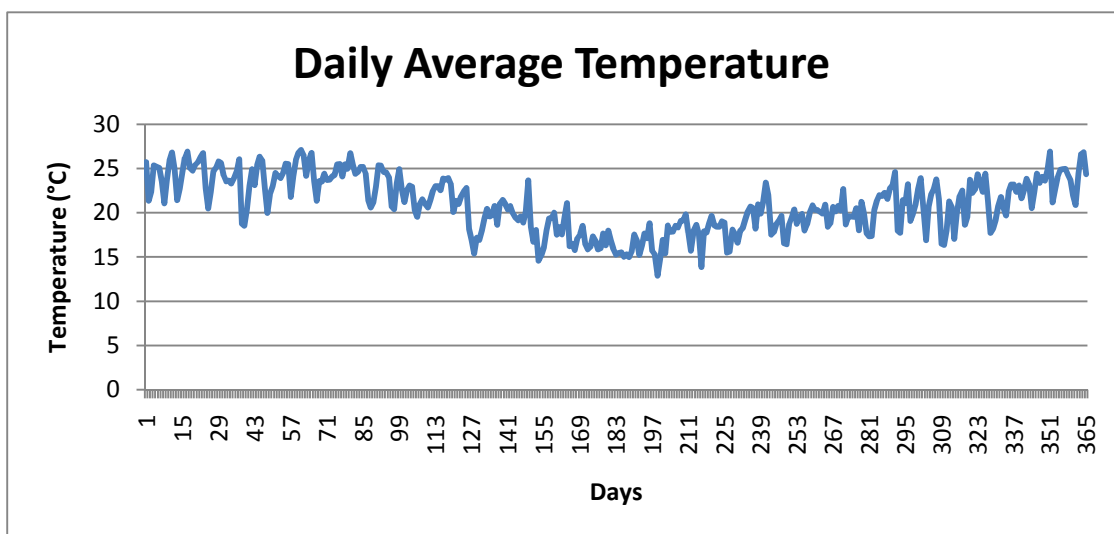


Figure 6.3: Gasese Daily Average Temperature over Year

6.3. Load Data Set

The load data for 84 residential households in Gasese is summed up to represent the hourly load profile for the entire village. The average monthly load values are shown in figure 6.4 and table 6.2 below. The load data is supplied by the National Load Research Program. This load data is used for the genetic algorithm after adding 5% onto them to allow for growth of load in the area.

Table 6.2: Monthly Average Load for Gasese

	Load (W)
January	9767.803
February	9505.526
March	8490.317
April	9491.633
May	10459.84
June	9787.575
July	9559.283
August	11326.39
September	11062.65
October	9008.533
November	7446.981
December	6772.863

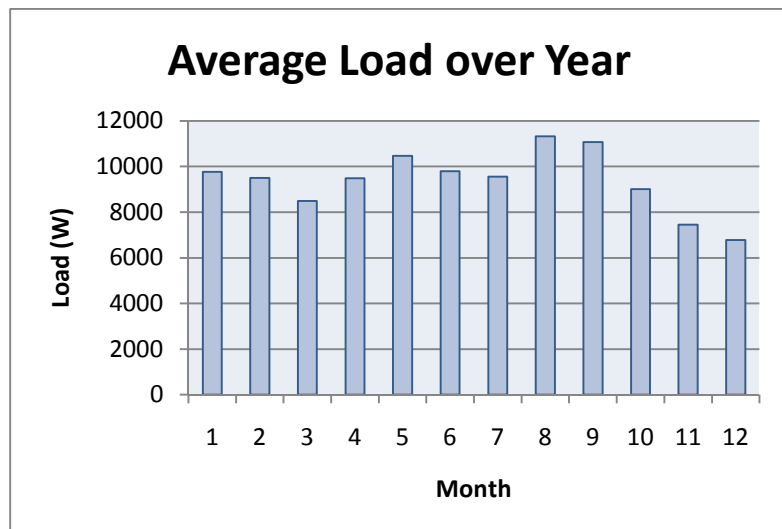


Figure 6.4: Histogram Showing Average Monthly Load for Gasese

6.4. Results of Optimisation

The genetic algorithm was run using the hourly climatic data and load data as specified above. The cost was minimised whilst keeping an LPSP of 1%. This means that the load is not met by the supply a maximum of 1% of the time under inspection, ie. 3.65 days is 1% of 1 year.

The resultant successive generations of populations of 20 reduced the objective function cost as shown below in table 6.3:

Table 6.3: Genetic Optimisation Results per Generation

Generation	Max f(x)	Stall Generations	Generation	Max f(x)	Stall Generations
1	8.27436e+006	0	49	2.76576e+006	4
2	7.25856e+006	0	50	2.76576e+006	5
3	5.90856e+006	0	51	2.76576e+006	6
4	5.90856e+006	1	52	2.76576e+006	7
5	5.39957e+006	0	53	2.76576e+006	8
6	5.39957e+006	1	54	2.76576e+006	9
7	5.39957e+006	2	55	2.76576e+006	10
8	5.39957e+006	3	56	2.76576e+006	11
9	4.56336e+006	0	57	2.76576e+006	12
10	4.56336e+006	1	58	2.76576e+006	13

11	2.94402e+006	0	59	2.76576e+006	14
12	2.94402e+006	1	60	2.76576e+006	15
13	2.94402e+006	2	61	2.76576e+006	16
14	2.81202e+006	0	62	2.76576e+006	17
15	2.81202e+006	1	63	2.76576e+006	18
16	2.81202e+006	2	64	2.76576e+006	19
17	2.81202e+006	3	65	2.76576e+006	20
18	2.81202e+006	4	66	2.76576e+006	21
19	2.81202e+006	5	67	2.76576e+006	22
20	2.81202e+006	6	68	2.76576e+006	23
21	2.81202e+006	7	69	2.76576e+006	24
22	2.81202e+006	8	70	2.76576e+006	25
23	2.81202e+006	9	71	2.76576e+006	26
24	2.81202e+006	10	72	2.76576e+006	27
25	2.81202e+006	11	73	2.76576e+006	28
26	2.81202e+006	12	74	2.76576e+006	29
27	2.81202e+006	13	75	2.76576e+006	30
28	2.81202e+006	14	76	2.76576e+006	31
29	2.81202e+006	15	77	2.76576e+006	32
30	2.81202e+006	16	78	2.76576e+006	33
31	2.81202e+006	17	79	2.76576e+006	34
32	2.81202e+006	18	80	2.76576e+006	35
33	2.81202e+006	19	81	2.76576e+006	36
34	2.81202e+006	20	82	2.76576e+006	37
35	2.81202e+006	21	83	2.76576e+006	38
36	2.81202e+006	22	84	2.76576e+006	39
37	2.81202e+006	23	85	2.76576e+006	40
38	2.81202e+006	24	86	2.76576e+006	41
39	2.81202e+006	25	87	2.76576e+006	42
40	2.81202e+006	26	88	2.76576e+006	43
41	2.81202e+006	27	89	2.76576e+006	44
42	2.81202e+006	28	90	2.76576e+006	45
43	2.81202e+006	29	91	2.76576e+006	46
44	2.81202e+006	30	92	2.76576e+006	47
45	2.76576e+006	0	93	2.76576e+006	48
46	2.76576e+006	1	94	2.76576e+006	49
47	2.76576e+006	2	95	2.76576e+006	50
48	2.76576e+006	3	96	2.76576e+006	51

The genetic algorithm is set to stop if it reaches 100 generations or else when the objective function has remained the same for 50 generations. If the objective value does not change between generations, it is called a stall generation. Table 6.3 highlights the generation number, the objective function and the number of stall generations. This optimisation ended at the 96 generations as 50 stall generations had been reached.

The output minimum cost of the system is R2 765 760, using 148 PV panels, 13 wind turbines at 12m heights and 100 batteries.

6.1.1. PV Panels

148x 200W PV panels were chosen as the optimal number of panels for the HRES for this area with the climatic data as shown above. At STC this gives 29.6kW of maximum solar PV power. Using the climatic data, the total PV power able to be supplied per hour to the system by all the PV panels is calculated and figure 6.5 shows the result over the period of the year, 0-8760 hours.

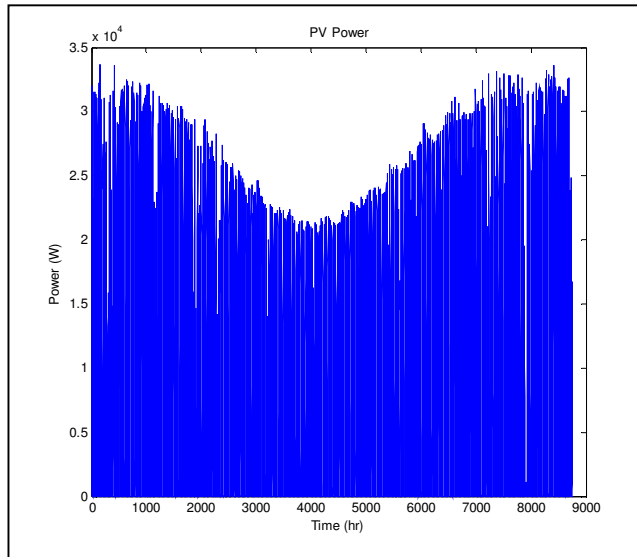


Figure 6.5: Power Able to be Supplied by PV Panels

6.1.2. Wind turbine

13x 3kW wind turbines were determined to be the optimal number of wind turbines for the HRES for this area with wind data as shown above. This is 69kW of wind power generation at rated wind speed. The turbines should be at a height of 12m to enable them to be most cost effective and provide as much power as possible. Figure 6.6 below shows the total power able to be provided to the system taking the wind speed into account.

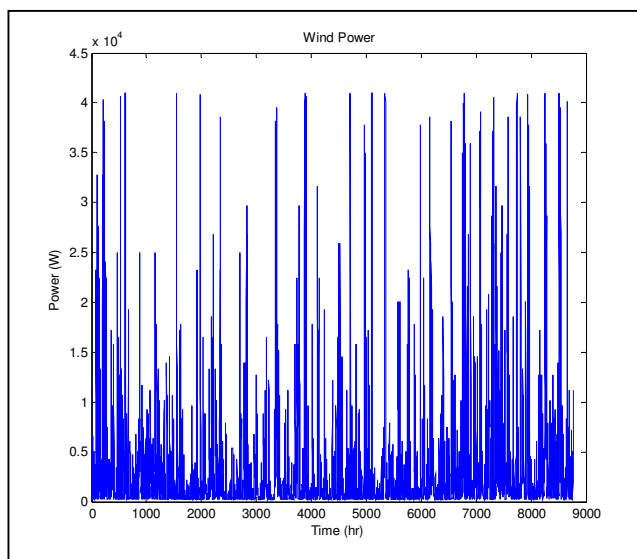


Figure 6.6: Power Able to be Supplied by Wind Turbines

6.1.3. Batteries

100x 200Ah batteries were selected for use for this system. There is therefore a capacity of 20000Ah. This will be used as energy storage to boost the power necessary to meet the load when weather conditions are not optimal.

6.1.4. Calculating LPSP

The LPSP calculated when checking the results from the genetic algorithm is 0.0083, which is lower than 0.01 which is the set LPSP. This means that the load will not be supplied 0.83% of the year on which calculations have been based. This is 72.7hrs or 3.02 days.

6.5. Resultant Controller and Simulation Results

The controller consists of four modes for the system to run in depending on the load and generation values, as discussed in chapter 3. The system consists of 4 modes, the first where only the wind turbine supplies the load, the second where the PV panels and wind turbine supply the load, the third where the PV panels, wind turbine and batteries supply the load and the fourth where the load is not supplied as the load is greater than the energy that can be generated by the system. Running the controller with the results from the genetic algorithm gives us the following information about the system. Firstly, we can gauge the load over the year, hour by hour, as well as the amount of the load that is supplied by the PV panels and the amount of the load supplied by the wind turbines. The following graphs show these components with figure 6.7 showing the load needing to be supplied over the year.

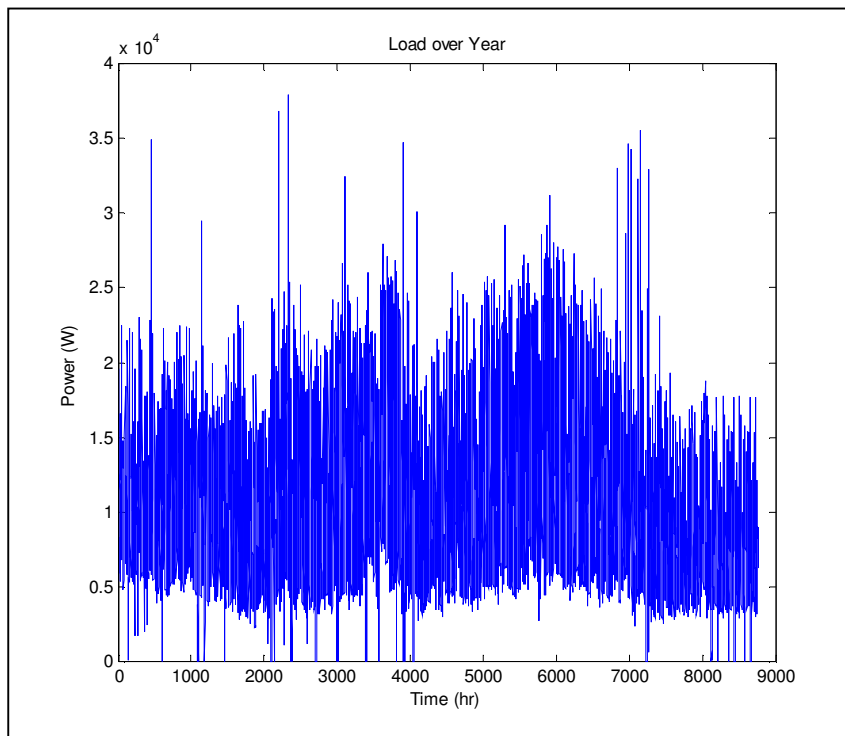


Figure 6.7: Load over the Year

The wind turbines supply the power to the system when the system is in mode 1, mode 2 and mode 3. In mode 1, the power generated by the wind turbine is sufficient to supply the system alone. Figure 6.8 shows the power supplied to the system by the wind turbines in mode 1, 2 and 3.

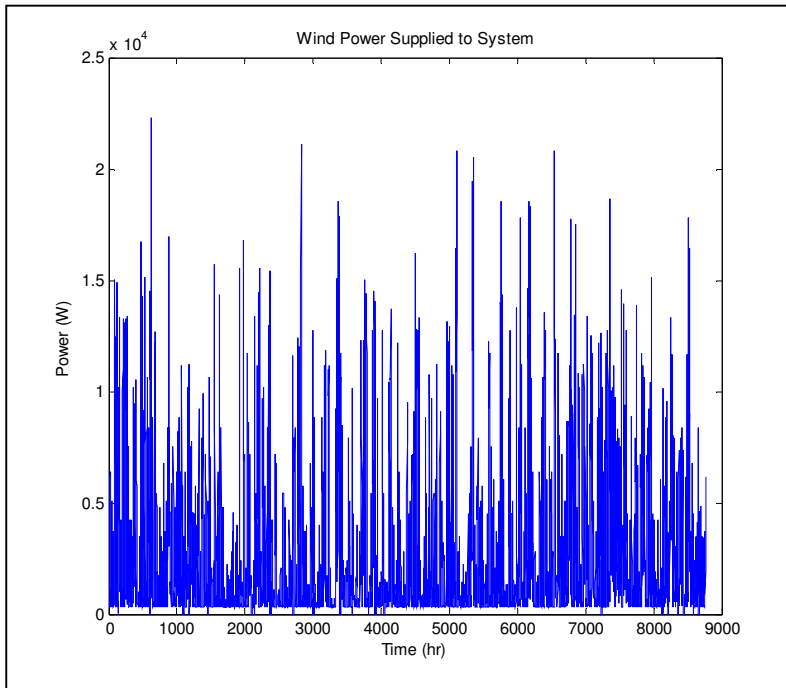


Figure 6.8: Power Supplied by the Wind Turbines

The PV panels supply power to the system in modes 2 and 3. Figure 6.9 shows the power that is supplied by the PV panels in those modes.

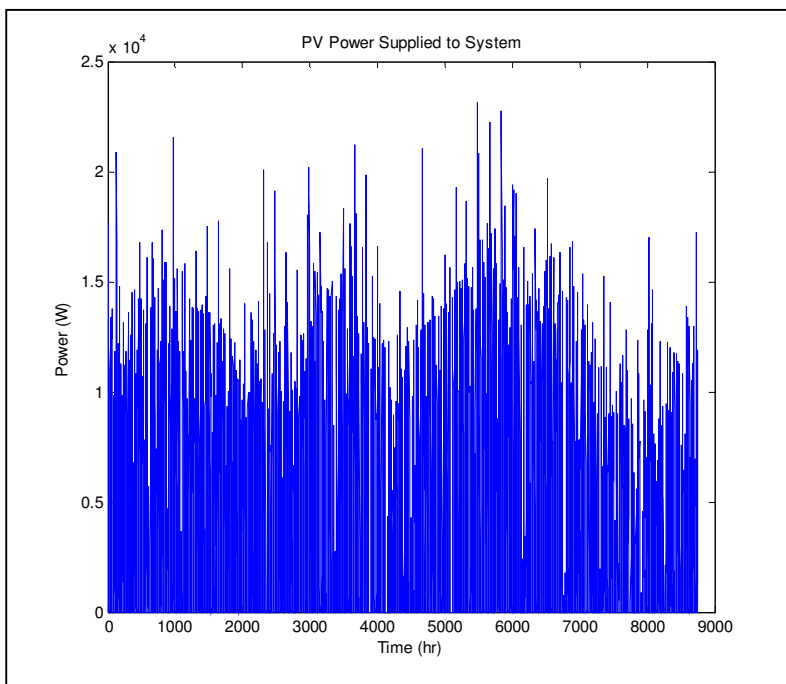


Figure 6.9: Power Supplied by the PV Panels

Another aspect of the system that can be monitored using the controller simulation is the State of Charge of the batteries and therefore the capacity of the system. The set depth of discharge for the batteries is 40%, which is 8000Ah for the battery system that we have for this system. Figure 6.10 outlines the battery capacity over the year. It can be seen that the battery capacity remains between 8000 and 20000Ah and therefore the controller is working as required in keeping the batteries between the minimum and maximum bounds.

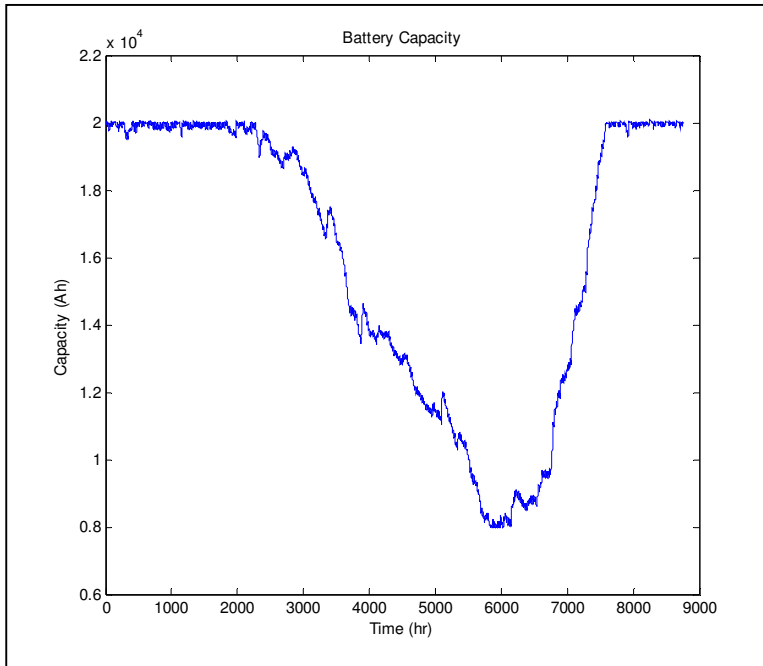


Figure 6.10: Capacity of Batteries

Figure 6.11 shows the histogram of the modes of the system. It can be seen that the system transitions between the different modes, as each mode accounted for on the histogram.

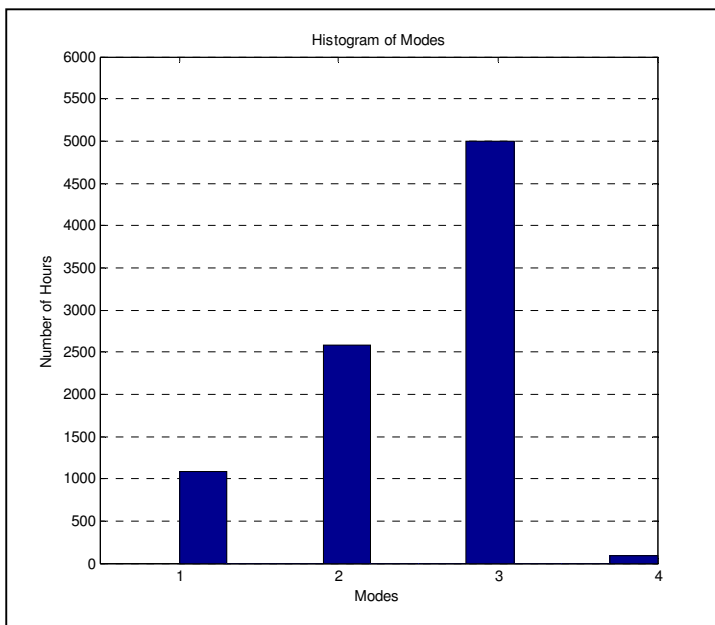


Figure 6.11: Histogram of modes of System

Mode 4 is the mode where the system is not supplied by the PV panel, wind turbine and batteries. This is the mode where the load is not supplied. From figure 6.11 it can be seen that the system is in mode 4 a very small percentage of the time, 78 hours (0.89%), which is below the set LPSP of 1%. It can be seen that the system is mostly in mode 3 where the wind turbine, PV panels and batteries are supplying the load. As there are a number of wind turbines as well as many PV panels, the system is split between modes 1 and 2, being in mode 1, 12% of the time and in mode 2, 30% of the time. As the wind turbines supply more power than the number of PV panels in the system, it is to be expected that the system will be in mode 1 for a portion of the time.

Figure 6.12 shows the total load to be supplied, EI, and the total supply, TSupply. It can be seen from the graph that the load is met the majority of the time, however there is a section of time around 6000 hours where the load is not met. As the LPSP has not been set to zero and therefore some loss of load is expected over the year, the concern is not that the load is not always met. The main concern is the amount of time that the load is met and not met. From the histogram in figure 6.11 and the load and supply graph shown in figure 6.12, we see that the load is not met around 0.9% of the time. This is appropriate as we have selected a LPSP of 1%.

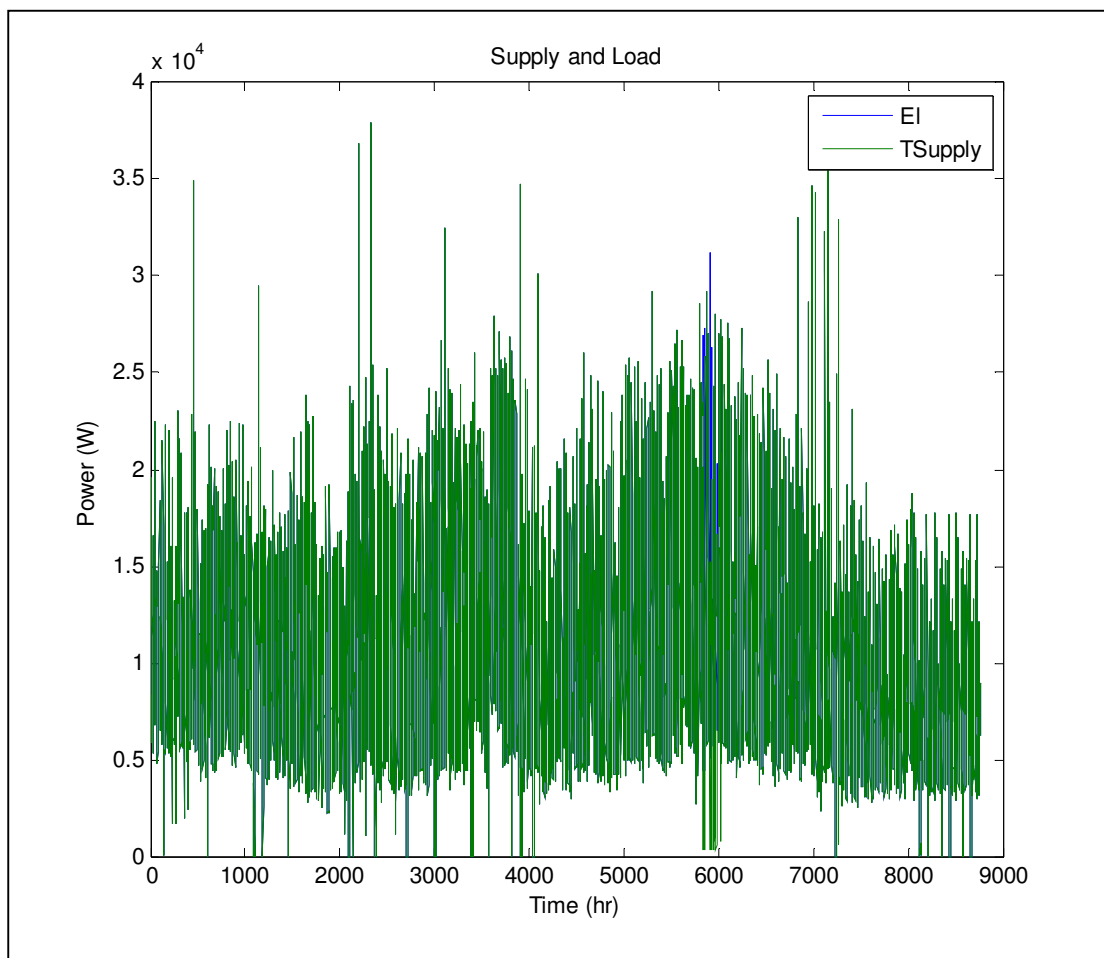


Figure 6.12: Load and Total Supply over Year

6.6. Conclusions

Using the hourly climatic and load data for Gasese over a year period, the genetic algorithm was run and a system of 148 PV panels, 13 wind turbines at 12m height and 100 batteries was deemed to be the most suitable for the conditions specified. This is a total energy generation capacity of 98.6kW and storage capacity of 20000Ah. This has a cost of R2 765 760. Running the LPSP checking test, an LPSP of 0.0083 was calculated giving a 0.83% loss of load probability over the period of the year. The controller simulation is run as a checking mechanism. Running the controller simulation shows that the state of charge of the batteries stays between 40% capacity to 100% capacity, the minimum and maximum bounds of the batteries, which shows that the control is working well. The system enters all four modes at different points in the year and the load is supplied around 0.9% of the year as can be seen from the histogram of modes in figure 6.11. This is very close to the output for the LPSP checking test, so the result is deemed to be validated.

The outcome of this case study can be used to set up a HRES in an area similar in climate and population dynamics to Gasese. Ideally the weather data for the area where the HRES is being designed for would be used in these calculations, but if it was not possible, this simulation could be used as a starting point for design. The outcome of this case study will be discussed in more detail in chapter 7.

7. Discussion of Results

7.1. Introduction

Three areas in South Africa were chosen for studying in this thesis, Garagapola in Limpopo Province, Antioch in Kwazulu-Natal and Gasese in the Northern Cape. Each is a good example of a rural residential area and rural residential load data has been gathered from each of these areas. This along with climatic data from nearby weather stations and solar irradiance data calculated from satellite images have been used to set up the genetic algorithm for optimising sizes of HRES which could be used to electrify villages of similar climatic type and load type. This chapter will discuss the results from these optimisation and look at all three studies together comparing the results and outcomes.

7.2. Climatic Data Set

Each area's climatic data set has been discussed in each case study chapter. This chapter will, therefore serve to look at the data sets together and compare them. Figure 7.1 shows a bar chart of the average monthly temperature in each of the areas.

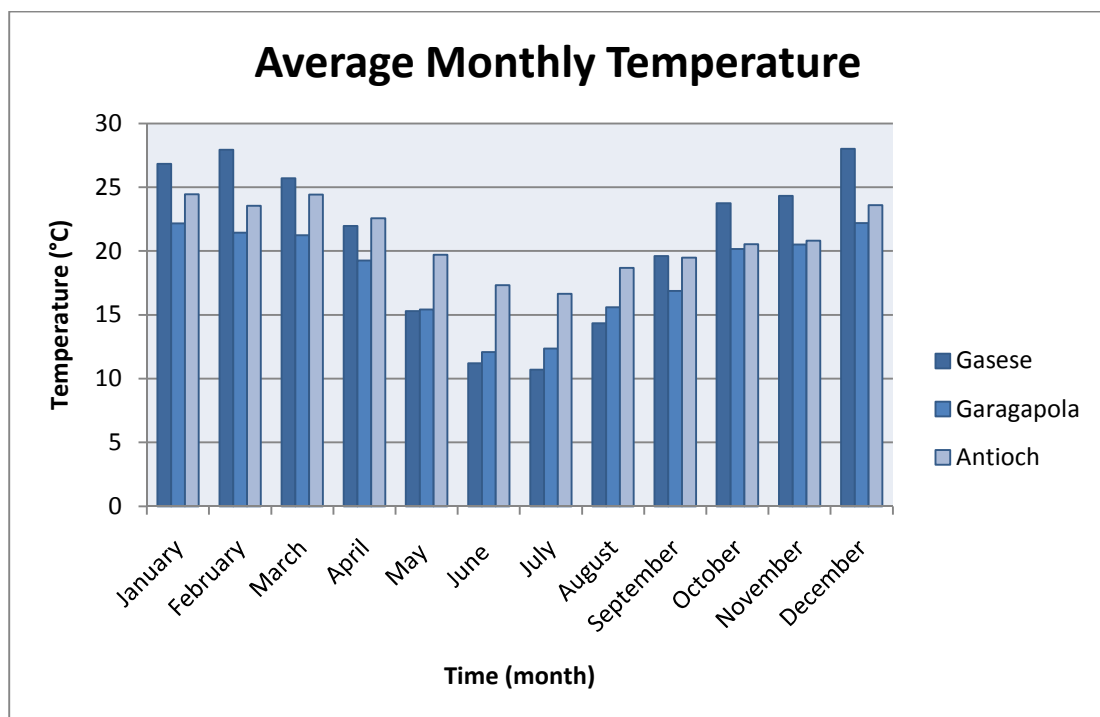


Figure 7.1: Average Monthly Temperature Bar Chart

From figure 7.1 we can see that Gasese has the most extreme temperature range having the highest temperatures in the summer months and the lowest temperatures of the three areas in the winter months. Antioch seems to have the most moderate temperature range with the difference in temperature between the summer and winter months not being very much. Garagapola has a temperature range between Gasese and Antioch, where the

difference between temperatures in winter in summer is significant, but not as extreme as that of Gasese. Figure 7.2 shows the average monthly solar irradiance.

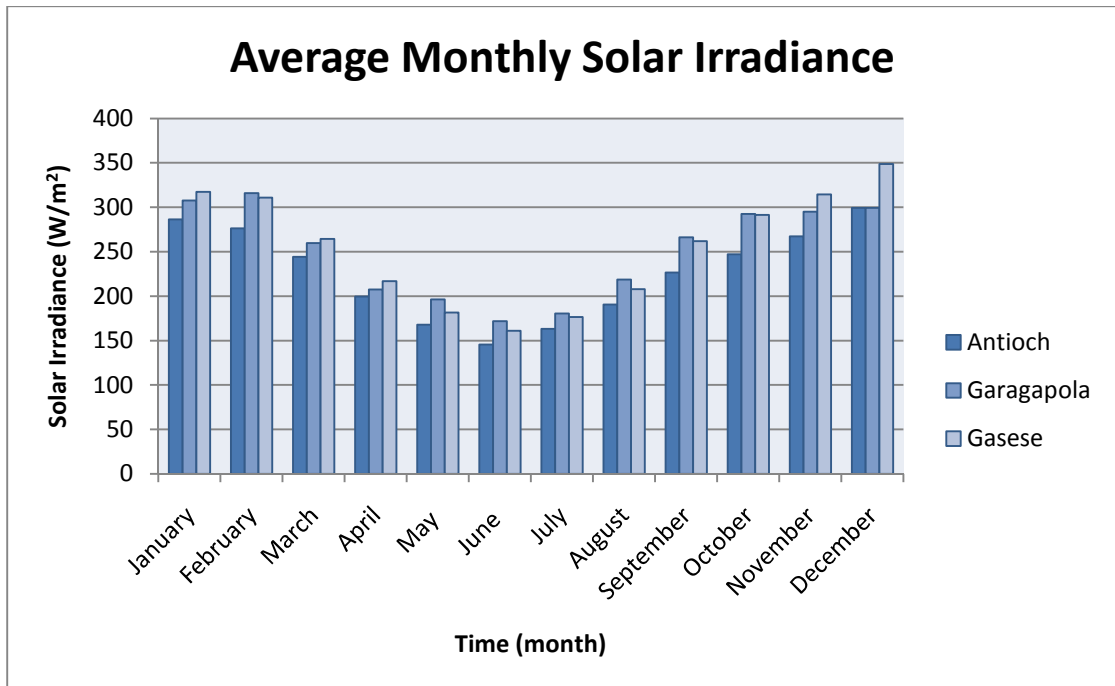


Figure 7.2: Average Monthly Solar Irradiance Bar Chart

The solar irradiance in figure 7.2 is follows a similar pattern, however the differences between the areas is less pronounced than those of figure 7.2. The solar irradiance for each of the areas is much lower during the winter months than those of the summer months.

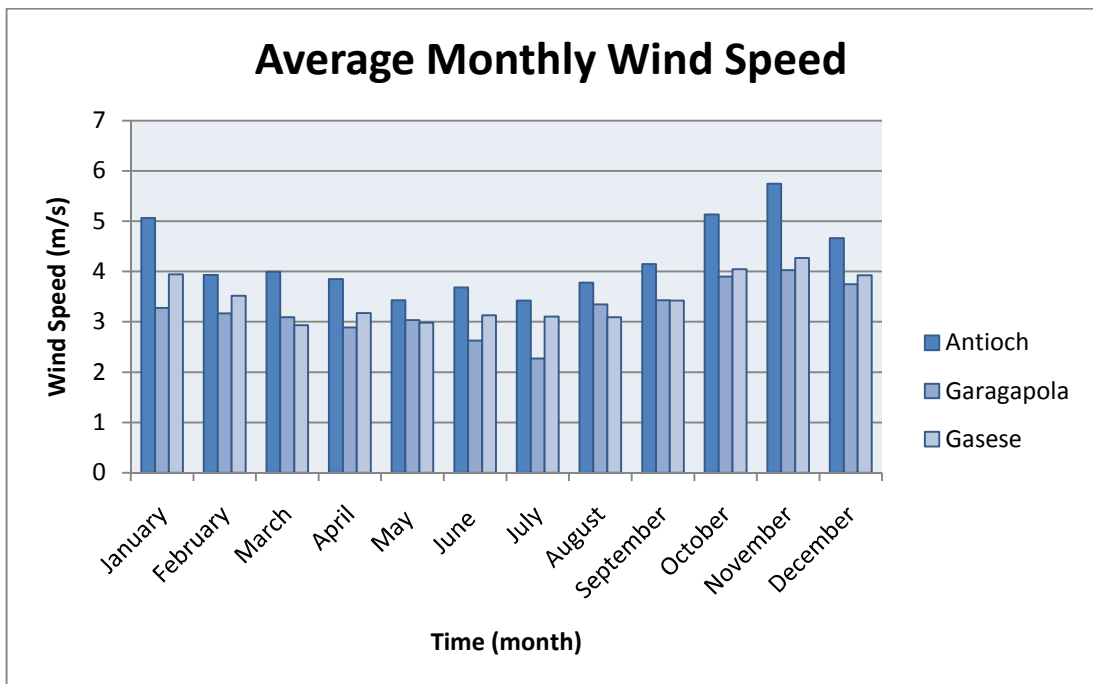


Figure 7.3: Average Monthly Wind Speed Bar Chart

Figure 7.3 shows the average wind speed per month in each of the three areas. It is clear that Antioch has the highest wind speed of the three areas all year round, with higher wind speeds in summer and lower wind speeds in winter. Garagapola and Gasese have similar wind patterns with slightly elevated values in summer and lower values in the winter months. Whilst there are slightly elevated values in summer than winter months in terms of wind speed, there is much less variation between the seasons than can be seen for the temperature.

From figure 7.1, 7.2 and 7.3 we can see that in general the wind and solar resources are higher in summer than in winter, in particular the solar resources. It can therefore be deduced that there will be more energy available from the wind turbines and PV panels in summer than winter.

7.3. Load Data Set

Each area's load data set has been discussed in each separate case study chapter. This chapter will, therefore serve to look at the data sets together and compare them. Figure 7.4 shows a bar chart of the average monthly load in each of the areas.

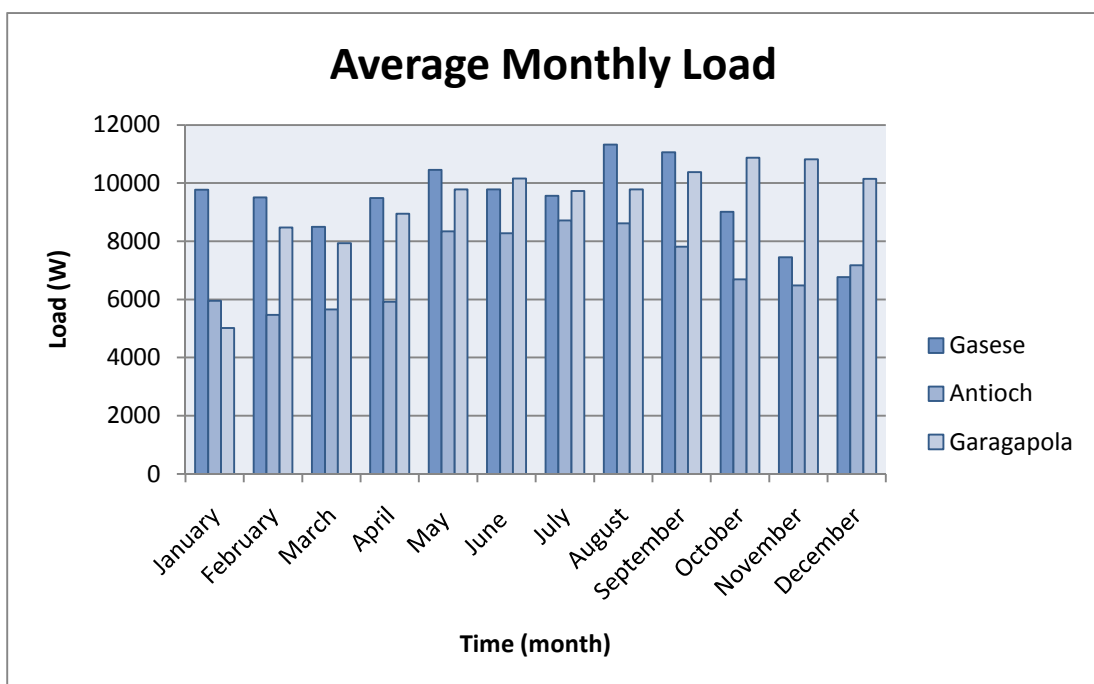


Figure 7.4: Average Monthly Load Bar Chart

From figure 7.4 it can be seen that for most of the year Gasese has the highest load with a maximum average in August of 11300W. Antioch has the most varying load with the highest load in the winter months and a lower load in the summer months. Garagapola has a fairly constant load throughout the year around 9000W, which however does dip substantially in January. It may be plausible to assume that the use of electricity in the area was growing over the year as though it is a fairly constant load, it does increase steadily from January to December.

It can be seen from figure 7.4 that whilst some areas have fairly constant loads, the demand does become higher in the winter months. When looking at that in the context of higher levels of energy being generated by the wind turbines and PV panels in the summer months, the necessity and importance of having some form of energy storage becomes obvious.

7.4. Results of Optimisation

The genetic algorithm was run using the climatic data and load data from each of the areas and the results as shown in table 7.1 were attained. Each individual result is discussed in more depth in each of the case study chapters.

Table 7.1: Comparison of Results

	Garagapola	Antioch	Gasese
Number of PV panels	220	203	148
Number of wind turbines	5	5	13
Height of wind turbines	10	10	12
Number of batteries	19	13	100
Cost	R1 952 665.5	R1 827 510	R2 765 760
LPSP	0.0045	0.0046	0.0083

7.1.1. PV Panels

From figure 7.1 it was seen that Gasese has the highest summer temperature and therefore highest potential for energy generation using PV panels. It is therefore not surprising that a large number of PV panels have been assigned to this design case, especially as Gasese has the largest load, throughout most of the year, of the three areas.

Garagapola, with the second highest temperature, as seen in figure 7.1, has also been assigned many PV panels to generate energy. This is also as Garagapola has the lowest wind speeds of the three areas and therefore PV generation will be the main form of energy generation for the area.

Antioch has the most moderate temperature range of the three areas and therefore the energy generated as a result of the PV panels does not vary substantially between summer and winter. This is therefore ideal as an energy generation method as the amount of energy generated in winter does not drop considerably as it does with the temperatures and therefore energy generated in the other two areas. It therefore follows that Antioch has a large amount of PV panels assigned to the HRES design.

7.1.2. Wind turbine

Gasese has a fairly consistent wind speed throughout both summer and winter with only slightly elevated values in summer. Wind energy generation is therefore a good base load energy supply and since a large load must be supplied, as seen in figure 7.4, both wind and PV panels are needed in larger quantities to enable consistent supply to the area.

As Garagapola has the lowest wind speeds of the three areas, wind is not a main source of energy generation and therefore only a small amount of wind turbines are needed to supply the load that the PV panels do not supply.

As from figure 7.3, it can be seen that Antioch has the highest wind speeds of the three areas, however it also has the most extreme difference in wind speed between the summer months and winter months. As the wind speeds are generally high, the wind turbines assigned to this area will generally operate near the peak power able to be produced, however as the wind fluctuates this changes. It therefore follows that whilst some wind turbines have been assigned to the HRES design, many PV panels have also been added.

7.1.3. Batteries

From figure 7.4 , it is seen that Gasese has the highest load for most of the year, of the three areas. Gasese also has the most varying load with the load peaking in the winter months and diminishing slightly in the summer months. As Gasese has the most extreme temperature range of the three areas, with the temperatures peaking in the summer months and dipping significantly in the winter months as well as wind speeds which are slightly elevated in the summer months and dip in the winter months, it can be assumed that the energy generated by the wind turbines and PV panels will be significantly higher in the summer months and lower in the winter months. As the load peaks in the winter month, it therefore follows that the system will need a large amount of energy storage in the form of batteries to balance the peak of load and dip in energy generation in winter.

Garagapola has a fairly steady load, with the load increasing slightly from January to December. There is, therefore no peak of load in the winter months, but a peak in the load in the summer months. As Garagapola has been assigned many PV panels as the main source of energy generation, it follows that the high in energy generation will be in the summer months and therefore the PV panels as well as the wind turbines will be able to supply the peak loads in summer. There is therefore not a large discrepancy in the peak of the load and peak of energy generation of the system and therefore not much energy storage is needed to ensure that the reliability of the system is maintained. It follows therefore that Garagapola would have the least amount of batteries assigned to it.

Antioch is slightly different to the previous two cases as Antioch has a more moderate temperature range and therefore the amount of energy that the PV panels produce throughout the year is fairly consistent, although elevated values do occur in the summer months. Because this difference is not vast, there is a smaller gap between the times of peak load and peak demand. Whilst the peak load for Antioch does occur in winter, the moderate temperatures allow the PV panels to generate energy even in these times. In addition the wind energy generated is also substantial throughout the year. There is therefore little need for energy storage and only 13 batteries are assigned to the system.

7.5. Conclusions

Looking at the climatic data, the load data and the genetic algorithm results for each of these areas, it is clear from the discussion of these results that the results gathered are plausible and the reasons for the differences in results between the three areas has been made clear.

Gasese has a largest load of the three areas and has a load profile which peaks in the winter months and dips in the summer months. Gasese also has the highest temperatures, but the most extreme temperature pattern with high temperatures in the summer months and low temperature in the winter months. Whilst the wind speed profile is more consistent throughout the year, there is an elevation in wind speed value in the summer months and a slight dip in the winter months. Gasese relies on both PV panels and wind turbines for energy generation as they both have good profiles and there is a large load to supply. As the peaks of generation and demand are mismatched, a large amount of energy storage is needed to supply the area.

Garagapola has a load profile over the year which increases slightly from January to December, leading to the maximum load over the end of the year summer months. As Garagapola has good temperatures and solar irradiance over the year, PV panels supply the bulk of the energy demand, whilst wind turbines supplement this energy generation. As the peaks of energy generation and energy demand match in the summer months, there is not a great need for energy storage and therefore only 19 batteries are needed for the HRES system designed for the area.

Antioch has the smallest load of the three areas and similarly to Gasese, has a load profile which peaks in winter and dips in summer. As Antioch has the most moderate temperature range over the year, many PV panels are used in the design as the base load. As Antioch has the best wind speed profile of the three areas, wind energy is also a substantial source of energy. Combining these factors, it is seen that the need for energy storage is diminished and only few batteries are needed to ensure the reliability of the system.

The results that were obtained are therefore well explained with the climatic and load data that we have used to generate these HRE systems.

8. Conclusions and Recommendations

8.1. Conclusions

The aim of this thesis as stated in chapter 1 was to design a tool which would size a Hybrid Renewable Energy System for a rural area. This was to be done to ensure a small specified Loss of Load probability, in this case 1%, whilst minimising the cost of the system as much as possible. This tool was designed using Genetic Algorithms to minimise the objective function of cost of the system. The choice of renewable energy sources were considered in the tool was limited to wind turbines and PV panels and lead-acid batteries were chosen as energy storage.

Climatic data in the form of hourly values of temperature, solar irradiance and wind speed were collected for the three areas selected as case study areas in South Africa. In addition, hourly load data for each of these areas was collected to be used in the model. 5% of the load was added to the load figures run through the models to ensure capacity in the system for future load growth in these areas. The areas selected as case study areas were Garagapola in Limpopo Province, Antioch in Kwazulu-Natal Province and Gasese in Northern Cape Province. These areas are already electrified areas, but are rural areas with average rural residential loads. Three different areas were used to see what effects differing climatic data and differing load data have on the optimisation of the sizing of a HRES.

The optimisation tool designed for the system was run on each of the case study sets of data and results were generated. These results were then tested to check the LPSP. Each of the results adhered to the limitation of a minimum of 1% LPSP that was set, ensuring that the design would allow a maximum of 3.65 days of loss of load over the year.

A controller was designed using modes and sliding control to control the amount of energy supplied to the load so as to ensure that the load was met as much as possible. This controller used a mode 1 of supply from the wind turbine, mode 2 being supply from the wind turbines and PV panels, mode 3 being supply from the wind turbines, PV panels and batteries and mode 4, being when the system is not able to supply the load. The batteries were controlled to ensure that they never reach below the set depth of discharge and therefore their lifetime is extended. The results from the GAs run for each area, the number of PV panels, wind turbine, height of wind turbine and number of batteries to be used, are used as inputs to the controller. Running the controller then shows the breakdown of energy generated and supplied for each hour over the year as well as the mode of control used in each hour. With this data the LPSP could be estimated to ensure that it correlated with the LPSP obtained. The results of the case studies correlated well with the LPSP set out as the constraint and that tested in checking the LPSP and therefore the optimisation tool and the controller were deemed to work well and accurately. The aim of this thesis is therefore thought to have been achieved.

The tool created for this thesis is able to be used in feasibility studies and initial design of HRE systems using wind turbines, PV Panels and batteries. The user will need to enter the

climatic and load hourly data for the area under investigation or use the load data already supplied for some rural areas. The Matlab files are easily customisable to allow the user to enter the costs and technical information of the PV panels, wind turbines and batteries which they plan to use if they differ to the ones included in this thesis. The LPSP can also be adapted for the user's purposes. The outcomes of using this tool will be a costing of many of the elements of the system to be used and the number of PV panels, wind turbines and batteries that should be used.

8.2. Recommendations

As discussed in the limitations of the scope of this project, rural electrification is not solely a technical issue. Often when a system similar to the one designed in this thesis is designed and implemented in an area, there are problems. These problems include tampering with the system, vandalism, neglect of system, improper maintenance and other issues.

To ensure that designed systems are well implemented and maintained, the area which is to be supplied by the system needs to be involved in the process, needs to be included and educated on the system that is going to be implemented to ensure that the community has a sense of ownership and pride in the system.

In addition to social aspects, it is felt that systems of such nature are best looked after by the community when the community has some monetary input to the electrification scheme. This may be monthly payments of a set amount or fluctuating payments; however this then becomes an economic issue too. In addition to the education and involvement on the technical aspects of the system, the community should also be included in, or at least notified of, the economic implications of the system. They must know the costs and limitations involved with the cost incurred to them, for example the 3.65 days per year of loss of load, before the system is implemented.

There are many other factors which should be considered when implementing a system of this kind to ensure a long lifetime for the system and good care of the system. Such other factors include the effect that electrifying the area will have on the community, the potential industry and development that will come from this and accounting for this in the design of the system and the load that will need to be supplied. Whilst other factors also need to be considered, it is obvious that the approach taken to rural electrification and implementations of systems of this kind is important. It needs to be approached holistically. This thesis, therefore, makes up only one aspect of this process and will need to have these other aspects added to it before implementation of this type of system could occur.

On a technical level, this thesis has looked at HRE systems consisting of PV panels, wind turbines and lead acid batteries. There are many other types of energy generation which could be included in a system such as this including: micro-hydro generation, biogas and other methods of energy generation. Diesel generators can be used in a system such as this for backup and many other options for batteries are available. These could be included in future work for a tool such as this.

This thesis has also aimed to look at the energy supplied to the area in question as purely electrical energy, however it may be more efficient to break up the load into heat and electrical demands and approach the electrical demands as this thesis has, but approach the heat demands differently, using solar heating or biogas production through digesters or some other method of heat generation. The needs and lives of each community need to be thoroughly analysed and considered as part of the design process. For instance, a farming village may be a great candidate for cooking using biogas and using the livestock excretion as fuel for a biogas digester, but a non-farming village may find it very difficult to fuel a biogas digester for cooking gas generation purposes.

There are therefore many more aspects to rural electrification and the manner by which it is approached. It is recommended therefore that each case be looked at and considered independently and design be approached looking at all these elements. The thesis outlined here can be used well within this design process, however it does not form the entire design process.

9. References

- [1] F. Mavromatakis, G. Makrides, G. Georghiou, A. Pothrakis, Y. Franghiadakis, E. Drakakis and E. Koudoumas, "Modeling the photovoltaic potential of a site," *Renewable Energy*, vol. 35, pp. 1387-1390, 7, 2010.
- [2] M. G. Villalva, J. R. Gazoli and E. R. Filho, "Comprehensive Approach to Modeling and Simulation of Photovoltaic Arrays," *Power Electronics, IEEE Transactions on*, vol. 24, pp. 1198-1208, 2009.
- [3] W. Zhou, C. Lou, Z. Li, L. Lu and H. Yang, "Current status of research on optimum sizing of stand-alone hybrid solar–wind power generation systems," *Appl. Energy*, vol. 87, pp. 380-389, 2, 2010.
- [4] R. F. Coelho, F. Concer and D. C. Martins, "A proposed photovoltaic module and array mathematical modeling destined to simulation," in *Industrial Electronics, 2009. ISIE 2009. IEEE International Symposium on*, 2009, pp. 1624-1629.
- [5] R. Belfkira, O. Hajji, C. Nichita and G. Barakat, "Optimal sizing of stand-alone hybrid wind/PV system with battery storage," in *Power Electronics and Applications, 2007 European Conference on*, 2007, pp. 1-10.
- [6] A. A. Ahmed, Li Ran and J. Bumby, "Simulation and control of a hybrid PV-wind system," in *Power Electronics, Machines and Drives, 2008. PEMD 2008. 4th IET Conference on*, 2008, pp. 421-425.
- [7] S. Chowdhury, G. A. Taylor, S. P. Chowdhury, A. K. Saha and Y. H. Song, "Modelling, simulation and performance analysis of a PV array in an embedded environment," in *Universities Power Engineering Conference, 2007. UPEC 2007. 42nd International*, 2007, pp. 781-785.
- [8] R. Faranda, S. Leva and V. Maugeri, "MPPT techniques for PV systems: Energetic and cost comparison," in *Power and Energy Society General Meeting - Conversion and Delivery of Electrical Energy in the 21st Century, 2008 IEEE*, 2008, pp. 1-6.
- [9] C. Liu, B. Wu, R. Cheung Advanced algorithm for MPPT control of photovoltaic systems, in the *Canadian Solar Buildings Conference*, Montreal, August 20-24, 2004.
- [10] J. Wen, Y. Zheng and F. Donghan, "A review on reliability assessment for wind power," *Renewable and Sustainable Energy Reviews*, vol. 13, pp. 2485-2494, 12, 2009.
- [11] F. Roques, C. Hiroux and M. Saguan, "Optimal wind power deployment in Europe—A portfolio approach," *Energy Policy*, vol. In Press, Corrected Proof.
- [12] S. C. Gupta, Y. Kumar and G. Agnihotri, "Optimal sizing of solar-wind hybrid system," in *Information and Communication Technology in Electrical Sciences (ICTES 2007)*, 2007. ICTES. IET-UK International Conference on, 2007, pp. 282-287.

- [13] J. Paska, P. Biczal and M. Klos, "Technical and economic aspects of electricity storage systems co-operating with renewable energy sources," in *Electrical Power Quality and Utilisation*, 2009. EPQU 2009. 10th International Conference on, 2009, pp. 1-6.
- [14] N. Jantharamin and L. Zhang, "A new dynamic model for lead-acid batteries," in *Power Electronics, Machines and Drives*, 2008. PEMD 2008. 4th IET Conference on, 2008, pp. 86-90.
- [15] A. Barin, L. N. Canha, K. Magnago, A. da Rosa Abaide and B. Wottrich, "Multicriteria decision making for management of storage energy technologies on renewable hybrid systems - the analytic hierarchy process and the fuzzy logic," in *Energy Market*, 2009. EEM 2009. 6th International Conference on the European, 2009, pp. 1-6.
- [16] K. C. Divya and J. Østergaard, "Battery energy storage technology for power systems—An overview," *Electr. Power Syst. Res.*, vol. 79, pp. 511-520, 4, 2009.
- [17] O. M. Toledo, D. Oliveira Filho and A. S. A. C. Diniz, "Distributed photovoltaic generation and energy storage systems: A review," *Renewable and Sustainable Energy Reviews*, vol. 14, pp. 506-511, 1, 2010.
- [18] H. Ibrahim, A. Ilinca and J. Perron, "Energy storage systems—Characteristics and comparisons," *Renewable and Sustainable Energy Reviews*, vol. 12, pp. 1221-1250, 6, 2008.
- [19] M. Dürr, A. Cruden, S. Gair and J. R. McDonald, "Dynamic model of a lead acid battery for use in a domestic fuel cell system," *J. Power Sources*, vol. 161, pp. 1400-1411, 10/27, 2006.
- [20] F. Valenciaga and P. F. Puleston, "Supervisor control for a stand-alone hybrid generation system using wind and photovoltaic energy," *Energy Conversion, IEEE Transactions on*, vol. 20, pp. 398-405, 2005.
- [21] M. E. Torres-Hernandez and M. Velez-Reyes, "Hierarchical control of hybrid power systems," in *Power Electronics Congress*, 2008. CIEP 2008. 11th IEEE International, 2008, pp. 169-176.
- [22] K. N. Hasan, M. E. Haque, M. Negnevitsky and K. M. Muttaqi, "Control of energy storage interface with a bidirectional converter for photovoltaic systems," in *Power Engineering Conference*, 2008. AUPEC '08. Australasian Universities, 2008, pp. 1-6.
- [23] Mei Qiang, Wu Wei-yang and Xu Zhen-lin, "A multi-directional power converter for a hybrid renewable energy distributed generation system with battery storage," in *Power Electronics and Motion Control Conference*, 2006. IPEMC 2006. CES/IEEE 5th International, 2006, pp. 1-5.
- [24] R. Kaiser, "Optimized battery-management system to improve storage lifetime in renewable energy systems," *J. Power Sources*, vol. 168, pp. 58-65, 5/25, 2007.
- [25] J. L. Bernal-Agustín and R. Dufo-López, "Simulation and optimization of stand-alone hybrid renewable energy systems," *Renewable and Sustainable Energy Reviews*, vol. 13, pp. 2111-2118, 10, 2009.

- [26] A. H. Shahirinia, S. M. M. Tafreshi, A. H. Gastaj and A. R. Moghaddomjoo, "Optimal sizing of hybrid power system using genetic algorithm," in Future Power Systems, 2005 International Conference on, 2005, pp. 6 pp.-6.
- [27] E. Koutroulis, D. Kolokotsa, A. Potirakis and K. Kalaitzakis, "Methodology for optimal sizing of stand-alone photovoltaic/wind-generator systems using genetic algorithms," Solar Energy, vol. 80, pp. 1072-1088, 9, 2006.
- [28] A. Roy, S. B. Kedare and S. Bandyopadhyay, "Optimum sizing of wind-battery systems incorporating resource uncertainty," Appl. Energy, vol. 87, pp. 2712-2727, 8, 2010.
- [29] H. Yang, Z. Wei and L. Chengzhi, "Optimal design and techno-economic analysis of a hybrid solar-wind power generation system," Appl. Energy, vol. 86, pp. 163-169, 2, 2009.
- [30] B. Ould Bilal, V. Sambou, P. A. Ndiaye, C. M. F. Kébé and M. Ndong, "Optimal design of a hybrid solar-wind-battery system using the minimization of the annualized cost system and the minimization of the loss of power supply probability (LPSP)," Renewable Energy, vol. 35, pp. 2388-2390, 10, 2010.
- [31] R. L. Haupt, Practical Genetic Algorithms. 1998.
- [32] (2011, August) SoDa Services. [Online]. <http://www.soda-is.com/eng/index.html>
- [33] Daming Xu, Longyun Kang, Liuchen Chang and Binggang Cao, "Optimal sizing of standalone hybrid wind/PV power systems using genetic algorithms," in Electrical and Computer Engineering, 2005. Canadian Conference on, 2005, pp. 1722-1725.
- [34] (2011, January) Tenesol TE200 Datasheet. [Online]. <http://www.tenesol.com/ged/gendoc.php?id=3&langue=EN&HD=no>
- [35] (2011, January) Kestrel e400i Datasheet. [Online]. http://www.kestrelwind.co.za/assets/brochures/kestrel%20e400i%20info%20leaflet_final%20for%20print.pdf
- [36] H. Yang, W. Zhou, L. Lu and Z. Fang, "Optimal sizing method for stand-alone hybrid solar-wind system with LPSP technology by using genetic algorithm," Solar Energy, vol. 82, pp. 354-367, 4, 2008.
- [37] (2011, August) MLT Drives Price list. [Online]. <http://www.mltdrives.com/price-list.htm>
- [38] (2011, August) Sustainable.co.za. [Online]. <http://www.sustainable.co.za/tenesol-solar-module-te-2000-200w-solar-module.html>
- [39] (2011, August) Battery Experts. [Online]. http://www.batteryexperts.co.za/batteries_sealed.html
- [40] (2011, August) Garagapola Google Map. [Online]. <http://maps.google.com/maps?q=-24.56%0930.16&hl=en&ll=-24.561468,30.163414&spn=0.010929,0.021136&sll=-26.767683,30.533752&sspn=1.37324,2.705383&vpsrc=6&t=h&z=16>

- [41] (2011, June) SoDa services Solar Irradiance. [Online]. http://www.soda-is.com/eng/services/services_radiation_free_eng.php
- [42] (2011, August) Antioch Google Map. [Online]. <http://maps.google.com/maps?q=-30.09++29.81&hl=en&ll=-30.028891,29.842172&spn=0.005202,0.014656&sll=37.0625,-95.677068&sspn=38.911557,86.572266&vpsrc=6&t=h&z=17>
- [43] (2011, August) Gasese Google Map. [Online]. <http://maps.google.com/maps?q=-27.11%0923.05&hl=en&ll=-30.145127,23.796387&spn=10.630414,21.643066&sll=37.0625,-95.677068&sspn=38.911557,86.572266&vpsrc=6&z=6>

10. Papers Published

- [1] G. Coppez, S. Chowdhury and S. P. Chowdhury, "Review of battery storage optimisation in distributed generation," in *Power Electronics, Drives and Energy Systems (PEDES) & 2010 Power India, 2010 Joint International Conference on*, 2010, pp. 1-6.
- [2] G. Coppez, S. Chowdhury and S. P. Chowdhury, "The importance of energy storage in renewable power generation: A review," in *Universities Power Engineering Conference (UPEC), 2010 45th International*, 2010, pp. 1-5.
- [3] G. Coppez, S. Chowdhury and S. P. Chowdhury, "Impacts of energy storage in distributed power generation: A review," in *Power System Technology (POWERCON), 2010 International Conference on*, 2010, pp. 1-7.
- [4] G. Coppez, S. Chowdhury and S.P. Chowdhury, "South African Renewable Energy Hybrid Power System Storage Needs, Challenges and Opportunities" in *IEEE PES General Meeting, 2011 International Conference*, 2011.

Appendix: Datasheets

PV Panel Datasheet: Tenesol TE200

Photovoltaic modules

TE190/220-54P

- ▶ High efficiency, reduced area

Tenesol manufactures its own photovoltaic modules in two facilities.

Tenesol's modules use the high-output technology of the polycrystalline cell. Each cell is individually measured and sorted before the encapsulation stage.

The combined use of tempered glass, EVA and back sheet keeps its weight to a minimum. The laminate guarantees total watertightness and long-term protection of the cells.

The reinforced 50 mm aluminium frame makes handling easy and allows for quick, easy and highly resistant assembly.

Each module is subject to an individual quality control process.

Product warranty: 10 years

Power warranty: 25 years*



The quality of TENESOL modules are CE certified.

Our production facilities are also certified according to ISO 9001 and ISO 14001 standards.



A rapidly expanding global player in the field of solar energy (with a turnover of €304 million in 2010, average 25% growth per year over last 3 years), Tenesol works on behalf of businesses, local authorities and private individuals.

For more than 28 years, Tenesol has been engineering, designing, manufacturing, installing and managing solar energy systems including production and consumption of supplied systems (Off-grid sites, general grid supply via direct connection, solar water heating) for its customers around the globe.

A benchmark player in its sector, Tenesol currently has a staff of more than 1.000 employees across 24 subsidiaries including 2 production facilities.



Sun access provider.

TENESOL
SOLAR GROUP

Property Tenesol. Duplication prohibited.

Photovoltaic modules

► TE190/220-54P

Electrical characteristics

Nominal Power	Wp	190'	200'	210'	220'
Minimum power		185	195	205	215
Maximum power		195	205	215	225
Sorting limits	Wp	-5 / +5			
Sorting limits	%	±2.5			
Voltage at max. power	(V)	25.0	25.85	26.25	26.5
Current at max. power	(A)	7.8	7.8	8.0	8.2
Open circuit voltage	(V)	32.1	32.5	32.9	33.3
Short circuit current	(A)	8.1	8.3	8.5	8.7

According to specifications of IEC 61215 (IEC 61730) and IEC 61730 (IEC 61215) test at ambient temperature $T = 20^{\circ}\text{C}$.

(*) - Models available upon request.

Nominal Power 45°C / 800W/m ² Wp		139,5	147,2	154,8	162,3
Voltage at max. power	(V)	22,7	23,3	23,9	24,5
Current at max. power	(A)	6,2	6,3	6,5	6,6
Open circuit voltage	(V)	29,7	30,1	30,5	30,9
Short circuit current	(A)	6,6	6,7	6,9	7,0

NOCT test realized with a maximum power (in Wp) junction temperature 45 °C; irradiation 800 W/m²; Air 1,5; Ambient temperature 20 °C; Wind speed 1 m/s.

Temperature coefficients

Temperature Coefficient of Voltage	-116,1 mV/°C
Temperature Coefficient of Current	+4,8 mA/°C
Temperature Coefficient of Power	+0,43 %/°C
NOCT	45 °C

Cells

Size	156 x 156 mm
Layout	54 cells / 6 x 9
Type	Polycrystalline

General information

Maximum system voltage	1000 V
Maximum reverse current	17 A
Diodes	3 by-pass
Type of connection	Typo connectors
Junction Box	IP55
Weight	18 kg
Operating ambient temperature	-40 / +85 °C

Certifications

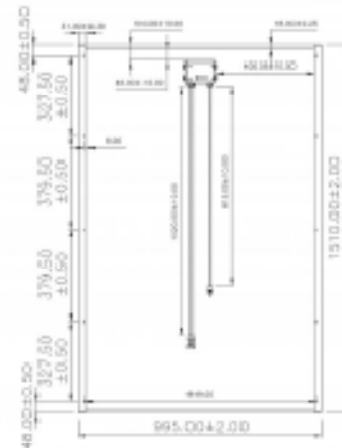
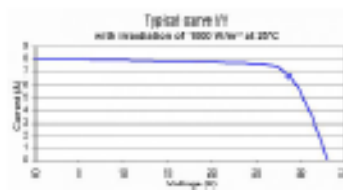
	IEC61215 + IEC61730
--	---------------------

Warranty

Product warranty	10 years
Power warranty (**)	25 years - 80 % of minimal power 10 years - 90 % of minimal power

Irradiance dependency

Irradiation (W/m ²)	Pm	Vpm	Ipm
1000	1	1	1
800	0,790	0,993	0,8
500	0,497	0,964	0,5
400	0,394	0,988	0,4
300	0,291	0,970	0,3
200	0,187	0,938	0,2
100	0,088	0,882	0,1



Wind Turbine Datasheet: Kestrel e400i



www.kestrelwind.co.za CO. ZA

e400i

Up to 3000 watts of power from a high performance three blade turbine
 Affordable clean electricity, adaptable to your needs
 Reliable and convenient with a long-life design
 Suitable for urban living

Power = Quality = Affordability

Specifications

The new e400i is the next level in small wind turbines. By optimising renewable power output and performance, the efficiency of the e400i makes it a valuable asset for fulfilling energy requirements.

Modern living requires a massive amount of energy that is depleting fossil fuels. The e400i generates regulated and optimised energy for increased energy efficiency that is adaptable to all installation requirements.

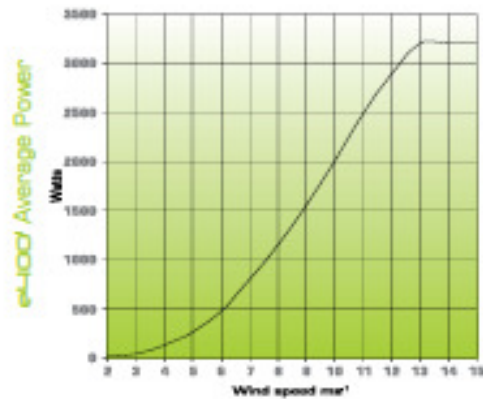
Design

The three aerofoil blades are managed by an advanced passive pitch control system that allows the e400i to continuously generate rated energy in wind speeds that exceed rated wind speed.

The three blade design, with a diameter of 4m, moderates noise emissions effectively, making it an unobtrusive and reliable method of renewable energy generation in all installations and environments. The e400i advanced direct drive alternator incorporates three main shaft bearings for longevity and increased reliability.

Applications

- Boost solar & other renewable energy installations increasing productivity, reliability & cost effectiveness
- Water pumping systems with suitable water pump controller to reduce utility costs
- Continual & reliable power for repeater stations, suitable for the telecommunications industry
- Grid tie applications using approved inverters to reduce energy costs
- Generate dedicated power for housing, community & health centres not connected to the national grid
- Small wind farm installations
- Adaptable to meeting many electrical needs



renewable power for life



kestrel
wind turbines

kestrel

Small Wind Turbine Class	□
Rated Output	3000w
Maximum Power	3300w at 12m/s ²
Rated Wind speed	11m/s ²
Cut-in Wind speed	2.8m/s ²
Generator Type	Permanent magnet Axial flux brushless
Rotor Diameter	4m
Number of Blades	3
Blade Material	Fibre glass
Tower Top Mass	150kg
Tower Height	12-15m
Tower Type	Tripod
Over-speed Protection	Pitch Control
Controller Type	Charge ONLY
Output Voltage	48V, 200 and 300 Vdc
Application	Battery charging Grid Tie Hybrid Water Pumping

* Available on request

Technical Specifications

Rated output is achieved at the rated wind speed at sea level. Rated power is the optimal power rating of the turbine at the rated wind speed, making it maintainable without a cut out wind speed.

Rated output is optimised by technology and design, namely by dynamically limiting the output by pitch control. The Axial Flux alternator type reduces the heat losses while energy is being generated in the form of polyphase high frequency output.

The full aerofoil blades are moulded from fibre glass and protected from dust and moisture. The e400 conforms to EC standards and follows the provisions in the directives ECR1400-2 (small wind turbines).

Kestrel Wind Turbines and its global affiliates and dealers are committed to renewable energy generation as well as reducing the use of fossil fuels. Wind power addresses most of the current issues of present renewable power generation options. Kestrel is continuously developing small wind turbine technology to supply personal or business energy demands.

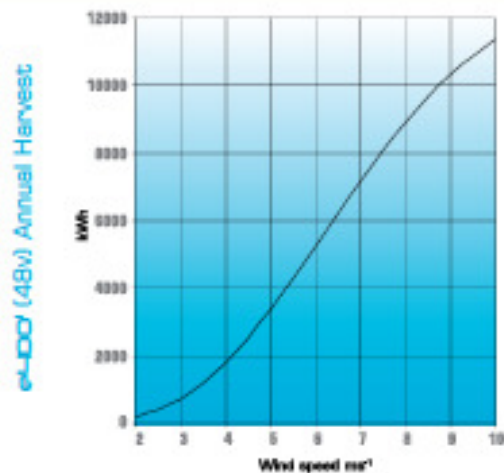
Kestrel is continuously improving current small wind turbines in the Kestrel range to ensure that the highest quality product is distributed. All Kestrel dealers share these values and are trained to support Kestrel's customers in understanding their power requirements and the local wind resource available to them. Also, to evaluate the turbines in the Kestrel range that best accommodate these requirements, assist installations and advise on maintenance procedures.

Power Generation

Generating your own renewable power is low maintenance as routine maintenance is largely based on visual assessments. Maintenance schedules are designed to suit the local, respective, wind area and power class. With a maximum instantaneous power rating of 3300W, annual energy harvests can exceed 13 800kWh. Energy may be harvested at any different wind speed exceeding cut in speed and rated output is maintained at any wind speed exceeding the rated wind speed through rotor turbulence. Energy output is intrinsically linked to regional wind distribution, topology and altitude as well as tower height. Potential energy harvest is estimated using an average wind speed in order to tailor the most suitable Kestrel wind system to your electrical need.

Results may vary based on wind distribution, topology, tower height and altitude. In order to estimate ones own potential energy harvest an average wind speed must be used.

Note: Specifications may vary with continuing development and innovation.



Eveready Road, Graunveld, Port Elizabeth, 6001, SOUTH AFRICA
PO Box 3191, North End, Port Elizabeth, 6056, SOUTH AFRICA
Tel: +27 (0) 41 401 2500 / 2599 - Fax: +27 (0) 41 394 8183
e-mail: kestrelwind@eveready.co.za - www.kestrelwind.co.za

we're renewable power for life